UNIVERSITÀ DEGLI STUDI DI MILANO

SCUOLA DI DOTTORATO IN MEDICINA MOLECOLARE

CICLO XXVI

Anno Accademico 2012/2013

TESI DI DOTTORATO DI RICERCA

MED/04

A METABOLIC APPROACH FOR THE CONTROL OF GLUTAMINE DEPENDENT TUMORS

Dottorando: Martina CHIU

Matricola N° R09183

TUTORE: Prof.ssa Raffaella CHIARAMONTE

CO-TUTORE: Prof. Ovidio BUSSOLATI

DIRETTORE DEL DOTTORATO: Ch.mo Prof. Mario CLERICI

ABSTRACT

Background. Deranged metabolism is a hallmark of cancer cells which need to sustain uncontrolled cell growth while maintaining a proper energy balance. Means to interfere with the cancer-associated metabolic alterations to control tumor cell proliferation are actively pursued. Most tumors rely on enhanced glucose consumption to supply Krebs cycle intermediates (a process called anaplerosis), which are continuously diverted to the macromolecular biosynthesis needed by proliferation. However, nutrients other than glucose may support anaplerosis in tumors, likely depending on the oncogenic mutations present in the particular type of cancer. Glutamine (Gln), the most abundant amino acid in blood, is a precursor of other amino acids (i.e. asparagine), nucleotides and glutathione, and stimulates mTOR. Tumors that rely on Gln instead of glucose for anaplerosis exhibit an enhanced requirement for the amino acid ("glutamine addiction"); however, reliable markers of "glutamine addiction" are still needed; in particular, the role of Glutamine Synthetase (GS), a key enzyme of Gln metabolism, has not been yet defined in this context. GS expression is known to be regulated at the protein level by intracellular Gln content, but, at transcriptional level, its expression is driven by the oncogene β-catenin. Consistently, its over-expression is a marker of β-catenin mutations in hepatocellular carcinoma (HCC), a liver cancer with poor prognosis. We have hypothesized that β-catenin-dependent GS expression may be a marker of a metabolic drift towards Gln-dependence and, hence, of Gln-addiction.

Aim of the thesis. The purpose of this study is to investigate the effects of Gln depletion on human HCC cells so as to verify the hypothesis that β-catenin-dependent GS expression points to a Gln-addicted phenotype.

In addition, the role of GS in the adaptation to Gln depletion of two other human cell models has been also assessed so as to achieve a general appraisal of the metabolic role of the enzyme under conditions of nutritional stress.

Methods. Gln depletion was achieved with the bacterial enzyme L-asparaginase (ASNase), a drug employed in the treatment of acute lymphoblastic leukemia, and the irreversible GS inhibitor methionine-L-sulfoximine (MSO). We have evaluated ASNase and MSO effects on cell viability and mTOR activity in β-catenin-mutated HCC cell lines, in two GS-negative human oligodendroglioma cells, and in bone marrow mesenchymal stem cells (MSCs). Moreover, ASNase and MSO effects were also assessed on HCC xenograft models.

Results. Gln depletion, obtained with ASNase and MSO, markedly hinders the proliferation of β-catenin-mutated, GS-positive, HCC cells in vitro and in vivo. The determination of mTOR activity in Gln-depleted HCC cells indicated that ASNase markedly inhibits the kinase, while MSO caused its paradoxical activation, suggesting that the GS inhibitor may deceive the intracellular amino acid sensors that regulate mTOR. ASNase causes massive cells death in GS-negative human oligodendroglioma cell lines, where MSO is ineffective. On the other hand, MSO prevents the adaptation of MSCs to Gln-depletion, suggesting that GS activity may contribute to the recently described trophic function of MSCs towards leukemic blasts.

Conclusions. These results indicate a role of β-catenin mutations in promoting Gln addiction in HCC and suggest that pharmacological Gln depletion represents a metabolic approach for the therapy of β-catenin-mutated liver cancers. Moreover, GS activity seems crucial for adaptation to Gln shortage, not only in HCC cells, but also in MSCs and oligodendroglioma cells. These evidences suggest that GS constitute a useful diagnostic tool and/or therapeutic target in selected types of human tumors.

SOMMARIO

Introduzione. Le alterazioni metaboliche sono una caratteristica delle cellule tumorali, le quali devono sostenere un'attiva proliferazione senza incorrere in una carenza energetica. Pertanto, la ricerca di approcci metabolici che interferiscono con la crescita tumorale è attivamente perseguita. La maggior parte delle cellule tumorali è contraddistinta da un aumentato consumo di glucosio, necessario per rifornire il ciclo di Krebs di intermedi estratti a scopo biosintetico (anaplerosi). Tuttavia, a seconda delle mutazioni oncogeniche presenti nel fenotipo tumorale, altri nutrienti oltre al glucosio possono essere utilizzati a scopo anaplerotico. Tra essi spicca la glutamina (Gln), il più abbondante amminoacido nel sangue, precursore di altri aminoacidi, di nucleotidi e del glutatione nonché attivatore di mTOR. Tumori che utilizzano Gln a scopo anaplerotico hanno un aumentato fabbisogno di tale aminoacido e vengono perciò definiti "glutamine addicted". Tuttavia non sono ancora stati identificati markers di "glutamine addiction" e, in particolare, il ruolo della Glutamina Sintetasi (GS), enzima chiave del metabolismo della Gln, non è ancora stato chiarito. L'espressione di GS è regolata a livello proteico dalla concentrazione intracellulare di Gln, ma, a livello trascrizionale, la sua espressione è dovuta all'oncogene β-catenina. Difatti l'iper-espressione di GS è un marker diagnostico di mutazione della β-catenina nel carcinoma epatocellulare (HCC), un tumore maligno del fegato con prognosi infausta. Pertanto l'espressione di GS causata dall'iperattivazione della β-catenina potrebbe indicare un metabolismo tumorale dipendente da Gln.

Scopo della tesi. Lo scopo di questo studio è valutare gli effetti della deplezione di Gln in linee umane di HCC, per verificare l'ipotesi che iper-espressione di GS dovuta a mutazioni di β-catenina possa essere un marker di "glutamine addiction". Inoltre è stato valutato anche il ruolo di GS nell'adattamento alla deprivazione di Gln di altri due modelli cellulari umani,

per ottenere una stima generale sul ruolo metabolico dell'enzima in condizioni di stress nutrizionale.

Metodi. La deplezione di Gln è stata ottenuta combinando l'enzima batterico L-asparaginasi (ASNase), in uso nella terapia della leucemia linfoblastica acuta, con la metionina-L-sulfoximina (MSO), un inibitore irreversibile di GS. Sono stati valutati gli effetti di ASNase e MSO sulla vitalità cellulare e sulla attività di mTOR in linee tumorali umane di HCC mutate in β-catenina (in vitro e in xenografts in modelli murini), in due linee di oligodendroglioma umano e in cellule mesenchimali staminali (MSC) umane derivate dal midollo osseo di donatori.

Risultati. Sia in vitro che in vivo, la deplezione di Gln ottenuta tramite ASNase e MSO, inibisce marcatamente la proliferazione delle linee cellulari mutate in β-catenina e positive per GS. Inoltre, mentre ASNase inibisce significativamente l'attività di mTOR, l'aggiunta di MSO, pur causando un'ulteriore diminuzione del contenuto intracellulare di Gln, determina un'attivazione paradossale della chinasi, suggerendo che l'inibitore di GS interagisca con dei sensori per aminoacidi a monte di mTOR. Nei modelli di oligodendroglioma umano GS-negativi ASNase causa una massiva morte cellulare, mentre l'aggiunta di MSO risulta inefficace. D'altra parte MSO previene l'adattamento delle MSC alla deplezione di Gln, suggerendo che GS possa contribuire alla funzione trofica, recentemente dimostrata, delle MSC nei confronti dei blasti leucemici.

Conclusioni. I risultati ottenuti indicano un coinvolgimento delle mutazioni di β-catenina nel favorire un fenotipo neoplastico dipendente da Gln e dimostrano che la deplezione farmacologica di Gln rappresenta un approccio metabolico per la terapia dei tumori al fegato caratterizzati da mutazioni di β-catenina. Inoltre GS sembra necessaria per l'adattamento alla deplezione di Gln in tutti i modelli cellulari testati. Questi risultati suggeriscono che GS possa essere un mezzo diagnostico e/o un target terapeutico in determinati tipi di tumore.

CONTENTS

FIGURE CONTENTS

ABBREVIATIONS

2-DG, 2-deoxyglucose

3-BrPA, 3-bromopyruvate

4E-BP1, eIF-4E binding protein 1

AAR, amino acids response

AFB1, aflatoxin B1

AFP, α-fetoprotein

ALL, acute lymphoblastic leukaemia

AML, acute myeloid leukaemia

AOA, aminooxyacetate

APC, adenomatous polyposis coli

Asn, asparagine

ASNase, L-asparaginase

ASNS, asparagine synthetase

Asp, aspartic acid

BM-MSC, bone marrow-derived MSC

BPTES, bis-2-[5-phenylacetamido-1,2,4-thiadiazol-2-yl] ethyl sulfide

BSA, bovine serum albumin

CK1, casein kinase 1

CLL, chronic lymphocytic leukaemia

CML, chronic myeloid leukaemia

CNS, central nervous system

COX2, cyclooxygenase 2

D-2-HG, (R)-2-hydroxyglutarate

DCA, dichloroacetate

DEBs, doxorubicin-eluting beads

DMEM, Dulbecco's modified medium

DON, 6-diazo-5-oxo-L-norleucine

D-Ser, D-serine

Dvl, Disheveled

EAA, essential amino acids

EBSS, Earle's Balanced Salt Solution

EGCG, epigallocatechin gallate

EGFR, epidermal growth factor receptor

eIF2α, eukaryotic initiation translation factor 2α

FAO, fatty acids oxidation

FASN, fatty acids synthase

FBS, fetal bovine serum

FH, fumarate hydratase

Fz, Frizzled

GAP, GTPase activating protein

GCN2, general control non repressed 2

GDH, glutamate dehydrogenase

Gln, glutamine

GLS, glutaminase

GLT1, glutamate transporter

Glu, glutamic acid

GLUT, glucose transporter

GPNA, γ-L-glutamyl-p-nitroanilide

GS, Glutamine Synthetase

GSH, glutathione

GSK-3β, glycogen synthase kinase 3β

HB, hepatoblastoma

HBV, hepatitis B virus

HCC, hepatocellular carcinoma

HCV, hepatitis C virus

HGF, hepatocyte growth factor

Hh, Hedgehog

HIF, hypoxia inducible factor

HSC, hematopoietic stem cell

HXK, hexokinase

i.p., intraperitoneal

ICN, Notch intracellular portion

IDH, isocitrate dehydrogenase

LDH, lactate dehydorgenase

LEF, lymphoid enhancer factor

Leu, leucine

LND, lonidamine

LRP, low-density lipoprotein receptor related protein

LRS, leucyl-tRNA synthetase

LSC, leukemic stem cells

MeAIB, N-methyl,α-methylaminoisobutyric acid

MSC, mesenchymal stem cells

MSO, methionine-L-sulfoximine

mTOR, mammalian target of rapamycin

NAFLD, non-alcoholic fatty liver disease

NASH, non-alcoholic steatohepatitis

NEAA, non-essential amino acids

OD, Oligodendroglioma

OXPHOS, oxidative phosphorylation

PB, peripheral blood

PBS, phosphate buffered saline

PCV, combination of procarbazine, lomustine, and vincristine

PDH, pyruvate dehydrogenase

PDK, pyruvate dehydrogenase kinase

PGM, phosphoglycerate mutase

PHD, HIF prolyl hydroxylase

PHGDH, phosphoglycerate dehydrogenase

PI, propidium iodide

PK-M2, pyruvate kinase

PPT, DL-phosphinothricin

PTEN, phosphatase and tensin homolog

Raptor, regulatory associated protein of TOR)

Rictor, rapamycin-insensitive companion of TOR)

ROS, reactive oxygen species

s.c., subcutaneous

S6K1, S6 kinase

SCO2, cytochrome c oxidase 2

SDH, succinate dehydrogenase

SHBG, sex-hormone-binding globulin

SSA, sulfosalicilic acids

TA, transamination

TACE, transarterial chemoembolization

TBG, thyroxine-binding globulin

TCA, cycle, tricarboxylic acid cycle

TCF, T-cell factor

TERT, telomerase reverse transcriptase

TIGAR, TP53-Induced Glycolysis and Apoptosis Regulator

TK, thymidine kinase

TOP, terminal oligopyrimidine tract

TSC2, tuberous sclerosis complex 2

UCP2, UnCoupling Protein 2

VDAC, voltage-dependent anion channel

α-KG, α-ketoglutarate

αMLT, α-methyl-DL-tryptophan

CHAPTER 1

INTRODUCTION

1.1 Metabolism & Cancer

Alteration in cell metabolism is now considered a hallmark of cancer [1]. Cancer cells must cope with the enhanced energy consumption and the increased synthesis of macromolecules necessary for support uncontrolled cell growth. As a result, the metabolism of tumor tissues differs from that of the normal tissue from which cancer arises [2]. The discover that several oncogene or oncosuppressor or mutations in metabolic enzymes may regulate cancer metabolism [3] boosted the interest on this field and is generating a thriving scientific production. Also, targeting rewired metabolism may provide useful tools for cancer control.

1.1.1 Metabolic alteration in cancer

1.1.1.1 The Warburg effect

It is now assumed that altered glucose metabolism is a common feature of cancer cells. Otto Warburg discovered in early 20s that tumor cells metabolize large amounts of glucose into lactate even in the presence of oxygen [4]. Now, this phenomenon is known as *aerobic glycolysis* or *Warburg effect* (Fig. 1).

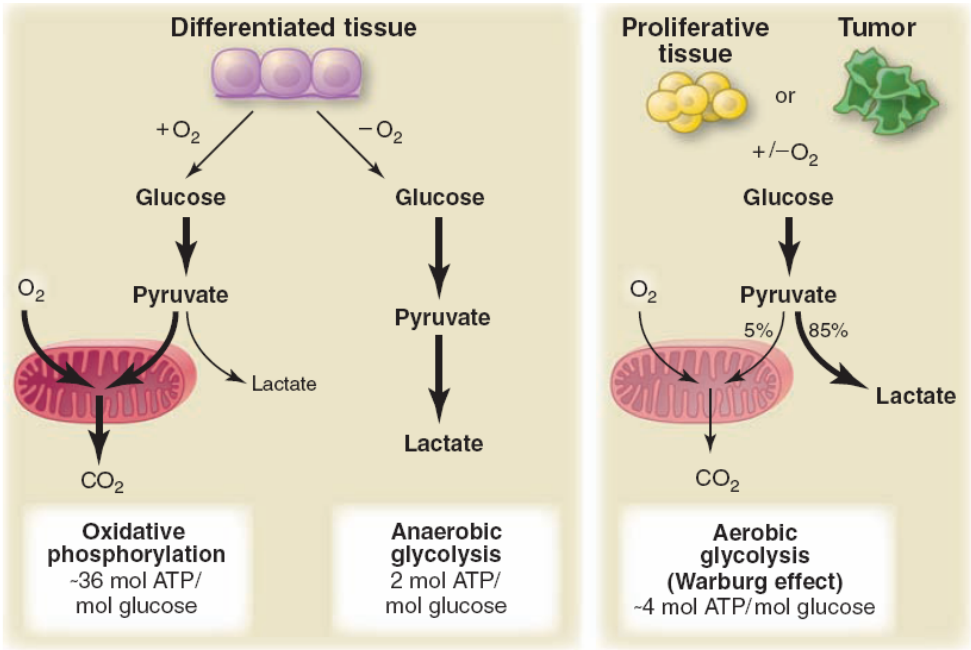

Fig. 1 ***Anaerobic glycolysis and Warburg effect (from [5]).***

Although Warburg's discovery laid the basis of the concept that cancer is also a metabolic disease, this idea was contrasted by other scientists of the same period and overcome by the tumultuous progress in viral carcinogenesis and molecular oncology, leading to the dominant concept of cancer as a genetic disease.

However, tumor cells that metabolize much larger amounts of glucose than normal tissue, also exhibit an extremely increased uptake of this carbon resource. This phenomenon has been translated in clinical practice and positron emission tomography (PET), with the radioactive modified hexokinase substrate ^{18}F-2-deoxyglucose (FDG), is routinely used to diagnose and monitor tumors [6]. This technique relies on the uptake of FDG, which is a transport analogue of glucose, in patient tissues; once FDG has entered in cells, it remains trapped by phosphorylation, and it does not undergo any further modification.

The molecular bases of the aerobic glycolysis are not clear; although it has been proposed that it is a consequence of mitochondrial damage (as Warburg himself thought) or an adaptive response to hypoxia, many tumors do not present any defect in mitochondria, and no consistent correlation between oxygen levels and glycolytic rate has been found yet.

The benefit for cancer cells of aerobic glycolysis is still a matter of debate, but several hypotheses have been proposed over the years. One is that the tumor may take advantage of enhanced lactic acid excretion. In fact, the high amount of extracellular lactate, derived from pyruvate, may lead to the acidification of the tumor microenvironment thus facilitating the disruption of tissue extracellular matrix and, hence, promoting cell invasion [7] and metastasis. This acidification may also support immune evasion; moreover, cell migration is pH dependent and several chemokines and cytokines are degraded faster under acid conditions.

Another fascinating idea is that glucose behaves as an anaplerotic substrate. Anaplerosis is defined as the act of replenish tricarboxylic acid cycle (TCA cycle) of molecules that have been diverted to biosynthesis. Thus, for a cancer cell, a large availability of anaplerotic substrates is a prerequisite to couple, under safe conditions, high proliferative activity (and, hence, high rates of anabolic reactions, such as protein and fatty acid synthesis) with high energetic charge [8].

Moreover, the high glycolytic rate increases the expression of *hexokinase II (*HXK II), which binds to mitochondria preventing mitochondrial dysfunction during cell stress and injury through the interaction with the *voltage-dependent anion channel* (VDAC) [9]. It has been shown that, in case of mithocondrial dysfunction, VDAC can assume a configuration that promotes the release of cytochrome c and, hence, apoptosis. Thus, the high HXK II may constitute an advantage in escaping apoptosis.

Furthermore, an excess of cytosolic ATP production through glycolysis inhibits mitochondrial ATP synthase, induces a chemiosmotic backpressure

and hyperpolarizes the mitochondrial membrane [8], fixing mitochondria in an anti-apoptotic state.

Additional benefits may derivate from the expression of the isoenzyme *pyruvate kinase M2* (PK-M2). This low-activity variant allows the diversion of glycolytic intermediates into subsidiary pathways such as the hexosamine, pentose phosphate, and amino acid biosynthetic pathways, thus supporting cellular biomass increase [10].

It should be noticed that other nutrients than glucose, including amino acids (i.e. glutamine, see below) may also provide energy and carbon moieties for macromolecular synthesis, and that the metabolism of many cancer cells relies on mutations which are often specific for a particular type of tumor.

1.1.1.2 Enzyme mutations and onco-metabolites in cancer

Many oncogenic mutations affecting both proto-oncogenes, tumor suppressor genes or genes for enzymes involved in the intermediate metabolism enhance the rates of utilization of anaplerotic substrates. Some of these mutations cause the accumulation of the so-called “onco-metabolites”; the abnormal levels of these compounds cause both metabolic and non-metabolic derangements and are often associated with the appearance of transformation clues [11].

For instance, p53 is involved in several aspects of cellular metabolism by regulating the levels of a series of genes that affect metabolic pathway rates and the abundance of metabolic products. Wild type p53 limits the glycolytic flux (see Fig. 2) either directly, by repressing the expression of glucose transporter 1 and 4 (GLUT1, GLUT4) [12], or indirectly, through the inhibition of NF-κB [13], the repression of the insulin receptor promoter and the regulation of *phosphoglycerate mutase* (PGM) stability. Moreover, p53 regulates glycolysis though *TP53-Induced Glycolysis and Apoptosis Regulator (*TIGAR), which causes a decline in Fru-2,6-P_2 levels, thus

inhibiting glycolysis and diverting glucose into the pentose phosphate shunt to produce NADPH [13]. Consistently, p53 has been shown to promote oxidative phosphorylation (OXPHOS) through mechanisms that include the transcriptional activation of cytochrome c oxidase 2 (SCO2) synthesis and favouring the use of the TCA cycle for energy production [14]. Furthermore, p53 seems to be involved in the regulation of glutaminolysis (see below) and fatty acids oxidation (FAO), inducing mitochondrial FAO during glucose starvation.

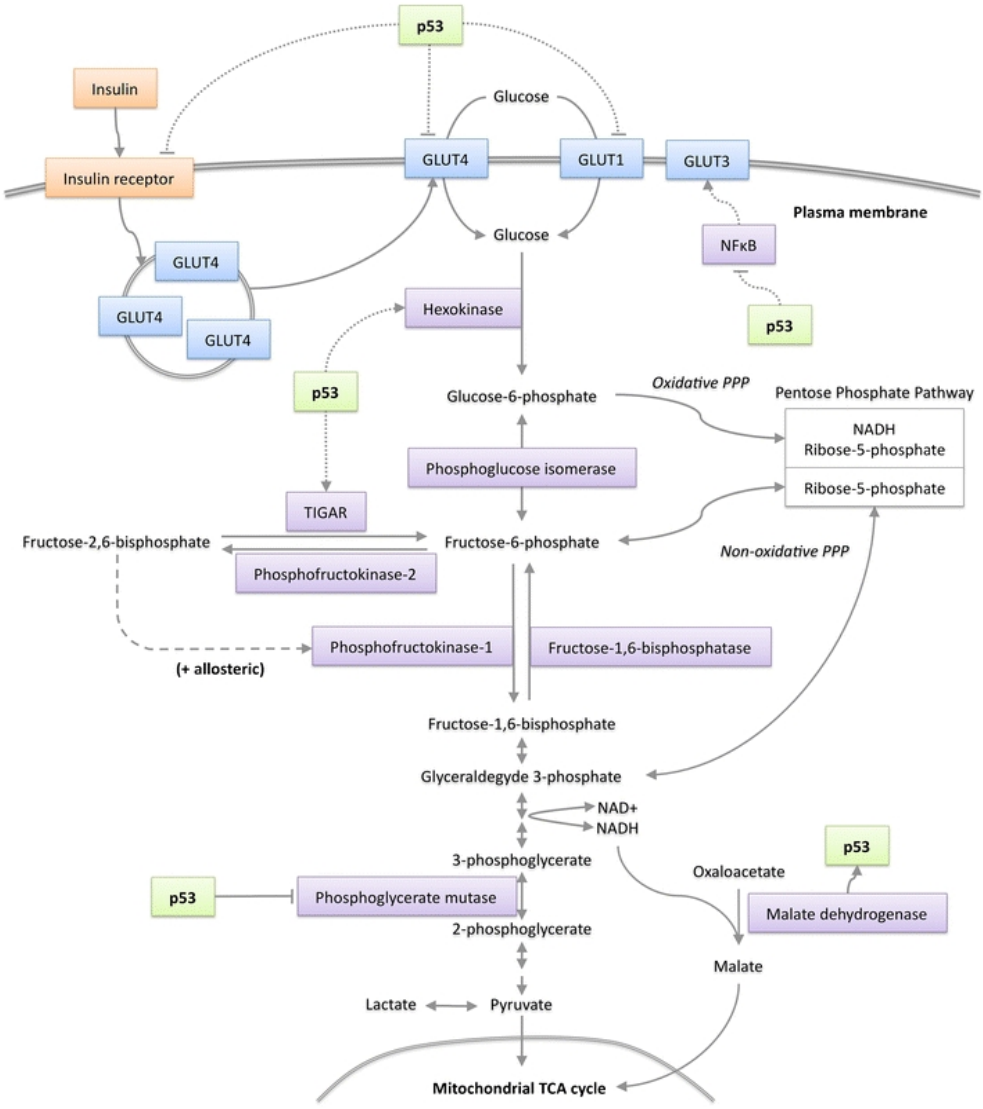

Fig. 2 ***p53 regulates glycolysis (from [14]).***

Loss-of-function germ-line mutations in genes encoding for Krebs cycle enzymes, such as *succinate dehydrogenase* (SDH) and *fumarate hydratase* (FH), promote oncogenesis behaving as oncosuppressor genes in rare forms of enhanced cancer susceptibility.

In particular, mutations of the SDH (subunits B, C and D) characterize familiar paragangliomas and pheochromocytomas, tumors of the parasympathetic and sympathetic nervous system [15]. These were the first tumor cells to be identified with a defined genetic defect of mitochondrial respiration, thus, conforming to Warburg's original hypothesis. SDH oxidizes succinate to fumarate (see Fig. 3), contributing to the generation of ATP by oxidative phosphorylation. Mutations of SDH lead to the accumulation of succinate, resulting in both a serious incapacity in the TCA cycle and a limited capacity to utilize respiration (OXPHOS) for ATP production [16].

Mutations of FH are found in familiar form of multiple cutaneous leiomyomas, benign smooth muscle tumours of the uterus (uterine leiomyomas), and aggressive renal cell carcinomas (HLRCC) of type II papillary or collecting duct morphology [17]. FH catalyses the hydration of fumarate to malate, which is the following step of SDH in TCA cycle (Fig. 3). Also for FH, mutations of its gene generate a not-functioning product leading to the accumulation of fumarate.

The accumulation of these onco-metabolites (succinate and fumarate) causes the inhibition of the HIF *prolyl hydroxylase* (PHD), resulting in the stabilization of the *hypoxia inducible factor* (HIF-1α) [18] and, as a consequence in the increase of expression of GLUT1 and lactate dehydorgenase (LDH) and, hence, of glycolytic rates. Normally, HIF-1α hydroxylation by PDH is oxygen dependent, and it is inhibited under hypoxic conditions by lack of oxygen. PHD, however, is also dependent on α-ketoglutarate (α-KG) levels; in fact, while using molecular oxygen to hydroxylate HIF-1α, PHD catalyses the oxidative decarboxylation of α-KG

to succinate (Fig. 3) [19]. The activation of HIF-1α by product-inhibition of PHD has been termed "*pseudo-hypoxia*", and this process can be reversed *in vitro* by the addition of α-KG [16].

Another onco-metabolite which causes the *pseudo-hypoxia* phenomenon, is the bio-product of *isocitrate dehydrogenase* (IDH1/IDH2) mutated enzymes. Somatic IDH1/IDH2 mutations occur in some astrocytomas (such as oligodendrogliomas), the majority of "secondary" glioblastomas and a certain percentage of acute myeloid leukaemias [8]. These isoenzymes catalyse the oxidative decarboxylation of isocitrate to α-KG, which is, then, available for the further oxidative decarboxylation into succinate operated by PHD (Fig. 3). It is unclear if these enzymes should be classified as oncogenes or tumor suppressors; however, the oncogenic potential of these mutations rely in a new catalytic activity. Mutant IDH, in fact, acquires the ability to convert α-KG into (R)-2-hydroxyglutarate (D-2-HG) [20], an onco-metabolite that can not be further metabolized. Consistently, gliomas with IDH1 mutations show elevated levels of D-2-HG. The production of D-2-HG lowers the availability of α-KG and, hence, causes the inhibition of PHD. However, cells carrying these mutations have also profound changes in glutamine, fatty acid, and citrate synthesis pathways.

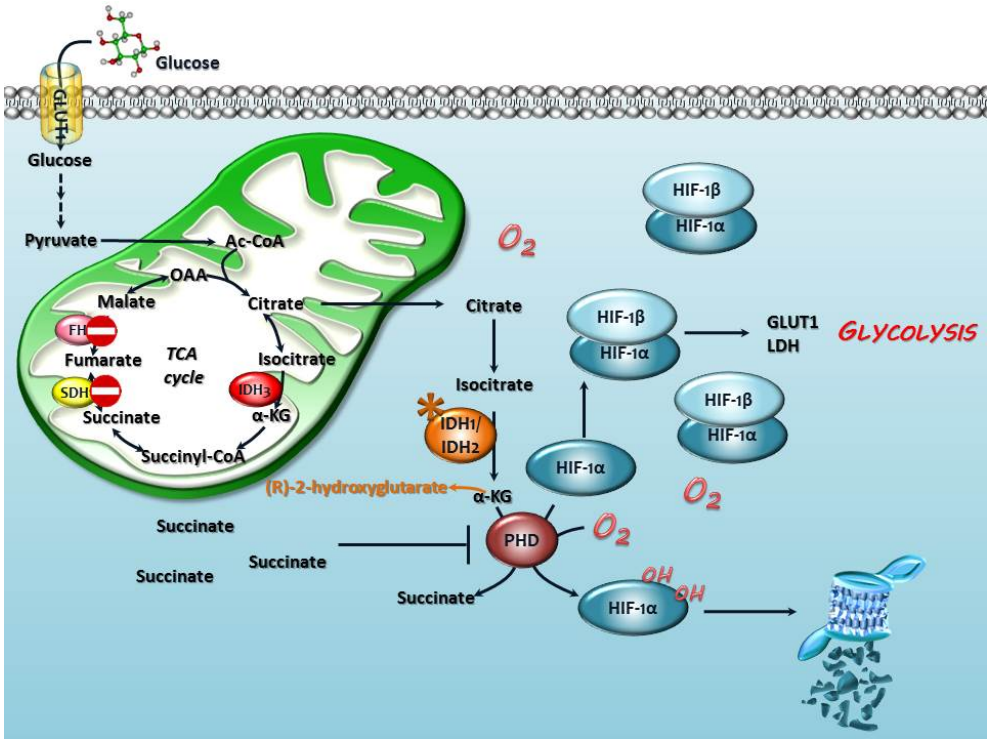

Fig. 3 ***SDH, FH, and IDH mutations enhanced glycolysis.***

Another enzyme frequently mutated in cancer is *phosphoglycerate dehydrogenase* (PHGDH), which is involved in the synthesis of serine and glycine (Fig. 4). These two amino acids are relatively abundant in the human plasma (more than 100 μM); however, some human cancer cells appear to need *de novo* synthesis of these two amino acids [21]. Both serine and glycine are intermediates of several metabolic pathways, which support cell survival and growth. Genomic amplification of the PHGDH gene, on chromosome 1p12, occurs in more than 15% of the human cancers including 40% of melanomas and a limited percentage of breast cancer.

Moreover, PHGDH is not only important for the synthesis of serine and glycine; in fact, it has been demonstrated that cells with high PHGDH activity produce large amount of the anaplerotic substrate α-KG (Fig. 4) through PSAT1 [22].

The list of enzymes, whose mutations are associated with transformation, is likely expected to elongate. Furthermore it has been proposed that in several cancers c-myc controls glutamine metabolism through the induction of *glutaminase 1* (GLS1), as described in 1.1.2 “Glutamine Addiction”: a new concept in cancer metabolism.

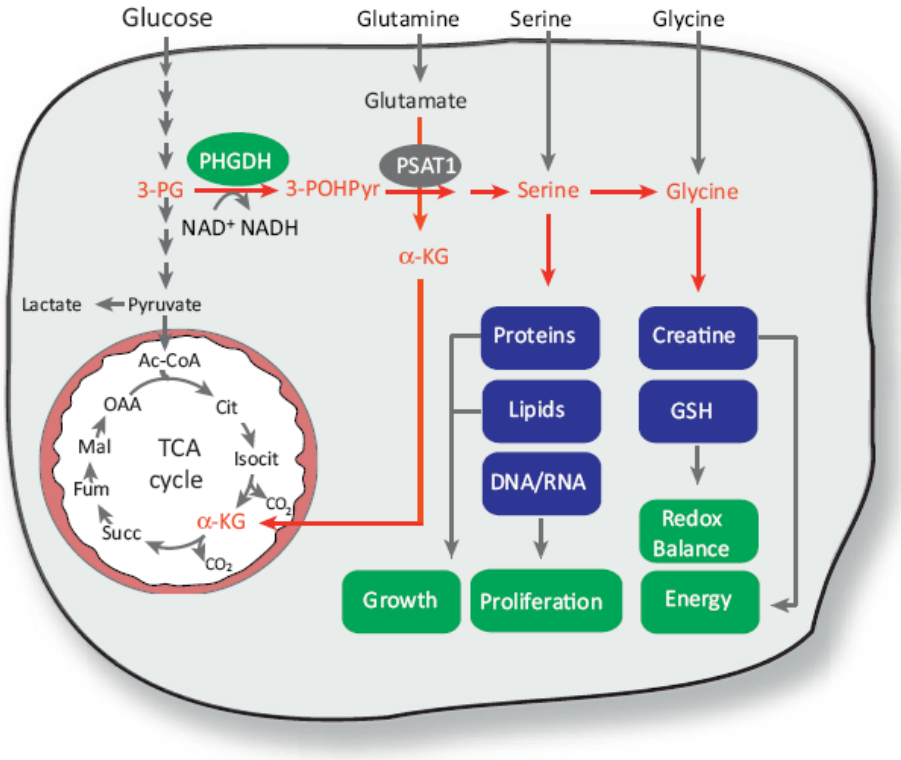

Fig. 4 ***Serine and glycine synthesis through PHGDH (from [3]).***

1.1.1.3 Metabolic alterations as therapeutic targets

The differences between normal and cancer cell metabolism suggest that targeting metabolic dependence could be a useful approach to control cancer. Moreover, deregulated metabolism is also linked to drug resistance.

Glycolysis is the main deranged metabolic pathways in most malignant phenotypes; thus, it is not surprising that the first approaches to target altered metabolism relied on non-metabolizable glucose analogue (see Fig. 5), such as 2-deoxyglucose (2-DG), 3-bromopyruvate (3-BrPA) and lonidamine (LND), which are in pre-clinical or in early-phase clinical trials [23].

HXK phosphorylates 2-DG glucose analogue into 2-DG-phosphate, a compound no more metabolizable. Accumulation of 2-DG inhibits glycolysis and ATP production and causes cell cycle arrest and cell death. No single trials with 2-DG are ongoing, since alone it does not seem to have significant effects on tumor growth; however, it potentiates the effects of radiation or chemotherapeutic agent [24]. 3-BrPA inhibits glycolysis targeting HXK and depleting cell ATP, which is determinant in some cases of drug resistance. For example, in leukaemic cells high ATP levels can activate *ATP-binding cassette* (ABC) transporters, which enhance drug efflux leading, hence, to drug resistance. Therefore, 3-BrPA favours drug retention and, hence, malignant cell death. Also LND, a derivate of indazole-3-carboxylic acid, targets HXK, suppressing glycolysis in cancer cells. Moreover it has been demonstrated that LND improved radiotherapy of brain tumors. Increased glycolysis is directly associated to glucocorticoid resistance, thus inhibition of glycolysis by 2-DG, 3-BrPA or LND increases prednisolone-induced toxicity in some cancer models [23].

Targeting HXK is not the only way to reduce glycolysis. Indeed, since the first limiting step of glycolysis is the availability of glucose itself, inhibitors of glucose transporters (i.e. WZB117 and ritonavir, which inhibits GLUT1 and

GLUT4 respectively) have been also synthesized and are under investigation.

Also the last glycolytic step, the conversion of pyruvate into lactate by LDH, has been tested as a therapeutic target; inhibitors of this enzyme produce an increase in mitochondrial respiration, a decrease of cellular ability to proliferate under hypoxic conditions, and, hence, suppress tumorigenicity [25].

However, it should be noticed that ATP levels negatively regulates glycolysis, thus, paradoxically lowering ATP content may enhance glycolytic flux, stimulating cancer proliferation. Consistently, some cancers express high levels of *UnCoupling Protein 2* (UCP2) to suppress ATP synthesis and favour glycolysis; in these cases the inhibition of UCP2 may yield an approach to reprogram metabolism in cancer cells and to suppress tumor cell growth [8].

Another important tumor suppressor metabolite is dichloroacetate (DCA). DCA inhibits *pyruvate dehydrogenase kinase* (PDK) causing the reactivation of *pyruvate dehydrogenase* (PDH) and, hence, diverting glucose from glycolysis to OXPHOS (see Fig. 5). The preclinical trials with DCA have shown its effectiveness in a variety of tumors via induction of apoptosis [23].

Besides targeting aerobic glycolysis, it is possible also to slower fatty synthesis by inhibiting *fatty acids synthase* (FASN). FASN expression in normal adult tissues is generally very low or undetectable, while it is significantly up-regulated in many types of cancer, where it promotes tumor growth and survival acting as a metabolic oncogene [26]. Several FASN inhibitors have shown antitumor activity including cerulenin, C75, orlistat, C93, GSK 837149A and natural plant-derived polyphenols (Fig. 5).

Also glutamine metabolism has been targeted for metabolic approaches of antitumor therapy as described in 1.1.2 “Glutamine Addiction”: a new concept in cancer metabolism. As a matter of fact, the first antitumor

“metabolic” drug used in clinical practice is L-asparaginase, a bacterial enzyme which hydrolyzes asparagine causing massive cancer cell death in childhood acute lymphoblastic leukaemia (ALL). This topic is extensively discussed below (1.1.3 The first anticancer metabolic drug: L-asparaginase (ASNase)).

Finally, diet may also influence cancer outcome. Ketogenic diet, a low-carbohydrate, high-fat regimen, mimics the effects of glycolysis inhibitors reducing glucose availability, and there are evidences of its antitumor effects on gliomas [27].

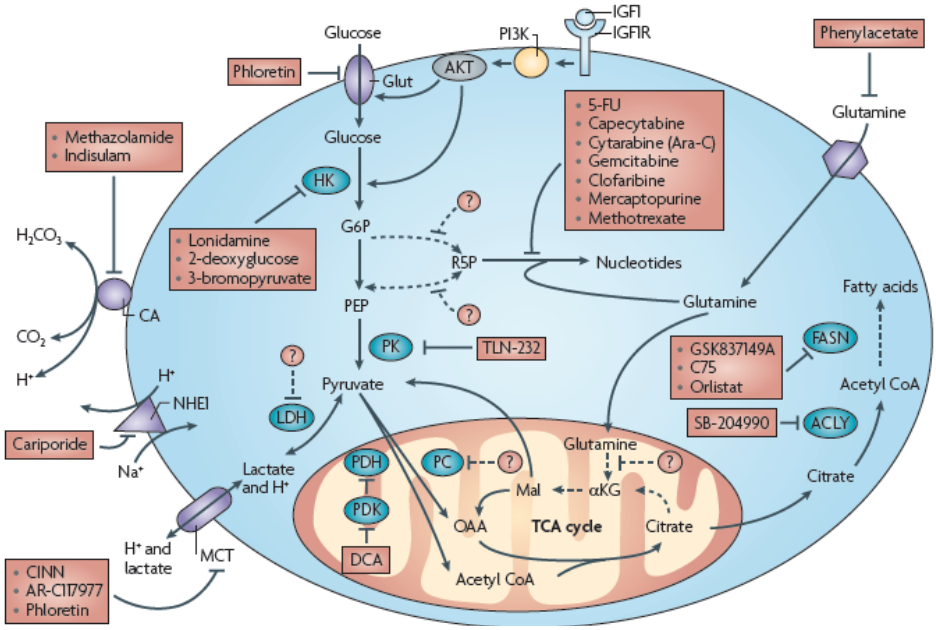

Fig. 5 ***Targeting tumor metabolism (from [28])***

1.1.2 “Glutamine Addiction”: a new concept in cancer metabolism

1.1.2.1 Glutamine is an anaplerotic substrate

Proliferating cells rely on TCA intermediates to synthesize macromolecules, lipids proteins, and nucleic acids. Therefore, TCA role is not only confined in ATP production from oxidizable substrates. Consistently, during cell proliferation, much of the carbon that enters the TCA cycle is used in biosynthetic pathways that consume rather than produce ATP [29]. Thus, a continuous leakage of TCA intermediates occurs, a phenomenon known as cataplerosis. Conversely anaplerosis, as previously described, is the act of replenish TCA intermediates which have been extracted for cataplerotic reaction (biosynthesis). Physiologically the balance between anaplerosis and cataplerosis depends upon the metabolic state and the specific tissue/organ involved. Besides glucose and precursors of propionyl-CoA (such as isoleucine, valine and fatty acids), one of the main anaplerotic substrate is glutamine.

Glutamine is the most abundant amino acids in human plasma (0.5-0.8 mM) and plays an important role in inter-organ nitrogen trafficking from muscle to intestine and liver. Mammals are able to synthesize glutamine in most tissues, but during periods of rapid growth or illness, the cellular demand for glutamine outstrips its supply, and glutamine becomes essential. Hence its designation as a “conditionally” essential amino acid. Proliferating cells display an intense appetite for glutamine, reflecting its incredible versatility as a nutrient and mediator of numerous processes [30].

Glutamine, indeed, is involved in several metabolic processes, which have a major impact on cell growth and proliferation, such as cell volume regulation, the mTOR –dependent control of protein synthesis (see below), and nucleotide synthesis (of both purine and pyrimidines).

As far as purine synthesis is concerned, the γ nitrogens of two glutamine molecules are added to the growing purine ring, and a third is used in the conversion of xanthine monophosphate to guanosine monophosphate. Pyrimidine rings, instead, contain one nitrogen from glutamine amido group and one from aspartate, and an additional amido nitrogen is added to uridine triphosphate to form cytidine triphosphate.

Moreover, glutamine is involved in the synthesis of other non-essential amino acids (i.e. glutamate, asparagine, serine, proline, and alanine) and in the redox balance allowing the synthesis of glutathione (GSH).

GSH is the more abundant intracellular antioxidant and counteracts the oxidative stress. This is crucial for the survival of tumor cells, which have to endure high levels of oxidative stress due to accelerated metabolism and presence of inflammation. GSH is a tripeptide (cysteine-glycine-glutamate) and its production is highly dependent on glutamine. In fact, not only glutamine metabolism produce glutamate, but the glutamate pool is also necessary to get cysteine, the limiting reagent for GSH production. This occurs through the X_c^- antiporter, which exports glutamate and imports cystine. Once taken up, cystine is converted to cysteine inside the cell and used in GSH synthesis.

Moreover, glutamine importance in tumor cell metabolism derives from the characteristics it shares with glucose. Both nutrients help to satisfy two important needs for proliferating tumor cells: bioenergetics (ATP production) and the provision of intermediates for macromolecular synthesis [30]. Actually, through the conversion into glutamate, glutamine carbon skeleton may replenish both TCA cycle intermediates, acting as an anaplerotic substrate, and the intracellular pool of glutamate, since glutamine is an abundant extracellular nutrient and glutamate is not (about 30 μM in plasma of healthy human [31]).

The conversion of glutamine into glutamate is catalyzed by the phosphate-dependent *glutaminase* (GLS), a mitochondrial enzyme highly expressed in

tumors and cancer cell lines. There are two types of GLS in mammals, the kidney-type (GLS1) and the liver-type (GLS2).

GLS1 expression is regulated by the oncogene c-myc, which suppresses the mircroRNA miR-23a/b that down-regulates the expression of this enzyme [32], and correlates with high growth rate and malignancy. Conversely, GLS2 is under p53 control [33] in several tissue, and it seems to function as tumor suppressor; however, its role appears context specific since its enhanced expression contributes to cell survival in some neuroblastomas. Once GLS deamidates glutamine to glutamate, the latter is, in turn, deaminated to α-KG by the *glutamate dehydrogenase* (GDH) or by transamination (TA) to produce other non-essential amino acids (NEAA). Under conditions of glucose shortage, or even under high-glucose conditions in a "glutamine addicted" cancer, GDH overbears transamination, providing glutamine carbon to TCA and, hence, allowing high rates of proliferation. This process, known as glutaminolysis, generates reducing equivalents for the electron transport chain and OXPHOS, supports macromolecular synthesis, and contributes to cellular production of NADPH and lactate (Fig. 6).

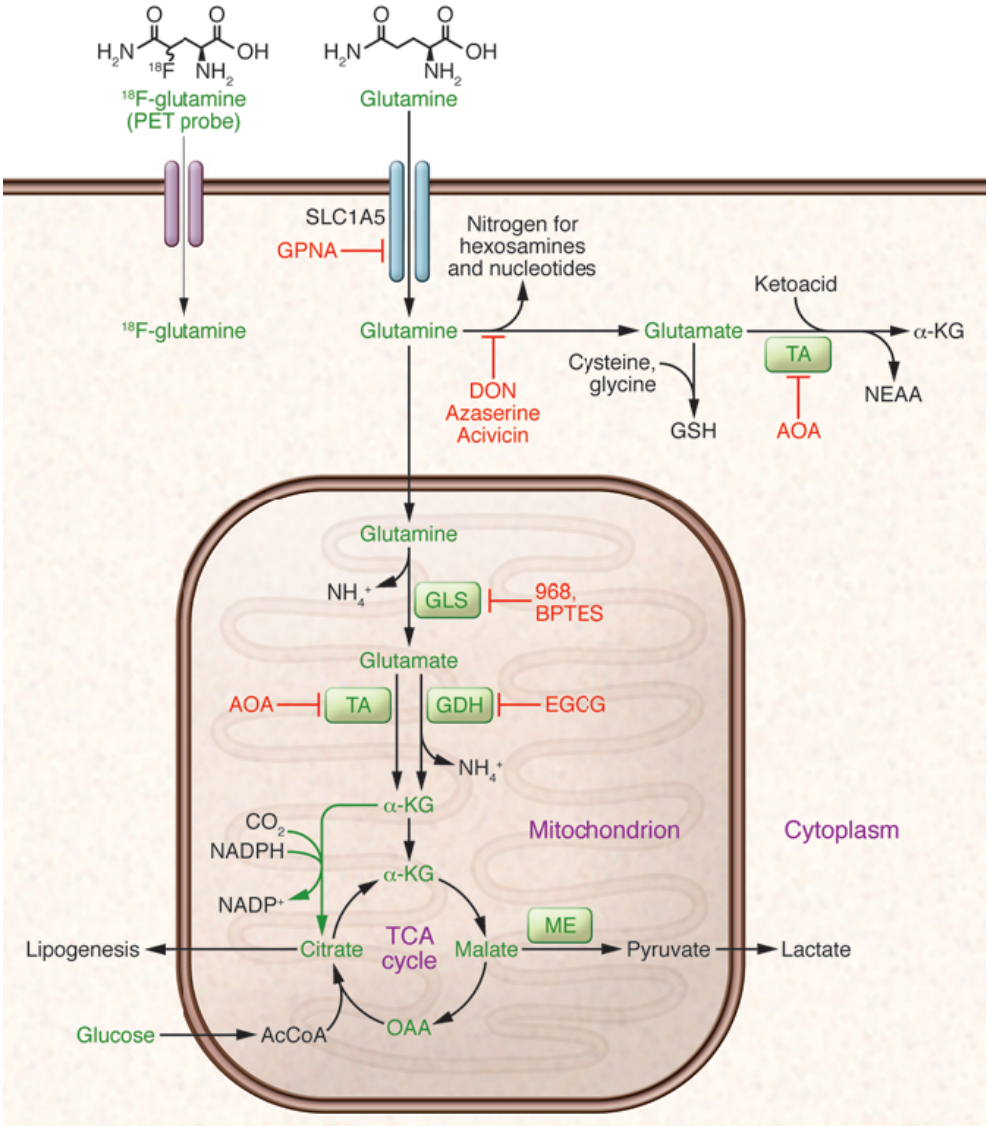

Fig. 6 ***Glutaminolysis (from [34]).***

These evidences are supported by several observations. First, nuclear magnetic resonance (NMR) spectroscopy using ^{13}C-labeled substrates has revealed the use of glutamine as the major anaplerotic precursor in proliferating glioma cells in both rats and humans [35]. Moreover, glutamine

deprivation of fibroblast cultures markedly affected the pool of the TCA cycle intermediates fumarate and malate [36]. Thus, since glutamine metabolism allows cells to maintain a sufficient anaplerotic flux to balance cataplerotic pathways, glutamine shortage may represent a severe nutritional stress that may lead to cell cycle arrest and, eventually, to cell death.

1.1.2.2 Glutamine is involved in mTOR stimulation

The highly conserved serine/threonine kinase *mammalian target of rapamycin* (mTOR) is the master regulator of protein synthesis, cell size and growth by integrating different signals from nutrients (amino acids), growth factors (i.e. insuline-like growth factor), energy status (ATP), and the presence of stress conditions.

mTOR operates through two different complexes mTORC1 and mTORC2, which interact with different partner, Raptor (*regulatory associated protein of TOR*) and Rictor (*rapamycin-insensitive companion of TOR*), respectively.

While mTORC2 controls cell survival by activating AGC kinases and AKT [37], mTORC1 regulates the translational machinery mainly through the activation of *S6 kinase* (S6K1) and the inhibition of *eIF-4E binding protein 1* (4E-BP1) [38].

The activation of S6K1 and the consequent phosphorylation of the 40S ribosomal protein S6 drive the translation of 5' terminal oligopyrimidine tract (TOP) RNAs. By controlling 5' TOP mRNA translation, mTOR upregulates the translational machinery under favourable growth conditions [38]. The phosphorylation of S6K1 is potently inhibited by rapamycin (especially at T389 residue, which is one of the upstream sites in the phosphorylation hierarchy). 4E-BP1 is a translation inhibitor; once phosphorylated, it dissociates from eIF-4E, the translation initiation factor that allows cap-

dependent translation. Also 4E-BP1 is blocked by rapamycin. Both S6K1 and 4E-BP1 phosphorylation are dependant on growth factor availability.

The binding of growth factors to their specific receptors results in the phosphorylation and, hence, the inhibition of *tuberous sclerosis complex 2* (TSC2), which, in complex with TSC1, has GTPase-activating protein (GAP) activity and stimulates the transition of the GTPase Rheb from its active (GTP-bound) to inactive (GDP-bound) state. The activation of Rheb is indispensable for mTOR activation in response of all stimuli [39]. The increasing Rheb-GTP and Rheb-GDP ratio, caused by the inhibition of TSC2 by growth factors, drives mTOR stimulation.

In order to balance anabolic and catabolic processes, single cells and multicellular organisms need to tightly coordinate their usage of energy as well as amino acids. It is not surprising that amino acids availability carefully regulates the phosphorylation of S6K1 and 4E-BP1. However, unlike the growth factor signalling, the precise mechanism by which amino acids powerfully stimulate mTORC1 is not completely understood.

It has been suggested that amino acids regulate the kinase in a TSC-independent way, since amino acid deprivation suppresses mTORC1 signalling even in TSC2-/- cells where mTORC1 is hyper-activated [40]. Consistently, it has been demonstrated that Rag GTPases (RagA, RagB, RagC and RagD) are crucial in transmitting amino acids content. The presence of amino acids favours the transition of the heterodimer RagA/RagB from GDP bound to GTP bound and of the heterodimer RagC/RagD from GTP bound to GDP, and, hence, sustains mTOR activity [41].

It has been proposed that in amino acids plenty cells, the system constituted by the lysosomal v-ATPase and the Regulator complex, is activated through a lysosomal ‘inside-out’ mechanism and promotes the GTP charging of RagA/B, which in turn recruits mTOR to the lysosome surface where it is activated by the lysosome-associated Rheb (see Fig. 7)

[42]. Consistently in amino acids starved cells mTORC1 has a cytoplasmic localization.

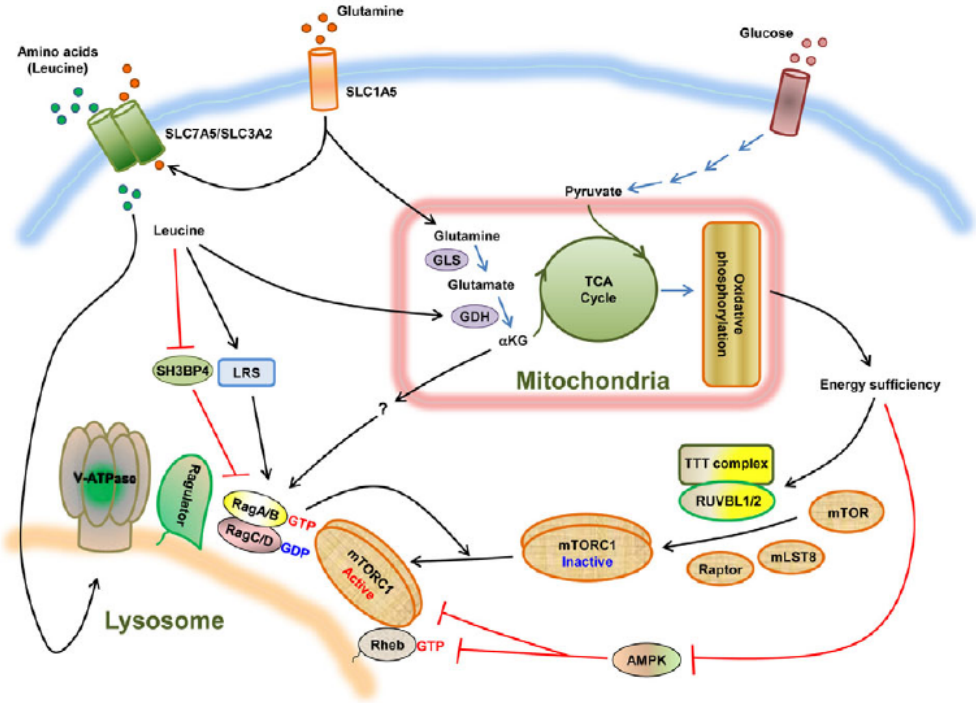

Fig. 7 ***Nutrient signalling to mTOR (from [39]).***

More recently, Sabatini laboratory has identified an octomeric complex, named GATOR, which is a critical regulator of the pathway that signals amino acids sufficiency to mTOR [43]. The GATOR1 sub-complex has GAP activity for RagA and RagB and its loss makes mTORC1 signalling insensitive to amino acid deprivation.

It is known that not all the amino acids are required for mTORC1 activation. In particular, leucine is one of the most powerful activators. It has been suggested that leucine content is sensed by another mechanism, different

from that described above. According to this theory, leucine availability is sensed by the *leucyl-tRNA synthetase* (LRS), which is the enzyme that charges leucine to its tRNA allowing protein synthesis. In mammals, LRS acts as a GAP for RagD, but not RagC, and stimulates the formation of the GDP-bound form of RagD, thereby promoting configuration of the active Rag heterodimer complex [44].

These findings suggest that mTORC1 activation via amino acid sensing may occur at various cellular localizations and by different mechanisms. Thus, it can not be excluded that different amino acids may contribute to mTORC1 activation through different pathways. Glutamine has also been repeatedly involved in mTORC1 stimulation, although its role is more controversial.

Nicklin et al. proposed that glutamine indirectly activates mTOR kinase by promoting leucine uptake through a tertiary active transport [45]. However, it has been demonstrated that glutaminolysis is necessary for GTP loading of RagB and, hence, for the activation of mTOR [46]. According to this theory, glutaminolysis may have a dual role in cancer cells, sustaining the TCA cycle and activating mTORC1, thus maximizing protein synthesis.

On the other hand, mTORC1 is able to promote glutamine-dependent anaplerosis by activating GDH, through the transcriptional repression of the GDH inhibitor *sirtuin 4* [47]. Moreover, the activity of the Na^+-dependent system A transporter (SNAT2), which mediates concentrative glutamine transport, has been linked to mTORC1 regulation [48]. These findings strengthen the links between glutamine and mTOR activation.

1.1.2.3 Targeting glutamine metabolism

Some malignancies rely on glutamine to fulfil TCA cycle, the so-called "glutamine addicted" tumors. Thus, targeting glutaminolysis may provide a useful tool for the control of these cancers.

For instance, it has been demonstrated that Bis-2-[5-phenylacetamido-1,2,4-thiadiazol-2-yl] ethyl sulfide (BPTES), an inhibitor of GLS (Fig. 6), slows the growth of glioblastoma cells with an isocitrate dehydrogenase 1 (IDH1) mutation, a cell model where glutamine use is enhanced [49]. As a consequence of BPTES treatment a decrease in glutamate and α-KG levels and an increase of glycolytic intermediates occur.

GLS may also be inhibited through 968, a compound that targets a specific carboxyl-terminal splice variant form of GLS1 (Fig. 6). 968 blocks the growth of human breast cancer and B lymphoma cells without affecting normal cells [50].

Moreover, three glutamine analogues, acivicin, 6-diazo-5-oxo-L-norleucine (L-DON) and azaserine (see Fig. 6), were demonstrated many years ago to have a significant cytotoxic activity *in vitro* but attempts to translate these effects *in vivo* were hampered by significant multi-organ toxicity [8], such as gastrointestinal alterations, myelosuppression, and neurotoxicity.

Furthermore, it has been demonstrated that glutaminolysis activates mTOR and, indeed, the inhibition of GLS with BPTES or DON prevents mTOR activation [46]. Thus, targeting glutaminolysis or GLS may sensitize cancer cells to common chemotherapeutic agents by reducing mTORC1 activity.

It is also possible to target the flux form glutamate to α-KG. For example, aminooxyacetate (AOA) inhibits aminotransferases and has demonstrated efficacy in breast adenocarcinoma xenografts and neuroblastomas in mice. Moreover epigallocatechin gallate (EGCG), a green tea polyphenol, inhibits GDH, and it has been used to kill glutamine-addicted cancers [34].

Since glutamine is a pleiotropic substrate, useful for several metabolic reactions, including mTOR activation, glutamine deprivation should be more efficient in killing cells than glutaminolysis inhibition.

On the basis of this assumption, it has been recently demonstrated that inhibiting glutamine uptake, via the knockdown of the Na^+-dependent neutral amino acid transporter ASCT2, induces apoptosis and inhibits tumor formation in a acute myeloid leukaemia (AML) xenotransplantation model [51]. Consistently the inhibition of ASCT2 through γ-L-glutamyl-p-nitroanilide (GPNA) limits lung cancer cell growth. Moreover, suppressing glutamine uptake with GPNA stimulates the uptake of 3-BrPA [34].

The antileukemic drug L-asparaginase has the ability to hydrolyze both asparagine and glutamine, causing a severe, although transient, glutamine depletion *in vivo* (see1.1.3 The first anticancer metabolic drug: L-asparaginase (ASNase)). Thus, the use of L-asparaginase is likely to be extended from ALL, where it still represents one of the first line drugs, to other haematological and non-haematological malignancies. It should be noticed that glutamine shortage stabilizes *Glutamine Synthetase* (GS), the enzyme that catalyzes glutamine synthesis from glutamate and ammonium. GS expression, in fact, is regulated in both a transcriptional and post transcriptional way [52, 53] and may cause resistance to glutamine-depleting treatments such as L-asparaginase. However, irreversible inhibitors of GS are available, such as methionine-L-sulfoximine (MSO) or phosphinothricin (PPT). These compounds have an amino acidic structure (Fig. 8) and mimic the phosphorylated intermediate of GS-mediated reaction, thus avidly binding the catalytic site of the enzyme. Furthermore, in asparaginase resistant models MSO powerfully synergizes ASNase cytotoxic effects [54, 55].

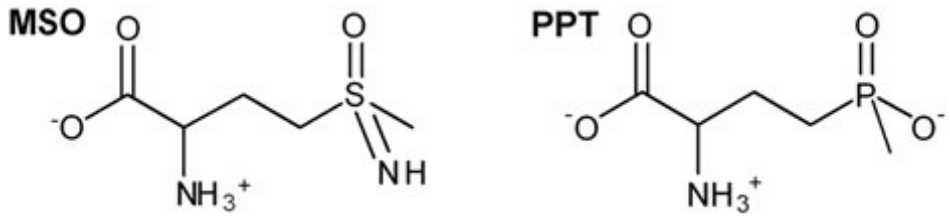

Fig. 8 ***Structures of MSO and PPT***

An alternative agent that deplete plasma glutamine is phenylbutyrate, an FDA-approved drug for the treatment of hyperammonemia in patients with acute liver failure or with congenital urea cycle disorders [56]. In humans, phenylbutyrate spontaneously breaks down to form phenylacetate, which is conjugated with glutamine by an hepatic enzyme into phenylacetylglutamine which is then excreted by urine [56].

1.1.3 The first anticancer metabolic drug: L-asparaginase (ASNase)

1.1.3.1 ASNase mechanism of action

The enzyme L-asparaginase (L-asparagine amidohydrolase, EC: 3.5.1.1, ASNase), has been the cornerstone of acute lymphoblastic leukaemia (ALL) therapy since 1970.

The antineoplastic properties of this enzyme were discovered in 1961 by Broome, who isolated ASNase from guinea pig serum and ascribed to its presence the anti-lymphoma effects of guinea pig serum described some years before [57]. Afterwards, ASNase has been isolated from several types of bacteria, mainly from *Escherichia coli* and *Erwinia chrysanthemi*, notably because of their use in the clinic.

The antileukemic effects of ASNase are related to its ability to catalyze the hydrolysis of asparagine into aspartic acid and ammonium. Asparagine is not essential for normal cells, but it becomes essential for leukemic blasts,

which cannot synthesize asparagine *de novo* [58] due to the low expression of *asparagine synthetase* (ASNS). However, the enzymes used in clinic are also endowed, with lower affinity, with a glutaminolytic activity, given that they hydrolyze glutamine into glutamic acid and ammonium (Fig. 9).

Although it is believed that several side effects of ASNase are attributable to glutamine depletion, it is also demonstrated that deamination of glutamine correlates with enhanced serum asparagine deamination *in vivo* [58], thus enhancing antileukemic effects of the drug.

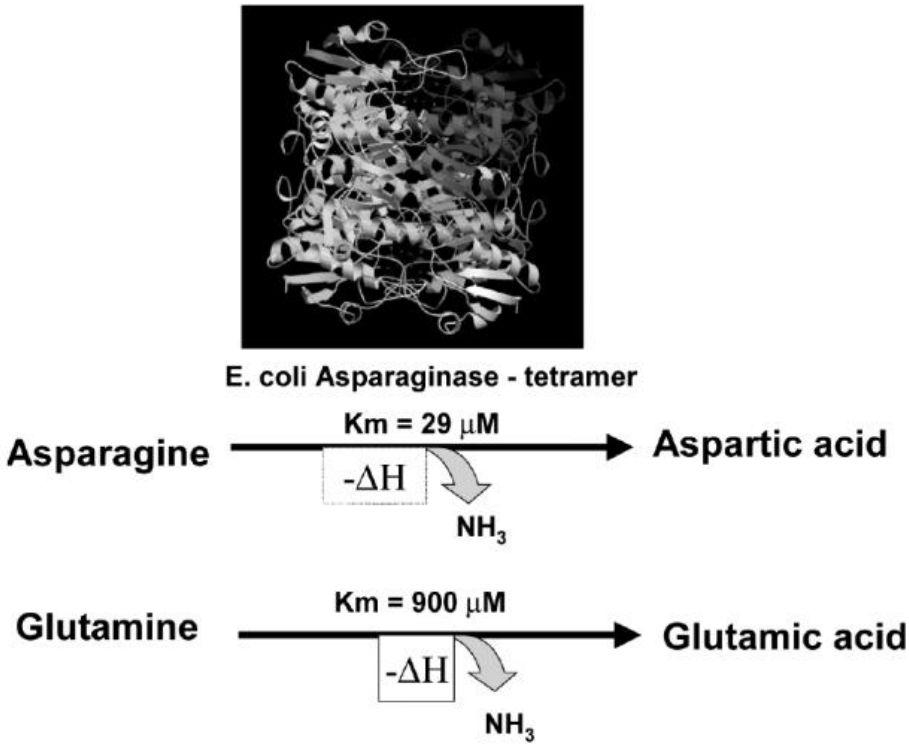

Fig. 9 ***ASNase deaminates both asparagine and glutamine (from [59]).***

Nowadays, three different ASNase preparations are available in clinical practice: the native *E. coli* (Colaspase), the pegylated *E. coli* asparaginase (Pegaspargase), and the native *E. chrysanthemi* (Crisantaspase or Erwinase).

Pegaspargase is the most used product available in the United States [60], because of its efficacy and low rate of allergic reactions. On the other hand, Crisantaspase has a 10-fold higher glutaminase activity than Colaspase, with favourable K_m and faster k_{cat} [61].

ASNases work as tetramers (133-141kDa) with four active sites, each constituted by the N-terminal domain of a given subunit and the C-terminal domain of another subunit [62].

ASNases are administered either by intramuscular or intravenous injections and maintain optimal enzymatic activity at 0.4-0.7 U/ml. In antibody-negative patients, asparagine is depleted from 50 μM to 3 μM or lower, while glutamine from 600 μM to less then 80 μM.

In vivo studies, revealed that the half-life of Crisantaspase and Colaspase are similar [63], while Pegaspargase has an higher stability, allowing reduction in administration frequency (every two weeks instead of every 2-5 days).

After administration, it is known that ASNase is mainly confined in the vascular space, although it has been detected in the pleural fluid and ascites, but not in the cerebrospinal fluid, even when used at high dosage. There are several opinions on ASNase clearance. Since it is not detected in the urine it has been suggested that it is eliminated by the reticuloendothelial system, otherwise it could be clived by proteolytic enzymes (i.e. cathepsin) [63].

Currently, ASNases are only used in the therapy of ALL and, more recently, of nasal-type NK lymphoma. However, there are several attempts to extend ASNase indications to other lymphomas of T-cell lineage and selected subtypes of AML. Moreover, ASNase therapeutic uses could be extended

to non-hematologic malignancies, for example ovarian cancers [64] and, possibly, other solid tumors with low ASNS expression. It has been recently proposed that local ASNase delivery would kill glutamine auxotrophic tumors [65].

1.1.3.2 Mechanism of resistance to ASNase

Considering the bacterial origin and the large molecular weight of ASNase it is not surprising that one of the mechanisms of drug resistance relies on antibody production against the exogenous enzyme.

The production of antibodies causes an accelerated clearance of ASNase that must be by-passed changing the type of enzyme used, commonly from the *E. coli* native product to the non-cross reactive *E. chrysantemi* asparaginase. In fact the immunogenic epitopes of Colaspase and Crisantaspase are different and frequently correspond to the flexible loops on the protein surface [62]. However, it is not uncommon that patients with clinical allergy to *E. coli* ASNase develop antibodies against Erwinase (7-20%).

Another factor that may causes ASNase resistance is the up-regulation of ASNS in the leukemic blast [62]. Transcription of ASNS increases in response to amino acid deprivation, a condition that activates the amino acid response (AAR). The AAR is composed of several transduction pathways that terminate in the induction of genes encoding for proteins involved in metabolic rescue or, if the stress is not relieved, apoptosis. In the absence of asparagine, uncharged tRNA activates *general control non repressed 2* (GCN2), a serine/threonine kinase which phosphorylates *eukaryotic initiation translation factor 2α* (eIF2α). The phosphorylation of eIF2α triggers a pleiotropic response that leads to the attenuation of protein synthesis and to the expression of transcription factors such as ATF4, followed by the increased transcription of *ASNS*.

Under these conditions, ASNase from *E. chrysanthemi* appears endowed with a significant advantage, due to its higher glutaminase moiety. Indeed, the synthesis of asparagine is strictly dependent on glutamine availability, since ASNS converts aspartate into asparagine, using the amido group of glutamine. Hence, glutamine shortage inhibits asparagine synthesis.

A few years ago, Iawamoto *et al.* proposed that resistance to ASNase may depend on a trophic relationship between bone-marrow mesenchymal stem cells (MSC) and leukemic blasts [66]. Confined *niches* in the bone-marrow microenvironment are a crucial place of interaction between MSC and haematopoietic stem cells (HSC), and it has been demonstrated that MSC could support cancer cell growth through several mechanisms [67]. In the work of Iawamoto, it has been demonstrated that MSC have a large amount of ASNS and, hence, can produce asparagine protecting ALL blasts from ASNase treatment *in vitro* (see the model in Fig. 10). Consistently, in the bone-marrow aspirates obtained during ASNase treatment an increase in aspartic acid content occurs [68, 69], probably due to a release of asparagine, which is rapidly cleaved by ASNase.

Moreover, ASNase resistance could be also supported by the release of glutamine: indeed, adipocyte-differentiated 3T3-L1 cells secrete glutamine reducing ALL blast sensitivity to ASNase [70].

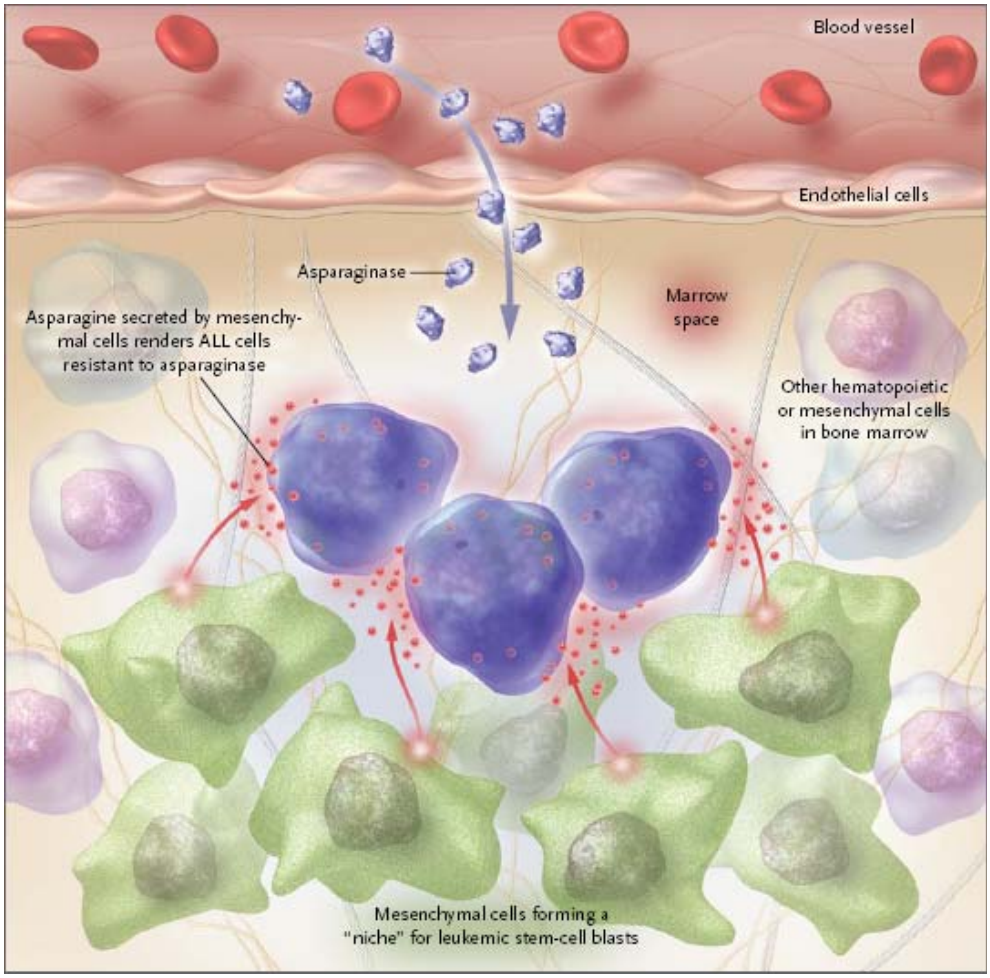

Fig. 10 ***Model of ASNase drug resistance (from [71])***

1.1.3.3 ASNase toxicity

Toxicity of ASNase is mainly related to immunological sensitization, with hypersensitivity reactions against the exogenous protein, and to the adverse event related to inhibition of protein synthesis.

The allergic reactions are the most common toxic effects and are caused by antibodies against ASNase in circulation; they mainly consist of urticarial but symptoms of hypersensitivity may range from localized erythema to

systemic anaphylaxis [63]. Moreover, tissues with high rate of protein synthesis, such as liver and pancreas, are affected by amino acid shortage caused by ASNase.

Liver disorders are common, in particular hepatotoxicity characterized by fatty acid accumulation, increase of transaminase and bilirubin levels and decrease in serum albumin, fibrinogen and lipoprotein levels. Moreover, reduced protein synthesis in the liver causes also endocrine disorders, *thyroxine-binding globulin* (TBG), the major thyroid hormone transport protein, and *sex-hormone-binding globulin* (SHBG), the glycoprotein that binds androgens and estrogens, are transiently, but markedly, decreased upon ASNase administration [72, 73]. However, hepatic functions usually return to normal when drug is cleared or discontinued.

Coagulation dysfunction, with decreasing levels of clotting factors, antithrombin III, plasminogen, and protein C and S [63], are frequently associated with ASNAse treatment. Bleeding or thrombotic complications are therefore reported with some frequency, while neutropenia and thrombocytopenia are rare.

10-16% of patients develop pancreatitis characterized by elevation of serum amylase and lipase, and associated with abdominal and/or back pain, anorexia, nausea and vomiting [74]. Some patients develop signs and symptoms of diabetes due to damage of islet cells, and subsequent decrease in the synthesis of insulin.

Nervous system disorders, like lethargy, somnolence, dizziness, confusion, may also occur. Neurotoxicity may be caused by glutamine deficiency or by increased blood ammonia levels, even if a correlation between ammonia levels and degree of toxicity has not been established [63].

1.2 Targeting glutamine in "glutamine addicted" cancers

As described before (see 1.1.2 "Glutamine Addiction": a new concept in cancer metabolism), glutamine withdrawal may produce a synthetic lethality in those tumors which preferentially use this amino acid to fulfil their anaplerotic demands. Although it has been proposed that c-myc hyperexpression, by enhancing glutaminolysis, is a marker of "glutamine addiction", it is also true that metabolic profiles of tumors depend on the tissue in which cancer arises [75]. Thus, markers of glutamine dependence are still unknown. GS, encoded by the gene *GLUL*, is the only enzyme able to catalyse glutamine synthesis and has been considered a factor of glutamine-depletion resistance. GS is not expressed ubiquitously, but it is abundant in skeletal muscle, perivenous hepatocytes, astroglial cells and other organs.

1.2.1 GS-positive HepatoCellular Carcinoma (HCC)

1.2.1.1 Epidemiology of HCC

Hepatocellular carcinoma (HCC) is the most common type of malignant liver tumor and the third leading cause of cancer death worldwide [76]. HCC is the fifth most common cancer in man and the seventh in woman, and most of the burden (85%) is in developing countries, especially in those regions where infection of hepatitis B virus (HBV) is endemic (South Asia, Sub-Saharan Africa). However the incidence is steadily rising across most of the developed world due to the use of alcohol, the rise of obesity, infection of hepatitis C virus (HCV), and increasing age. HCC rarely occurs before the age of 40 years with an overall sex ratio man : female of 2.4 [77]. Many aetiological factors of HCC are well known: HBV or HCV infection, aflatoxin exposure, alcohol abuse, obesity. The distribution of these risk

factors among patients with HCC is highly variable, depending on the geographic region and the ethnic group. These agents promote chronic hepatitis and cirrhosis, favouring the formation of dysplastic nodules, defined as pre-neoplastic lesions. More rarely, HCC occurs in a healthy liver, and it is often due to a malignant transformation of a hepatocellular adenoma [78].

HBV and HCV infection are presents in 70-80% of the causes of HCC. HBV is a small enveloped DNA virus, member of the *Hepdanaviridae* family, and integrates its DNA into the host genome [79]. Although the mechanisms underlying transformation may be complex, it is known that viral DNA integration disrupts the functioning of several genes favoring transformation. HBV is the leading risk factor for HCC globally and is thought to account for at least 50% of the cases of HCC. On the other hand, HCV infection incidence depends on geographical region and it is found in 70-80% of HCC patients in Japan, 40-50% in Italy and Spain, about 20% in the United States [80]. HCV is an RNA virus, member of *Flaviviridae* virus, unable to integrate into the host genome. It is thought that HCV increases the risk of HCC by promoting inflammation and fibrosis of the infected liver that, eventually, results in liver cirrhosis.

Aflatoxins are food-borne secondary fungal metabolites that are hepatotoxic, hepatocarcinogenic, and mutagenic. Aflatoxins are produced mainly by *Aspergillus flavus* and *A. parasiticus*, which commonly contaminate foods such as peanuts, grain, legumes, and corn [81].

The most potent carcinogen among aflatoxins is the aflatoxin B1 (AFB1). AFB1 is metabolized by cytochrome P_{450} into a reactive epoxide, able to form a covalent bond with guanine. The resulting adducts can promote cellular and macromolecular damage, including the GC → TA transversion mutation at the third position of codon 249 of the p53 gene [82].

The risk of HCC significantly increases with an exposure of > 80 g ethanol per day, and was elevated 54-fold in the presence of both viral infection

and alcohol exposure. However, no molecular evidence of alcohol-induced carcinogenesis has been already defined. Alcohol *per se* is not cytotoxic, but its metabolism is a powerful source of cell damage. Ethanol, indeed, is metabolized by alcohol dehydrogenase, catalase and cytochrome P_{450}2E1 (CYP2E1). All these reactions lead to the highly reactive, protein synthesis inhibitor acetaldehyde; additionally, CYP2E1 reaction leads to the formation of reactive oxygen species (ROS) and, hence, to DNA, protein and membrane damage [83].

More recently, it has been proposed that another cause of HCC is obesity. Fatty enriched, hyper-caloric diets can alter hepatic metabolism and promote inflammation leading to non-alcoholic fatty liver disease (NAFLD) or, even worse, to the more severe non-alcoholic steatohepatitis (NASH). NASH is characterized by prominent steatosis and inflammation, and enhances HCC incidence [84].

1.2.1.2 Therapy of HCC

The poor prognosis of HCC is often due to late diagnosis. Thus, screening and surveillance are highly important for the early detection of HCC especially in patients considered to be at high risk (i.e. patients with cirrhosis or HBV infection). This screening is based on ultrasounds and α-fetoprotein (AFP) dosage.

The treatment of HCC is particularly challenging because of patient-associated variables and the high resistance to classical chemotherapeutics, such as cisplatin and doxorubicin, to hormone therapy, or to immunotherapy. Currently, HCC therapeutic approaches are based on liver transplant, surgical resection, embolization, thermal ablation, and biological therapies.

Liver transplant is considered the most effective method to treat both cancer and liver disease, from which cancer arise. Patients receiving a transplant have a 4-year overall survival of 75% and only an 8% risk of

recurrence [85]. However the limited availability of donor reduces the efficacy of this approach.

Surgical resection remains the golden standard for patients with early-stage HCC, whose hepatic functions have not yet been impaired. However, the recurrence rate after resection is approximately 50% at 2 years and 75% at 5 years [86].

Transarterial chemoembolization (TACE) involves the intra-arterial injection of a cytotoxic agent (doxorubicin, cisplatin, or mitomycin), with or without lipiodol, plus an embolic agent into the hepatic artery that supplies the tumor. This technique is used in patients who can not undergo surgery for the extent or the distribution of the neoplasia. However, the efficacy of this approach is limited, with a long-term outcome of only 30% overall survival [87]. Conventional TACE has been improved by developing a new drug delivery system: the doxorubicin-eluting beads (DEBs). DEBs are preformed deformable microspheres loaded with up to 150 mg of doxorubicin. Encouraging results, with 1-year and 3-year survival rates of 89.9% and 66.3% respectively, have been reported [86].

One of the most used approaches is thermal ablation (radio-frequency, microwaves, laser-induced interstitial thermotherapy, high-intensity focused ultrasound, cryoablation). Another kind of ablation used is the chemical ablation with ethanol or acetic acid. These methods cause necrosis inside and around the tumor. In general they are preferentially used in the presence of small lesions (< 3 cm), since the long-term efficacy of these techniques drops with increasing size and numbers of lesions [88].

Recently, it has been approved a biological therapy for HCC based on a multikinase inhibitor, sorafenib. This drug inhibits tyrosine-kinase receptor (VEGF-R2 and PDGF-R-β) and several intracellular serine/threonine-kinases involved in cell proliferation and angiogenesis. Although sorafenib represents the major advancement in the management of unresectable advanced-stage HCC, the clinical benefit appears to be modest and short-

lived, even in patients with preserved liver function. In addition, there is currently no reliable predictive biomarker for indicating susceptibility to treatment [87].

1.2.1.3 Carcinogenesis of HCC

It is known that HCC carcinogenesis is a multi-step process. After liver injury a continuous cycle of destructive–regenerative process begins and promotes chronic liver disease. This condition fosters liver cirrhosis culminating in malignant transformation (Fig. 11).

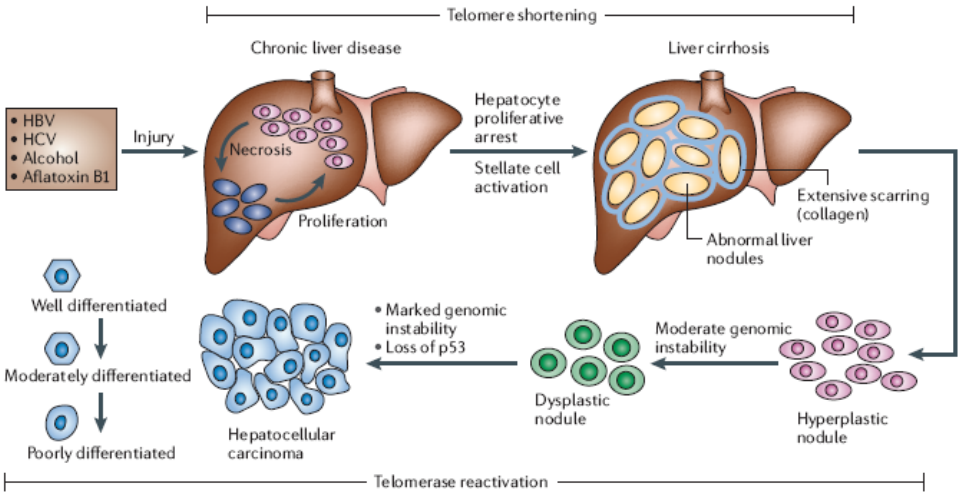

Fig. 11 ***Histopathological progression of HCC, from [89].***

During this process, genetic and epigenetic alterations occur and result in the altered expression of cancer-related genes such as oncogenes and tumour-suppressor genes (Fig. 12) including TP53, Rb and p16, PTEN, c-MYC, β-catenin, ErbB receptor family members, MET and its ligand *hepatocyte growth factor* (HGF), E-cadherin and *cyclooxygenase 2* (COX2).

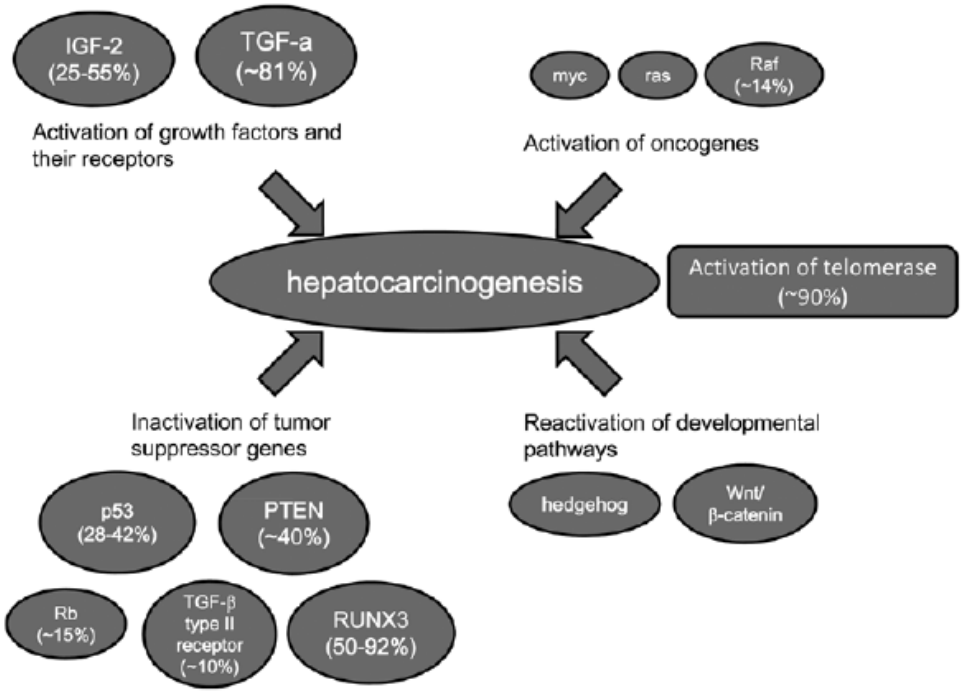

Fig. 12 ***Gene alteration in HCC, from [90].***

p53 arrests cell cycle after DNA damage, promotes DNA repair, and triggers apoptosis. It is the most extensively studied gene in solid tumors and its mutations are present in at least 30% of HCC. It seems plausible that p53 mutations might operate in either early or late stages of HCC development, depending on the context [89].

The retinoblastoma (Rb) gene negatively regulates cell cycle through the binding of the transcription factor E2F. The p16 gene, also known as cyclin-dependent kinase inhibitor 2A gene, is the regulator of the Rb pathway. Inactivation of either Rb or p16 is frequently found in HCC (81%) [90].

Phosphatase and tensin homolog (PTEN) is involved in cell survival regulating the phosphoinositide-3-kinase/Akt signalling pathway. At least

40% of HCC poorly express PTEN, a phenomenon attributable to the increased expression of miR-21 [91].

Myc is a potent proto-oncogene which codes for a protein involved in mediating the cellular response to growth factors. It has been reported a correlation between myc expression and HCC tumor size [92].

The ErbB family of receptor tyrosine kinases consists of four members (ERBB1–ERBB4), which have been implicated in the development of various types of human cancers. ERBB1, known as *epidermal growth factor receptor* (EGFR), and ERBB2 have been found over-expressed in 68% and 84% of HCC cases, respectively and correlated with a more aggressive phenotype, such as a high proliferation index, intrahepatic metastasis, de-differentiation and large tumour size [89].

Aberrant DNA methylation patterns have been reported in human HCC; moreover specific hypermethylation events targets p16, E-cadherin, and COX2. In fact, HCC cells treated with de-methylating agents increases p16 and COX2 expression, and this increase is associated with the inhibition of cell proliferation.

Re-activation of developmental pathways, such as the Wnt/β-catenin signal (see below), Notch (see below) and Hedgehog (Hh), often occurs in HCC.

Hh pathway is an evolutionarily conserved signaling mechanism that controls many aspects of cell differentiation and the development of tissues and organs during embryogenesis, promoting cell growth and inhibiting apoptosis. Significant hyper activation of Hh signaling has been observed in liver injury and cirrhosis and plays an important role in the progression of HCC, where an increase of Hh related molecules has been reported [93].

Lastly, the re-activation of telomerase, correlating with increased *telomerase reverse transcriptase* (TERT) mRNA levels, arises in nearly 90% of human HCC. Telomerase re-activation may promote HCC progression and recurrence after resection [94].

1.2.1.3.1 Wnt/β-catenin hyper-activation in HCC

Since its discovery in 1982, the Wnt pathways have been associated with cell proliferation and cancer, as they trigger G1 phase progression through Cyclin D1 expression and c-Myc transcriptional inductions [95]. In 1998, the link between Wnt signaling and the liver was initially established through the demonstration that β-catenin activating mutations occur in 20 to 40% of HCC. Moreover, β-catenin mutations characterize at least 70% of hepatoblastomas (HB), the most frequent malignant paediatric liver tumor. Thus, β-catenin is the most frequently altered oncogene in liver cancers.

Wnt signalling has a prominent role in stem cell biology, including self-renewal, pluripotency, and differentiation of both embryonic and adult stem cells. Moreover, it is crucial for the development of liver by regulating hepatoblast proliferation, survival and differentiation. In adult liver β-catenin is mainly a cytoskeletal protein, localized mostly at the hepatocyte membrane, which connects E-cadherin with F-actin.

In the absence of Wnt ligand, free β-catenin is rapidly bound in a complex with Axin, *adenomatous polyposis coli* (APC), *casein kinase 1* (CK1) and *glycogen synthase kinase 3β* (GSK3β), which collectively constitute the destruction complex. β-catenin is phosphorylated by CK1 and GSK-3β at specific serine/threonine residues located at the N-terminal region of the protein, a reaction facilitated by the scaffolding proteins Axin and APC [96]. Once phosphorylated β-catenin is ubiquitinated and eventually destroyed by the proteasome (Fig 13).

The binding of Wnt lingands with the seven-pass transmembrane Frizzled (Fz) receptors on the surface of cells induces the association with the low-density *lipoprotein receptor related protein* (LRP) 5/6. This co-receptor complex triggers activation of the canonical Wnt pathway. *Dishevelled* (Dvl) is recruited to the Fz receptor and the Fz/Dvl complex, in turn, relocates Axin to LRP5/6. Then, Axin-bound GSK-3β and CK1 phosphorylate LRP5/6, leading to the inactivation of GSK-3β.

The hypophosphorylated form of β-catenin is more stable and it is accumulated in the cytoplasm. Although β-catenin lacks a nuclear localization sequence, it then translocates to the nucleus through an unknown mechanism which may involve an interaction with both components of the nuclear pore complex and lymphoid enhancer factor or T-cell factor (LEF/TCF), its nuclear binding partners. Once in the nucleus, β-catenin binds to LEF/TCF (Fig 13), displacing the transcriptional inhibitor Groucho, and, in complex with TCF, initiates transcription of target genes [97], such as c-Myc, Cyclin D1, VEGF, and GS.

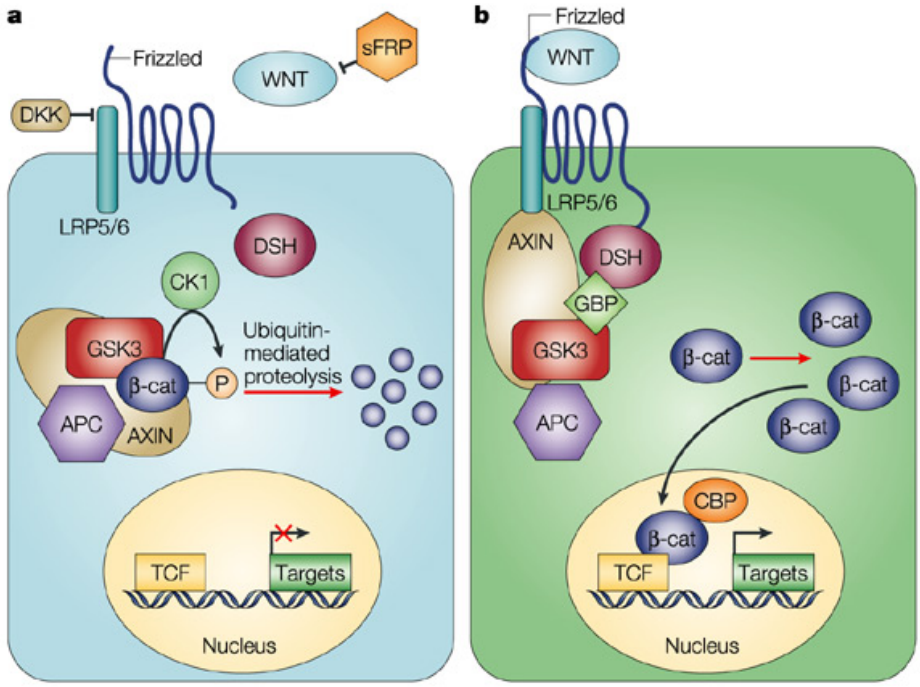

Fig 13 ***Wnt pathways off state (a) and on state (b), from [98].***

In normal adult liver, this pathway is important for imparting zonation [99]. In fact, pericentral (PC) hepatocytes express cytoplasmic and nuclear β-catenin in addition to membranous localization (Fig. 14). Here, β-catenin regulates the expression of genes that encode for enzymes critical in ammonia and xenobiotic metabolism (GS, glutamate transporter-1 (Glt1), and cytochrome P_{450} family members). Conversely, the hepatocytes in the periportal (PV) zone show higher APC protein expression and, as a consequence, less dephosphorylated β-catenin.

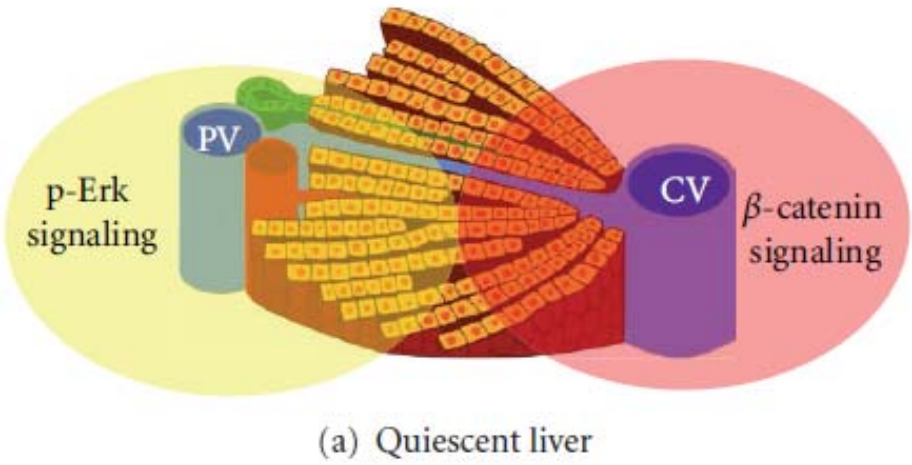

Fig. 14 ***Liver zonation.*** *PV = portal vein, CV = central vein, from [95].*

Moreover β-catenin is essential for maintaining adherens junctions through the E-cadherin binding. This binding is controlled by the phosphorylation of β-catenin at a specific tyrosine residue (Y654). The disruption of adherens junctions causes an impairment in the apical trafficking of specific proteins and results in many morphogenetic processes that contribute to motility and metastasis in the presence of aberrant growth [100].

Another important function of β-catenin is the contribution to liver regeneration. Adult liver, in fact, has the unique capacity to regenerate after insult and loss of most of its mass. During liver regeneration, i.e. after partial hepatectomy, β-catenin accumulates and translocates into the nucleus. This mechanism is due to a decrease in serine phosphorylation and a subsequent decrease in protein degradation, and not a result of changes in gene expression [97]. As a consequence, an increase in cyclin-D1 and c-myc expression is observed after partial hepatectomy, confirming the positive impact on cellular proliferation of β-catenin. Furthermore β-catenin is also one of the downstream effectors of hepatocyte growth factor, which itself is a significant player in the process of liver regeneration [101].

Considering the importance of Wnt/β-catenin in the liver homeostasis, it is not surprising that the hyper-activation of this pathway contributes to the development of a malignant phenotype, although it is not sufficient for initiation and progression of HCC.

The dys-regulation of this pathway may be caused by mutation (i.e. point mutation or deletion) affecting the exon 3 of *CTNNB1*, the gene encoding for β-catenin itself (about 12-26% of HCC) or the *AXIN1* and *AXIN2* genes (8-13%) [102]. In both cases, the affinity of β-catenin for the degradation complex is lowered, and β-catenin results hypophosphorylated, accumulates in the cytoplasm and, hence, in the nucleus. The activation of this pathway leads to the increased expression of a number of target genes among which a preeminent position is held by *GLUL*, the gene encoding for GS.

The relationship between β-catenin activation and *GLUL* expression is so strong that GS positivity in immunocytochemistry is considered a *bona fide* indicator for β-catenin pathway activation in human HCC [103].

1.2.1.3.2 Notch signalling in HCC

The Notch signalling is a highly conserved system and plays an important role in stem cell self-renewal and differentiation.

This pathway is constituted of four different notch receptors (Notch1, Notch2, Notch3, and Notch4). Each receptor is a single-pass transmembrane protein, with a large extracellular portion and a small intracellular region. Maturation of Notch receptor consists in the synthesis as a single transmembrane polypeptide and in post-translational rearrangements. These modifications, such as glycosylation and cleavage, occur during translocation to the cell surface through the trans-Golgi system (see Fig. 15).

Neighboring cells send signals through five ligands, belonging to two different groups. The first group includes Jagged1–2, the second group Delta-like -1, -3 and -4 (DLL-1, -3, -4) [104]. The receptor is normally triggered via direct cell-to-cell contact, in which the transmembrane proteins of the cells in direct contact form the complex between ligands and Notch receptors. Ligand binding promotes a conformational change which allows two proteolytic processing events mediated by an ADAM/TACE metalloprotease acting outside the cell, and the γ-Secretase, which operates at the cytoplasmic side [105]. As a result of proteolysis, the Notch intracellular portion (ICN) is released and is able to translocate into the nucleus. Once in the nucleus, ICN displaces the transcriptional repressor complex CSL and recruits co-activators, such as PCAF, GCN5, p300, and MAML1, thereby activating the transcription of several downstream target genes. Among direct or indirect Notch effectors, several are involved in proliferation, including c-myc, p21, p27, Cyclin D1 [104] (Fig. 15).

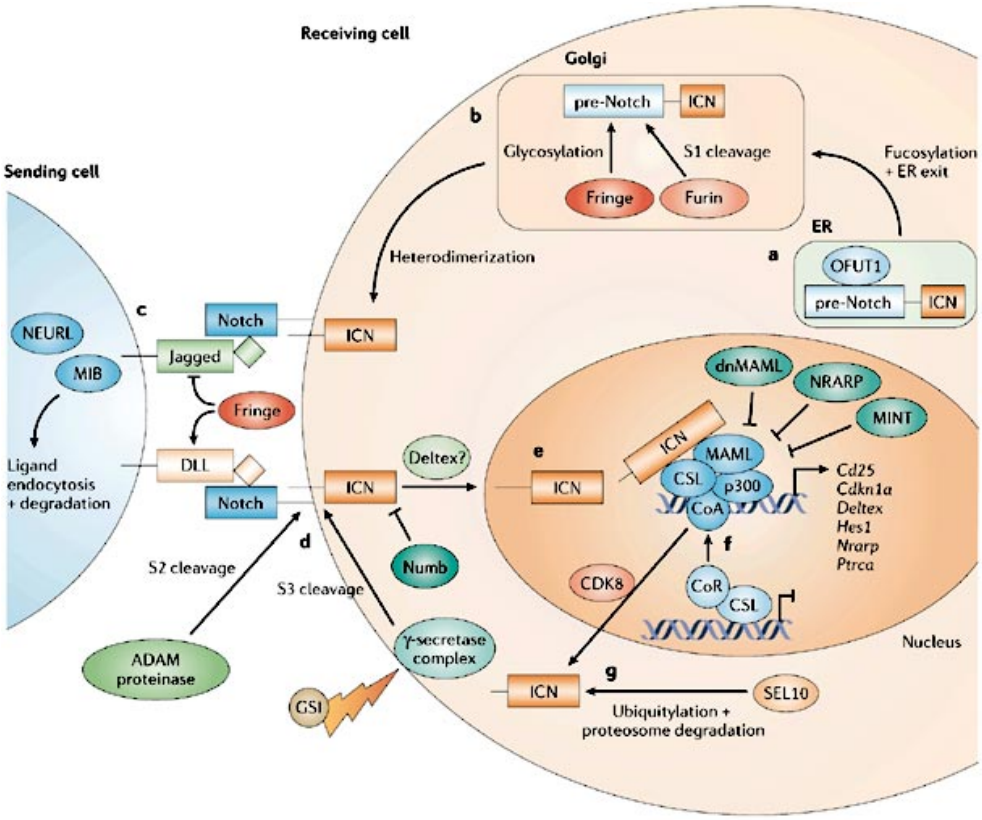

Fig. 15 ***Notch pathway, from [106].***

Notch activation has been described in different kinds of cancer (i.e. leukaemia or solid tumor as prostate and breast cancer [107, 108]), although in other case it has been considered as tumor suppressor [109]. In fact, other signalling pathways influence whether Notch functions as a tumor suppressor or oncogene in a particular tissue.

In the liver, Notch acts in a temporal- and dose-dependent manner to coordinate biliary fate and morphogenesis [110]. It has been proposed that Notch1 over-expression inhibits HCC progression by promoting cell cycle arrest and apoptosis [111, 112]. Conversely, there are growing evidences of the oncogenic role of Notch activation in hepatocarcinogenesis [113].

Significant over-expression of Notch1 and Notch3 was detected through immunohistochemistry in HCCs [114]. In addition, the depletion of Notch3 by specific shRNAs increased p53 expression and enhanced doxorubicin-sensitivity by promoting apoptosis. Moreover, a recent study found that HBV x protein upregulates key molecules in Notch signaling (Notch1, HES1, and Jagged1) [115].

1.2.2 GS-negative Oligodendroglioma (OD)

Oligodendroglioma (OD) is a low-grade glioma originating from oligodendrocytes or, more likely, from glial precursor cells.

OD is the third most common glioma overall, accounting for 2%–5% of primary brain tumors and 5%–18% of all glial neoplasm. OD generally occurs in adult age, with an average age at diagnosis of 35, while a low percentage (about 6%) arises in children and rarely manifests as fetal tumor [116]. OD arises more frequently in males with an overall sex ratio male : female of 2.

While no definite inheritance pattern or known genetic risk factors have been documented, occasional familial groupings of oligodendroglioma and oligoastrocytoma have been reported [117].

The etiology of this cancer is still unknown since no causative environmental or lifestyle factors have been unequivocally identified [118].

It has been observed that losses of portions of chromosomes 1p and 19q are a characteristic lesion of OD; this 1p/19q co-deletion is mediated by an unbalanced translocation of 19p to 1q: der(1;19) (p10;q10) [119]. About 25% of anaplastic oligodendrogliomas have deletion of the tumor suppressor gene p16 located on the short arm of chromosome 9, while mutation of p53 is more typical for astrocytoma.

Histological criteria for distinguishing OD from astrocytoma remain subjective, with significant inter-observer variability; however it has been

demonstrated that OD is usually histologically GS negative, whereas GS-positivity is a specific marker for astrocytes [120].

Similarly to astrocytoma, OD remains localized to the central nervous system (CNS). Extra-CNS metastases (especially to bone) have been described, but this is a very rare evenience and occurs in the occasional patient only at later stages of the disease.

Therapeutic approaches for OD rely on surgery and chemotherapy.

Surgical resection is the main form of therapy for most patients with an oligodendroglial tumor; however, because of its infiltrative nature, the tumor may frequently be poorly delineated from the normal brain parenchyma, making complete resection impossible [116].

Chemotherapy of OD was improved in 1988, when the efficacy of the combination of procarbazine, lomustine, and vincristine (PCV) was demonstrated [121]. Subsequently the efficacy of PCV treatment has been demonstrated since approximately two-thirds of patients have either a complete response or partial response to PCV. However, the cumulative haematological toxicity and gastrointestinal side effects, associated with standard PCV, often limit the duration of its administration [118].

More recently, an alkylating agent, temozolomide, has shown promise, although at a lower response rate compared to PCV, as an effective chemotherapeutic alternative. Similar to outcome after PCV chemotherapy, response is more frequent and with longer duration in patients with combined 1p/19q loss. Moreover, the better tolerability and the ease of administration of temozolomide as compared to PCV have made temozolomide the drug of choice in most institutions.

Apart from temozolomide and PCV, few agents (i.e. paclitaxel, CPT-11, carboplatin, etoposide plus cisplatin), have been investigated but response rates are low.

Despite the achievement of gross total resection, the recurrence of this disease is extremely common and usually occurs several years following resection and at the surgical site. Malignant transformation of the recurrence to an anaplastic oligoastrocytoma or glioblastoma multiforme may occur, although at lower rates compared with typical astrocytomas [116].

Thus, although the prognosis of OD is better than astrocytomas or other gliomas, the overall prognosis is still guarded. The median postoperative survival period for patients with oligodendrogliomas ranges from 3 to 17 years, and although occasional long-term survivors (up to 40 years) have been reported, almost all patients die for their disease [122].

1.2.3 Mesenchymal stem cells interaction with acute lymphoblastic leukaemia blasts

1.2.3.1 Mesenchymal stem cells (MSC)

Mesenchymal stem cells (MSC) are multipotent stromal cells which have the capability to differentiate into several cell types, such as adipocytes, chondrocytes and osteoblasts (see Fig. 16).

During the past decade, a large amount of publications were focused on MSC, because of their ability to proliferate *ex vivo*, their potential for multilineage differentiation and their immunomodulatory properties [123].

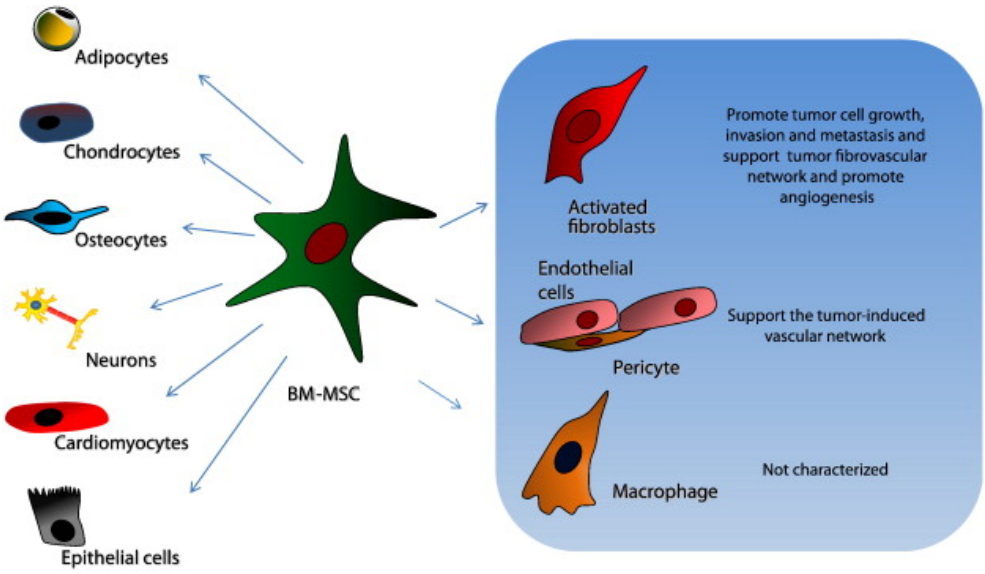

Fig. 16 ***BM-MSC trasndifferentiation ability (from [123]).***

MSC were first isolated from bone-marrow by Friedenstein in 1976 [124]. However, MSC are widely distributed in a variety of adult tissues such as the umbilical cord, Wharton's jelly, adipose tissue, peripheral blood and the lungs, but also in fetal tissues and placenta.

In adult tissues, MSC are either constantly present or their pool is replenished by the migration of bone marrow-derived MSC (BM-MSC) [125]. Thus, bone marrow is the main source of MSC extraction, although an invasive surgical procedure is required for cell recovery, and the percentage of MSC isolated is relatively low (0.001%–0.01%) and inversely correlated with the age of the donor [123]. Despite this limitation, once isolated, MSC are easy to grow *in vitro*, without apparent modification of the phenotype and/ or loss of function. Generally, MSC are cultured at low density (1,500 -3,000 cells/cm^2) to avoid differentiation.

There is still a wide perception in the literature that MSC represent a phenotypically heterogeneous population of cells and no distinctive typical markers are still available.

However, the International Society for Cell Therapy has proposed the following criteria for human BM-MSC characterization:

1. adherence to plastic in standard culture conditions;
2. expression of surface molecules such as CD73, CD90, and CD105 in the absence of CD34, CD45, HLA-DR, CD14 or CD11b, CD79a, or CD19, as assessed by fluorescence-activated cell sorter analysis;
3. capacity to differentiate into osteoblasts, adipocytes, and chondroblasts *in vitro* [126].

MSC morphologically appears with a small cell body endowed with a few processes that are long and thin. The cell body contains a large, round nucleus with a prominent nucleolus (see Fig. 17).

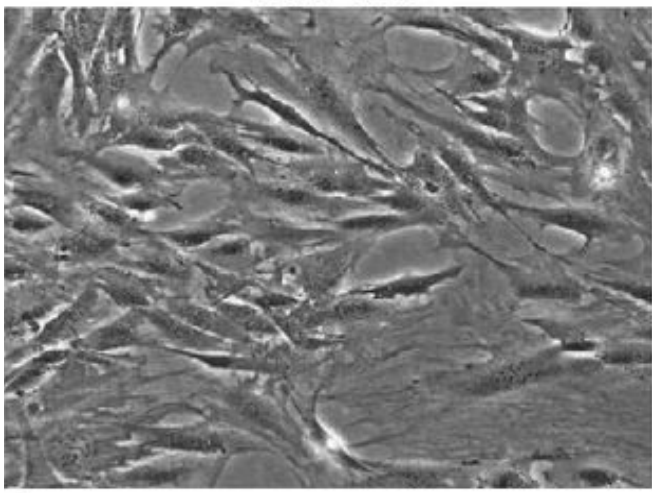

Fig. 17 ***BM-MSC. Magnification 200x (from [127]).***

1.2.3.2 Acute lymphoblastic leukaemia (ALL)

Acute lymphoblastic leukaemia (ALL) is a form of leukaemia that occurs more often in childhood, with an incidence peak at 2-5 years of age.

ALL is generally characterized by gross chromosomal alterations. In B-cell disease, these alterations include high hyperdiploidy of at least five chromosomes (including X, 4, 6, 10, 14, 17, 18, and 21), hypodiploidy with fewer than 44 chromosomes, and recurring translocations [128].

Many of this chromosomal rearrangements disrupt genes that regulate normal haemopoiesis and lymphoid development (i.e., *RUNX1, ETV6*), activate oncogenes (i.e., *MYC*), or constitutively activate tyrosine kinases (i.e., *ABL1*), hence contributing to malignant transformation (Fig. 18).

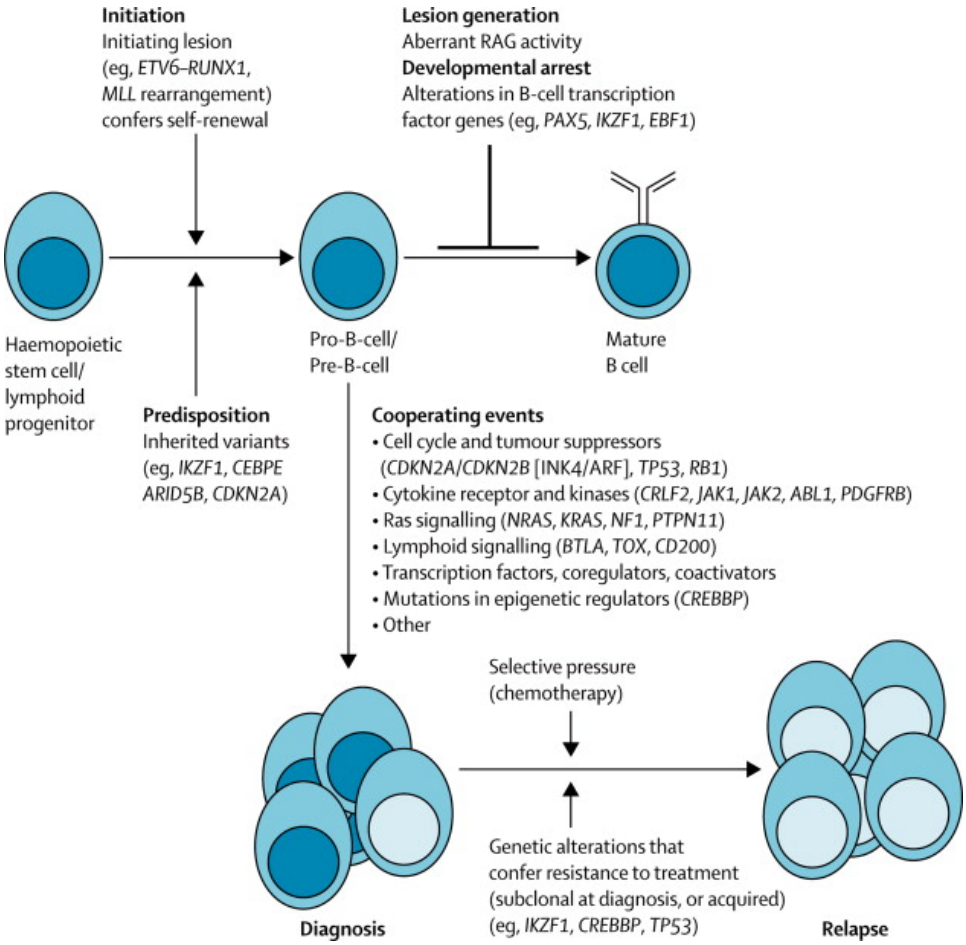

Fig. 18 ***Pathogenesis of B-lymphoblastic leukaemia (from [128])***

The treatment of ALL has been markedly improved during the past 40 years and nowadays the 5-year free disease survival exceeds 90% in the child. Treatment typically spans 2–2.5 years, and comprises 3 phases: induction of remission, intensification (or consolidation), and continuation (or maintenance) [129].

The remission-induction therapy is aimed to eradicate the initial leukemic cell burden and restore normal haemopoiesis. During this phase chemotherapy is based on vincristine and glucocorticoid (prednisolone or dexamethasone) combined with one of the three preparation of ASNase (for details see 1.1.3 The first anticancer metabolic drug: L-asparaginase (ASNase)).

The intensification-therapy is given after the remission-induction treatment, and is aimed to eradicate residual leukemic cells [130]. High-dose methotrexate with mercaptopurine is often given, together with frequent pulses of vincristine and glucocorticoids, uninterrupted asparaginase for 20–30 weeks, and reinduction therapy with drugs similar to those used during remission-induction therapy.

The continuation-therapy typically lasts 2 years or longer and comprises mainly daily mercaptopurine and weekly methotrexate with or without pulses of vincristine and dexamethasone [128].

However, some subsets of acute lymphoblastic leukaemia still have an adverse prognosis.

1.2.3.3 MSC implication in haematological malignancies

In the bone-marrow MSC are crucial for the maintenance of the hematopoietic microenvironment.

One of the roles of MSC is the participation in the formation of the hematopoietic stem cell (HSC) niche. In fact, in the bone marrow there is a structurally unique niche made of MSC–HSC paired populations, tightly regulated by local input from the surrounding microenvironment and by long-distance cues from soluble factors and the autonomic nervous system [131]. MSC generate a number of stromal cells, which have been shown to have an impact on HSC behaviour, including adipocytes, pre-osteoblast, osteoblasts and chondrocytes [132]. This niche is directly involved in self-renewal and differentiation of HSC.

The role of MSC in tumor is not completely ascertained and conflicting opinions have arisen.

On one side, there are evidences confirming that MSC may allow and support tumor growth [123]. For example, it has been recently demonstrated that MSC support the growth of chronic lymphocytic leukemic (CLL) blast. CLL blasts exhibit low expression of X_c^- transporter and, hence, low uptake of cystine. MSC, conversely, are able to transport cystine, which is converted into cysteine and released into the microenvironment for uptake by CLL cells to promote GSH synthesis [67] and, hence, survival of CLL blasts. Furthermore, MSC are known to have an anti-apoptotic effect on acute promyelocytic leukaemia cells and to promote leukemic cell survival. BM-MSC have been shown to play a protective role on leukemic cells isolated from acute myeloid leukaemia (AML) and chronic myeloid leukaemia (CML) patients, contrasting apoptosis induced by FI700 (FLT3 inhibitor) and imatinib, respectively [133]. BM-MSC also induce resistance to apoptosis in ALL cells exposed to ASNase, through the release of asparagine (for details, see 1.1.3 The first anticancer metabolic drug: L-asparaginase (ASNase)) [66].

On the other hand, several studies have shown that BM-MSC can also interact with leukemic stem cells (LSC) and exert an inhibitory effect on K562 cell line proliferation through Wnt-inhibitor Dickkopf-1 (DKK-1) or by inhibiting cell cycle progression. Additionally, BM-MSC can inhibit the proliferation of leukemic cells from patients having CML [133].

It has been proposed that MSC can be friend or foe of cancer cells depending on their origin (BM, adipose tissue, cord blood), differentiation state (STRO-1+CD56+TNAP$^{-/dim}$[21]or total stromal cells), and the type of tumor cells they interact with [134] (i.e. acute or chronic leukaemia).

CHAPTER 2

AIM OF THE THESIS

Considering the importance of Gln in cancer cell metabolism, the aim of my thesis is to evaluate the effects of pharmacologically induced Gln withdrawal on cancer cell viability, so as to assess if and in which tumors this metabolic approach may induce cytotoxicity and, hopefully, cancer control. Since mTOR activity is needed for cell proliferation and is often over-activated in many kinds of cancer, the effect of Gln depletion on the kinase has been also investigated.

To obtain a severe glutamine depletion, I have combined L-asparaginase, targeted to deplete extracellular Gln, with the inhibition of Glutamine Synthetase (GS). This double-hit approach was applied first on β-catenin mutated human hepatocellular carcinoma (HCC) cells, because (1) the liver is rapidly exposed to amino acid variations in blood and (2) a subset of HCC present over-expression of GS, caused by activating mutations of β-catenin. Thus, β-catenin mutations may drive metabolism towards "glutamine addiction" and, hence, that β-catenin-mutated HCC should be more sensitive to Gln depletion.

Moreover, to assess if GS expression plays a role in the cell adaptation to glutamine depletion, I have also extended the same approach to "GS-negative" human oligodendroglioma cell lines and to co-cultures of normal bone marrow mesenchymal stem cells (MSC) and acute lymphoblastic leukaemia cells.

CHAPTER 3

MATERIALS AND METHODS

3.1 Cell lines and treatments

3.1.1 Cell culture

The human β-catenin mutated HCC HepG2 (a gift of Prof. Giovanni Raimondo, Laboratory of Molecular Biology and Hepatology, Department of Internal Medicine, University of Messina, Italy) and the HB Huh6 (a gift by Dr. Nadia Lampiasi, IBIM C.N.R., Palermo, Italy) cell lines and the β-catenin wild type HCC Huh7 (a gift by Prof. Giovanni Raimondo, Laboratory of Molecular Biology and Hepatology, Department of Internal Medicine, University of Messina, Italy) cells were grown in low-glucose (1 g/l) Dulbecco's modified medium (DMEM, EuroClone) supplemented with 4 mM glutamine (Gln), 10% fetal bovine serum (FBS) and antibiotics (100 U/ml penicillin, and 100 µg/ml streptomycin).

The paediatric β-catenin mutated HCC HC-AFW1 cell line was isolated from a liver neoplasm of a 4-year-old boy culturing primary tumor specimens [135] and kindly provided by Prof. Armeanu-Ebinger, Department of Pediatric Surgery and Urology, University Children´s Hospital, Eberhard Karls University Tübingen, Germany. HC-AFW1 were cultured in high-glucose (4.5 g/l) DMEM (EuroClone) supplemented with 2 mM Gln, 10% FBS and antibiotics.

HeLa cells, obtained from ATCC, were maintained in high-glucose DMEM (EuroClone), enriched with 1 mM sodium pyruvate, 4 mM Gln, 10% FBS and antibiotics.

The oligodendroglioma (OD) cell line, HOG (provided by Dr. G. Dawson University of Chicago, USA), and the glioma cell line, U87 (a gift of Prof. D. Parolaro of Universiy of Insubria, Italy) were grown in high-glucose DMEM (EuroClone) supplemented with 4 mM Gln, 10% FBS and antibiotics.

The OD cell line Hs683 (provided by Dr. R. Kiss, University of Bruxelles) was grown in low-glucose DMEM (EuroClone) supplemented with 2 mM Gln, 10% FBS, antibiotics and 2.1 g/l sodium bicarbonate.

After thawing, HepG2, Huh6, Huh7, HC-AFW1, HeLa, HOG, U87, and Hs683 cultures were not used for more than 12 passages (6-12 weeks depending on the cell line).

Bone-marrow mesenchymal stem cells (MSC) were isolated as described by [132], and kindly provided by Dr. Giovanna D'Amico, Centro Ricerca Tettamanti, Department of Pediatrics, University of Milano-Bicocca, Ospedale S.Gerardo, Monza, Italy. MSC were cultured in low-glucose DMEM supplemented with 2 mM Gln, 10% FBS, antibiotics at cell density of 3,000 cell/cm^2. After thawing, MSC were not used for more than 7 passages.

The pre-B acute lymphoblastic leukaemia, RS4;11, REH, and Nalm6, cell lines (a gift of Dr. Giovanna D'Amico, Centro Ricerca Tettamanti, Department of Pediatrics, University of Milano-Bicocca, Ospedale S.Gerardo, Monza, Italy) were grown in RPMI 1960 Advanced medium (Invitrogen), supplemented with 4 mM Gln, 10% FBS (for RS4;11 and Nalm6) or 20% FBS (for REH), and antibiotics.

All cells were maintained at 37 °C in an atmosphere of 5% CO2 in air, pH 7.4.

For the experiments reported in Fig. 39, cells were incubated in pyruvate- and glucose-free DMEM containing 4 mM Gln (Gibco), supplemented with 1 g/l glucose.

3.1.2 Treatments

Unless otherwise stated, ASNase (*E. chrisanthemy* ASNase, Erwinase®, Crisantaspase, a generous gift of EUSA*Pharma*, an internal division of Jazz Pharmaceutics) was used at 1 U/ml, the GS inhibitors methionine-L-sulfoximine (MSO) and DL-phosphinothricin (PPT) at 1 mM, and the Notch inhibitor DAPT at 75µM.

For the experiments shown in Fig. 19, Fig. 20, Fig. 21, Fig. 22, Fig. 25, Fig. 26, Fig. 27, Fig. 28, Fig. 29, Fig. 30, Fig. 31, Fig. 36, and Fig. 81 cells were washed with Earle's Balanced Salt Solution (EBSS, composition in mM: NaCl 116, KCl 5.3, $CaCl_2$ 1.8, $MgSO_4 \cdot 7H_2O$ 0.81, $NaH_2PO_4 \cdot H_2O$ 0.9, $NaHCO_3$ 26, glucose 5.5, supplemented with 0.02 % Phenol Red) and incubated in DMEM with or without glutamine or GS inhibitors, supplemented with dialyzed FBS. For the experiments shown in Fig. 23 and Fig. 24 cells were washed and incubated in EBSS for 3 hours. Starved cells were then incubated for 1 hour with glutamine (4 mM) and/or essential amino acids (EAA) from the MEM EAA solution (Invitrogen).

For the experiments shown in Fig. 32 and Fig. 33, cells were washed and incubated for 6h in EBSS alone or supplemented with glutamine (4 mM) or MSO (4 mM) and PPT (4 mM) and/or EAA from the MEM EAA solution (Invitrogen).

Treatment periods and amino acid concentration are detailed for each experiment.

3.1.3 Viability assay

For viability assay of adherent cell lines, cells were seeded in complete growth medium in 96-well or 24 well-plates and grown for 24 hours. Growth medium was then substituted with fresh medium containing the drugs to be tested. For non-adherent cell lines, cells were seeded in 96-well-plates in medium containing the drugs to be tested. Cell viability was assessed with

resazurin methods [136], incubating cells in a solution of resazurin (44 μM) solved in the line-specific medium without FBS. After 1 hour, fluorescence was measured at 572 nm with a fluorimeter (EnSpire® Multimode Plate Readers, Perkin Elmer). Alternatively, the cytotoxic effects were assessed counting cell with a Coulter Z1 particle counter.

3.1.3 Co-culture of MSC and ALL cells

For co-culture experiments, shown in Fig. 82, MSC were seeded at 3000 cells/cm^2 in complete growth medium. After 48 hours medium was replaced with fresh medium containing 2.5 *10^5 ALL cells and drugs to be tested. After 48 hours cells were collected, centrifuged and the pellet was washed with phosphate buffered saline (PBS, composition in mM: NaCl 137, KCl 2.7, $Na_2HPO_4 \cdot 2H_2O$ 10, KH_2PO_4 2, pH 7.4) and resuspended in 300 μl of PBS containing 20 μg/ml propidium iodide, 10 μg/ml ribonuclease A, and 0.1% Nonidet P-40. After 1h-staining in the dark at 4°C, the samples were analyzed by means of a FACSCanto cytofluorimeter (Becton & Dickinson, San Jose, CA) equipped with a doublet discrimination module. 100,000 cells were analyzed for each experimental condition. Flow cytometric data analysis was performed using the FACSdiva software.

3.2 Gene and protein expression

3.2.1 qRT-PCR

Gene expression was evaluated with RT-qPCR. 1 μg of total RNA, isolated with GenElute™ total RNA Miniprep Kit (Sigma, Italy), was reverse transcribed as described previously [136]. For real time PCR (35 cycles), cDNA was amplified with GoTaq® qPCR Master Mix (Promega, USA) along with the primers (5 pmol each) reported in Table1. Quantitative PCR was performed in a 36 well Rotor Gene 3000 (Corbett Research, Rotor-Gene™ 3000, version 5.0.60, Mortlake, Australia). Each cycle consisted of

a denaturation step at 95 °C for 30 s, followed by separate annealing (30 s, 55-58 °C) and extension (30 s, 72 °C) steps. Fluorescence was monitored at the end of each extension step. A no-template, no-reverse transcriptase control was included in each experiment. At the end of the amplification cycles a melting curve analysis was added. Data analysis was made according to the Relative Standard Curve Method [137].

GENE	***PRIMERS***
GLUL *(Glutamine Synthetase)*	for 5' TCATCTTGCATCGTGTGTGTG 3' rev 5' CTTCAGACCATTCTCCTCCGG 3'
ASNS *(Asparagine Synthetase)*	for 5' GATTGCCTTCTGTTCAGTGTCT 3' rev 5' GGGTCAACTACCGCCAACC 3'
SLC38A2, SNAT2 *(Solute carrier family 38 member 2)*	for 5' ATGAAGAAGGCCGAAATGGGA 3' rev 5' TGCTTGGTGGGGTAGGAGTAG 3'
SLC1A5, ASCT2 *(Solute carrier family 1 member 5)*	for 5' TGGTCTCCTGGATCATGTGG 3' rev 5' TTTGCGGGTGAAGAGGAAGT 3'
SLC6A14, ATB0+ *(Solute carrier family 6 member 14)*	for 5' GCTGCTTGGTTTTGTTTCTCCTTGGTC 3' rev 5' GCAATTAAATGCCCCATCCAGCAC 3'
c-MYC	for 5' GCTGCCAAGAGGGTCA 3' rev 5' CGCACAAGAGTTCCGTAG 3'
HES-1	for 5' ACGACACCGGATAAACCAAA 3' rev 5' CGGAGGTGCTTCACTGTCAT 3'

CTNNB1 *(β-catenin)*	for 5' CCTCTGATAAAGGCTACTGTTGGAT 3' rev 5' CTGATGTGCACGAACAAGCA 3'
CCND1 *(cyclin D1)*	for 5' CCCTCGGTGTCCTACTTCAA 3' rev 5' AGGAAGCGGTCCAGGTAGTT 3'
GLS1 *(glutaminase 1)*	for 5' GCTGTGCTCCATTGAAGTGA 3' rev 5' GCAAACTGCCCTGAGAAGTC 3'
CHOP	for 5' CTTCTCTGGCTTGGCTGACT 3' rev 5' TCCCTTGGTCTTCCTCCTCT 3'
RPL-15 *(ribosomal protein L15)*	for 5' GCAGCCATCAGGTAAGCCAAG 3' rev 5' AGCGGACCCTCAGAAGAAAGC 3'

Table 1 *Primers*

3.2.2 Western Blot

After the experimental treatments, cells were rinsed twice in PBS with Ca^{2+} and Mg^{2+} and lysed in a buffer containing 20 mM Tris-HCl, pH 7.5, 150 mM NaCl, 1 mM EDTA, 1 mM EGTA, 1% Triton, 2.5 mM sodium pyrophosphate, 1 mM β-glycerophosphate, 1 mM Na_3VO_4,1 mM NaF, 2 mM imidazole, and a cocktail of protease inhibitors (Complete, Mini, EDTA-free, Roche). Lysates were transferred in Eppendorf tubes, sonicated for 5s, and centrifuged at 12000*g* for 10 min at 4 °C. After quantification with the Bio-Rad protein assay the equivalent of 30 µg of proteins, was mixed with Laemmli buffer 4x (250 mM Tris-HCl, pH 6.8, 8% SDS, 40% glycerol, 0.4 M DTT), warmed at 95°C for 5 min, and loaded on a 10% gel for SDS-PAGE. After electrophoresis, proteins were transferred to PVDF membranes (Millipore—Immobilon-P). Non-specific binding sites were blocked with an incubation of 2 hours at RT in 5% non-fat dried milk in

TBS-Tween solution. The blots were then incubated at 4 °C overnight with the following antibodies diluted in a 5% BSA TBS-Tween solution: anti p70S6K1 phospho T389 (rabbit, monoclonal, 1:1000, Cell Signaling), anti p70S6K1 phospho T421/S424 (rabbit, monoclonal, 1:1000, Cell Signaling), anti p70S6K1 total (mouse, monoclonal, 1:1000, Cell Signaling), anti-eIF2α phospho S51 (mouse, monoclonal,1:1000, Abcam), anti-GS (mouse, monoclonal, 1:1500, BD, Transduction Laboratories), anti-β-catenin (mouse, monoclonal, 1:1000, Dako), anti-ASNS (rabbit, polyclonal, 1:1000, Santa-Cruz Biotecnology), anti-GADPH (rabbit, polyclonal, 1:4000, Sigma), anti-β-tubulin (mouse, polyclonal, 1:1000, Santa-Cruz Biotecnology). After washing, blots were exposed for 1 hour at room temperature to HRP-conjugated anti mouse or anti-rabbit antibody (Cell Signaling Technology), diluted 1:10000 in blocking solution. Immunoreactivity was visualized with Immobilon Western Chemiluminescent HRP Substrate (Millipore).

3.2.3 Immunofluorescence

To study the subcellular distribution of β-catenin we used immunofluorescence. Briefly, HCC cells were seeded on 4-chamber CultureSlides (Falcon, Becton & Dickinson Company, San Jose, CA) at a density of $4*10^4$ cells/cm^2. When 70% of confluence was reached, cells were rinsed twice in PBS and fixed for 10 min in 3.7% paraformaldehyde in PBS. After two further rinses, cells were permeabilized for 7 min in 0.1% Triton X-100 in PBS. Cells were then incubated for 1 hour in blocking solution (5% of BSA 10% of goat serum, and 0.3 M glycine in PBS) followed by an overnight incubation at 4 °C with anti-β-catenin monoclonal antibody (DakoCytomation, M35359, 1:200 in PBS 5% BSA), two washes in PBS, and an additional 1hour-incubation with an Alexa Fluor 488 anti-rabbit IgG antibody (Invitrogen, Paisley, UK, 1:400). After one rinse, cells were incubated for 30 min with a 100 µg/ml RNAase A solution, and then

with a 1 µg/ml solution of propidium iodide (PI) in PBS for 10 min to stain nuclei. Cells were observed with a confocal microscope Zeiss® 510 LSM Meta (Carl Zeiss SpA, Arese, Milan, Italy), using an oil 60x objective. λ_{ex} of 488nm and 540nm and λ_{em} of 545nm and 595 nm were used for Alexa Fluor 488 and propidium iodide, respectively.

3.3 Amino acid analysis

3.3.1 Amino acid extraction

The intracellular content of amino acids was determined as previously described [138] with minor modifications. Briefly, cell monolayers were washed twice with ice-cold PBS, extracted in a solution of acetic acid (6.6 mM) in ethanol and processed for protein determination with the Lowry method. After lyophilization, samples were reconstituted in LiOH buffer (pH 2.2). For serum amino acid analysis, sera were deproteinized with 10% (w/v) of sulfosalicilic acids (SSA) on ice for 30 min. Then, samples were centrifuged at 12000*g* for 10 min at 4 °C, and supernatants were mixed with 1 volume of LiOH buffer (pH 2.2). For tissue amino acid extraction, liver and tumor samples were homogenized in 6.6 mM solution of acetic acid in ethanol with an high-speed drive motor for small volumes homogenizer (Ingenieurbüro CAT, M Zipperer GmbH, Germany) for 30 s on ice. Afterwards, samples were centrifuged at 12000*g* for 10 min at 4 °C, the supernatant was collected, lyophilized and reconstituted in LiOH buffer (pH 2.2).

3.3.2 Amino acid determination

The intracellular content of the single amino acids was determined by HPLC analysis with a Biochrom 20 amino acid analyzer (Amersham Pharmacia Biotech, UK), employing a high resolution column (Bio 20 Peek Lithium) and the physiological fluid chemical kit (Amersham Pharmacia Biotech) for elution. The column effluent was mixed with ninhydrin, passed through the high-temperature reaction coil and read by the photometer unit. Data are expressed as nmol/mg of proteins, mmol/l serum or nmol/mg of tissue.

3.4 Amino acid transport and protein synthesis

3.4.1 L-Leu uptake

The initial influx of L-Leu was measured in 96-well multidish plates (Falcon, Becton Dickinson Biosciences, Franklin Lakes, NJ, USA) where 20,000 cells/well had been seeded 24 hours earlier. Before the experiments cells were rinsed and incubated for 1 hour in EBSS with Tris-HCl at pH 7.4 supplemented with 5 µg/ml cycloheximide. Then, cells were rinsed twice with 200 µl of EBSS Na^+-free and incubated in EBSS, with or without Na^+, supplemented with L-[4,5-3H] Leu (10 µM, 10 µCi/ml, Amersham Biosciences) and with specific inhibitors of system ATB0+ and system A. After 2 min, multiwell dishes were washed twice with ice-cold urea (300 mM) and cell monolayers were extracted with 50 µM of cold absolute ethanol. The extracts were added to 200 µl of scintillation fluid and counted with a Wallac Trilux2 liquid scintillation spectrometer (Perkin-Elmer, Boston, MA, USA). Transport values were normalized for the cell protein, determined directly in the well with a modified Lowry procedure and measured with a Wallac Victor2 Multilabel Counter (Perkin-Elmer).

L-Leu transport has been characterized using the following inhibitors to discriminate the transporter subtypes: L-Leu (2 mM) ; α-methyl-DL-tryptophan (αMLT, 2.5mM); D-serine (D-Ser, 2.5mM); N-α-methylaminoisobutyric acid (MeAIB, 2.5mM).
Transport assay under Na^+-free conditions was performed in a modified EBSS in which NaCl was replaced by N-methyl-Dglucamine chloride and pH kept at 7.4 with Tris–HCl.

3.4.2 Protein synthesis

L-[4,5-^{3}H]leucine (10 μCi/ml, Amersham Biosciences) was added to the incubation medium during the last 45 min of incubation. At the end of the incubation, cells were washed with PBS and extracted with a 6.6 mM solution of acetic acid in ethanol. After discarding of the acid-soluble fraction, proteins were suspended in 150 μl of 5% sodium-deoxycholate in 1 N NaOH. While 50 μl were used for the determination of total proteins with Lowry method, scintillation fluid was added to the remaining aliquot and the incorporated radioactivity counted with a scintillation spectrometer (Wallac Microbeta Trilux counter). Data were expressed as CPM/mg prot/min.

3.5 Gene manipulation

3.5.1 β-catenin silencing

HepG2 and Huh-6 cells were transfected with a scrambled siRNA (ON-TARGETplus Non-targeting Pool) or with a siRNA targeting β-catenin (ON-TARGETplus SMARTpool, CTNNB1, Thermo Scientific DharmaFECT) following with modifications the procedure described by Cairo et al. [139]. Briefly, HepG2 and Huh-6 cells were seeded in complete growth medium without antibiotics in 12-well plates, at a density of $1.5*10^5$/well and $2.5*10^4$/well, respectively. After 24 hours cells were incubated in a FBS-

and antibiotic-free medium containing DharmaFECT transfection reagent and the siRNAs. After further 16 hours medium was replaced with fresh complete growth medium and cultures underwent the experimental treatments.

3.5.2 Luciferase assay

HCC cells were seeded in 6-well-plates in standard growth medium. After 24 hours cells were washed with PBS and incubated in DMEM in the presence or in the absence of glutamine without serum and antibiotics. After 24 hours, the cells were transiently transfected with the reporter construct TOPflash (Upstate, Lake Placid, NY), kindly provided by Prof. Monga, University of Pittsburgh. TOPflash has three copies of the Tcf/Lef sites upstream of a thymidine kinase (TK) promoter and the *firefly luciferase* gene. All transfections were performed using 1.8 µg of TOPflash plasmids and FuGene HD reagent (Roche, Indianapolis, IN). To normalize transfection efficiency in reporter assays, the cells were cotransfected with 0.2 µg of the internal control reporter *Renilla reniformis* luciferase under the TK promoter (pRL-TK; Promega, Madison, WI). 20 hours after TOPflash transfection, luciferase assay was performed, using the Dual Luciferase Assay System kit, in accordance with the manufacturer's protocols (Promega). Luminescence was detected with a Wallac Microbeta Trilux (Perkin Elmer, Wellesley, Ma, USA). Relative luciferase activity (in arbitrary units) was reported as fold induction after normalization for transfection efficiency.

3.6 In vivo experiments

3.6.1 Animals and treatments

Experiments in athymic nude nu/nu mice were performed at the Laboratory of Genetic Engineering for the Production of Animal Models (LIGeMa) at the Animal House of the University of Firenze. In the experiment shown in Fig. 47, Fig. 48, and Fig. 49 male five-weeks old mice (Harlan Italy, Udine, Italy) were treated with intraperitoneal (i.p.) injections of ASNase (5 U/ml) and MSO (10 mg/kg), both in 0.9% NaCl, or vehicle alone, MSO was injected 3 hours after ASNase injection. Treatment was performed three times a week for three weeks, after which peripheral blood (PB) and liver were collected for analysis. After collection PB was centrifuged and serum was frozen (-80°C).

In the experiment shown in Fig. 50, Fig. 51, Fig. 52, Fig. 53, Fig. 54, and Fig. 55 mice were subcutaneously (s.c.) injected with HepG2 cells (2.5 x 10^6 cells). After 8 days, mice were i.p. treated with ASNase and MSO, alone or in combination. Tumor growth was monitored for 19 days by external measurement using a caliper and tumor volume was calculated by applying the ellipsoid equation. 3 hours after the last MSO injection, which corresponds to 6 hours after ASNase injection, mice were sacrificed, and PB, tumor masses and livers were collected for analysis. After collection PB was centrifuged and serum frozen. In the experiment shown in Fig. 56 and Fig. 57 mice were s.c. injected with 2.5 x 10^6 cells of HepG2 (left flank) or Huh7 cells (right flank). After two weeks the combined treatment with ASNase and MSO (see above) started. Control animals were injected with vehicle alone. Tumor growth was monitored by external measurement using a caliper and tumor volume was calculated by applying the ellipsoid equation. Three weeks after treatment, 3 hours after the last MSO injection (6 hours after ASNase injection) mice were sacrificed, and tumor masses dissected and weighted.

In the experiment shown in Fig. 64, Fig. 65, Fig. 66, and Fig. 67, HC-AFW1 cells were engrafted in NOD.Cg-Prkdcscid IL2rgtmWjl/Sz (NSG) mice, purchased from Charles River (Sulzfeld, Germany) and bred in the Department of Pediatric Surgery and Pediatric Urology, University Children's Hospital, Tübingen, Germany. Eight-week-old mice were s.c. injected with $2*10^6$ cells and kept in filter-top cages at 22°C, 60% humidity. Sterilized food and water were accessible ad lib. After two weeks mice were treated as described above with ASNase, MSO or ASNase + MSO. Tumor length, width and height were measured every 3 days and tumor volumes were calculated by applying the ellipsoid equation. Mice were weighted every 3 days. After 10 days of treatment mice were sacrificed and PB, tumors and livers were explanted for further analysis.
Animals received human care and study protocolos comply with the institutional guidelines for animal welfare.

3.6.2 GS activity

GS activity was assayed measuring the γ-glutamyltransferase activity of the enzyme [140]. Tissues were lysed in 500 µl of a solution containing 50 mM imidazole-HCl, pH 6.8, 0.5 mM EDTA, 1 mM DTT, supplemented with protease inhibitors (Complete, Mini, EDTA-free, Roche), transferred into a 1.5 ml microtube, sonicated in ice (Sonicator Ultrasonic Processor XL, Misonix), and centrifuged at 12000*g*, 30 min, 4°C. After quantification (Bio-Rad Protein Assay), protein concentration of the supernatant was adjusted to 1 µg/µl. An aliquot of 150 µl was used for the assay in a mixture (final volume 300 µl) consisting of 50 mM imidazole-HCl (pH6.8), 50 mM Gln, 25 mM hydroxylamine, 25 mM sodium arsenate, 2 mM $MnCl_2$, and 0.16 mM ADP. After incubation at 37°C for 30 min, the reaction was stopped adding 600 µl of a solution containing 2.42% FeCl3 and 1.45% TCA in HCl 1.82%. Precipitates were removed by centrifugation (2,000 rpm for 5 min) and

supernatants were read at 540 nm using a spectrophotometer (Helios-γ, Spectronic Unicam). Values of GS activity, expressed as pmol/min/µg protein of γ-glutamylhydroxamate, were calculated with a calibration curve using aliquots of the product.

3.6.3 Histological evaluation

The tumor samples were routinely fixed in buffered formalin and embedded in paraffin. Sections (4 µm) were stained with haematoxylin - eosin for histological diagnosis and examined according to predefined histological variables. Immunohistochemical analyses were performed on all available specimens using the following primary antibodies: anti β-Catenin (BD Transduction Laboratories, CA, USA; 1:1000) and anti Glutamine-Synthetase (BD Transduction Laboratories, CA, USA; 1:10000). After deparaffinization and rehydration, sections were treated with 3% hydrogen peroxide. For antigen retrieval, sections were immunostained with HRP Polymer (Advance HRP Kit, Dako) in accordance with the manufacturer's specifications. 3-3[1]Diaminobenzidine (DAB) was used for staining development. In negative controls, normal serum replaced the primary antibody.

3.6.4 Ki67 index

Deparaffinized tissues were exposed to citrate buffer pH 6.0 at 90 °C for 20 min. Endogenous perodixase was blocked with 3% H_2O_2 for 10 min in dark. After washing, non-specific binding sites were blocked with an incubation of 1h at room temperature in 3% goat serum (DAKO) and the tissues were then exposed at 4°C for 20 min to the anti-Ki67 antibody (mouse monoclonal, 1:75, DAKO) diluted in 5% bovine serum albumin TBS Tween solution. After washing, HRP-conjugated antibody (HRP One-Step polymer anti mouse/rabbit/rat, ZYTOMED) was added and incubated for 45 min at

room temperature. Incubation of 10 min with DAB (DAB substrate kit for peroxidase, SK-4100, Vector Laboratories) was performed to detect the signal. Slides were counterstained in hematoxylin (Mayer´s Hemalaun, AppliChem) for 10 s and rinsed in running tap water for 10 min. Ki67 index was calculated counting a minimum of 10 randomly selected high-power (x40) fields containing representative sections of tumor and calculated as the percentage of positively stained cells to total cells [141].

3.7 Statistics

Data were expressed as means ± SD. For statistical analysis, two-tail Student's t test for unpaired data or one-way ANOVA were used, whenever appropriate. GraphPad Prism 5.0™ was used for all the statistical analyses and p values < 0.05 were considered statistically significant.

CHAPTER 4

RESULTS AND DISCUSSION

4.1 mTOR activity is modulated not only by essential amino acids (EAA) intracellular content

Mammalian target of rapamycin (mTOR) plays a pivotal role in the control of cell growth and protein synthesis. Many upstream signals converge on the regulation of this kinase, such as growth factors, energy status (via AMPK pathway), hypoxia and glucose content [142]. However, the main factor which determines mTOR activation is definitely amino acid, and in particular leucine, availability [143]. Also glutamine is critical for mTOR activation, although there are contradictory opinions on the role of this amino acid in mTOR stimulation.

Recently, it has been proposed that glutamine has an indirect role on mTOR activation by allowing leucine entry through a tertiary active transport [45]. However, due to its importance as nitrogen donor and anaplerotic substrate, we hypothesized that glutamine may directly influences mTOR activity.

4.1.1 Glutamine regulates mTOR independent on EAA content

4.1.1.1 Glutamine depletion down-regulates mTOR in a dose and time dependent manner

To evaluate the effects of glutamine (Gln) on mTOR activity HepG2 cells were incubated in DMEM supplemented with decreasing concentrations of Gln, from 4 mM to 0 for 24 hours. mTOR activity was assessed by the phosphorylation of S6K1 at the sites: T389 and T412 (for the p70 and p85

isoforms, respectively), which are the selective target of the mTORC1 complex, and T421/S424 and T444/S447 (for p70 and p85 isoforms, respectively), which are the target of both mTORC1 and MAP kinases [144]. Western blot analysis revealed that mTOR activity decreases in a Gln-dependent manner (Fig. 19). However the activity was not completely suppressed, since the phosphorylation of S6K1 is still visible in the absence of Gln. S6K1 phosphorylation was suppressed by rapamycin, confirming its dependence upon mTORC1 (data not shown). Glutamine Synthetase (GS) expression was increased by Gln depletion. Since GS protein abundance is regulated by Gln intracellular concentration [52, 53], this pattern suggests a progressive fall of intracellular Gln content during the incubation in media supplemented with decreasing concentrations of the amino acid.

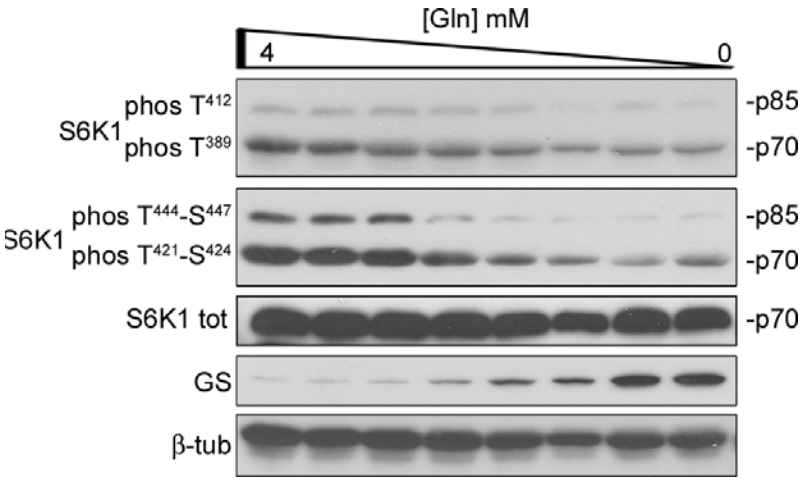

Fig. 19 ***mTOR activity was regulated by Gln concentration.*** *The expression of p70S6K1 (phospho T389 and T421/S424), p85S6K1 (phospho T412 and T444/S447), S6K1 (total), and Glutamine Synthetase (GS) was assessed in HepG2 cells incubated for 24 hours in DMEM supplemented with 10% dialysed FBS at the following Gln concentrations (mM): 4, 2.26, 1.25, 0.71, 0.4, 0.22, 0.125 and 0. β-tubulin was used as a loading control. The experiment was repeated three times with comparable results.*

Recently, it was proposed that, in HeLa cells, Gln stimulates mTORC1 increasing the intracellular availability of leucine through a transport exchange mechanism [45]. However, in that paper intracellular leucine was not measured. To ascertain if the modulation of mTOR was due to Gln availability itself or to a consequent decrease in leucine (Leu) content, we measured intracellular amino acids in HepG2 cells incubated in the presence (4 mM) or in the absence (0 mM) of Gln for 24 hours. HPLC analysis revealed that Gln starvation caused a clear cut decrease of intracellular Gln, Glu and Ala, but, paradoxically, a significant increase of the essential amino acids (EAA) and, in particular Leu, content was detected (Fig. 20), suggesting that intracellular leucine does not appear to be the only factor that regulates mTORC1.

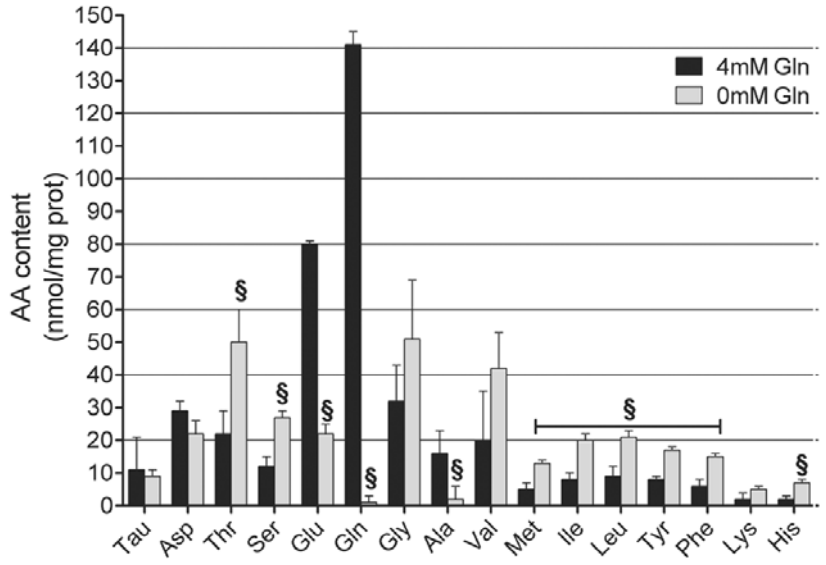

Fig. 20 ***Leucine intracellular content increased in the absence of extracellular Gln.*** *HepG2 cells were incubated for 24 hours in DMEM supplemented with 10% dialyzed FBS and 4 mM (black bars) or 0 mM (gray bars) Gln and cell content of amino acids were determined as described in Methods. Data are means ± SD of three independent experiments. § p<0.05 vs. control (4 mM Gln).*

Time course of changes in mTORC1 activity during Gln starvation indicated that the activity of the kinase was almost abolished at earlier times (3-9 hours) but seemed to increase at later times (24-48 hours), although it remained lower compared to control (4 mM Gln) (Fig. 21 A). Also in HeLa cells, Gln depletion caused a biphasic changes in mTOR activity, which decreased at earlier times and showed a partial restoration at later times (Fig. 21 B).

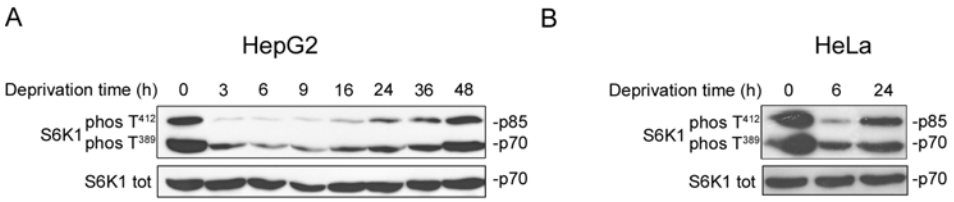

Fig. 21 ***mTOR activity was partially restored at later times of Gln starvation.*** *Western Blot of S6K1 (phospho T389 and T412) and S6K1 total was performed in HepG2 (A) and HeLa (B) cells incubated for the indicated times with DMEM supplemented with 10% dialysed FBS without Gln. The experiment was repeated three times with comparable results.*

To understand the reason of the partial restoration of mTORC1 activity, amino acid content was analysed in both HepG2 and HeLa cells. In both cell lines Gln and Glu continued to decrease during the experiment, while Leu content increased, reaching levels higher than control (Fig. 22). The behaviour of Leu was shared by other EAA (not shown, see [145]).This observation suggests that the increase of Leu may be sensed upstream of mTOR and partial rescues kinase activity. However, given that activity restoration was not complete, we speculate that two signals, one from Leu and the other from Gln, are required to attain a full mTOR activation.

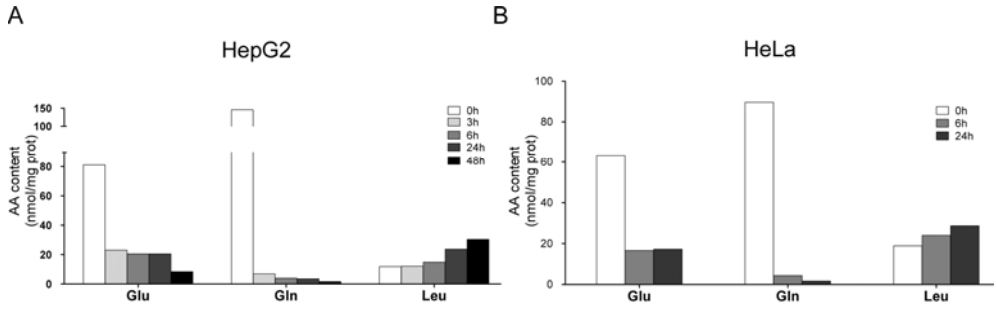

Fig. 22 ***Leucine content increased at later times of Gln deprivation.*** *Amino acids content was determined, as described in Methods, in HepG2 (A) and HeLa (B) cells incubated for the indicated times with DMEM supplemented with 10% dialyzed FBS without Gln. A single representative experiment is shown.*

4.1.1.2 Essential Amino Acids alone are not able to fully activate mTOR

To confirm the hypothesis that two signals, one from Gln and the other from EAA, are needed for a complete mTOR activation, we incubated both HepG2 and HeLa cells in unsupplemented saline solution (EBSS) for 3 hours. This condition led to a marked reduction of mTOR activity, since the phosphorylation of S6K1 was not detectable at all (Fig. 23). In HepG2 cells, the restitution for 1 hour of Gln (4 mM) to starved cells does not caused any increase in the phosphorylation of S6K1. Likewise, the restitution of EAA, in absence of Gln, was not able to increase the phosphorylation of S6K1 even when added at doubled (2x) or tripled (3x) concentration than standard growth medium. Instead, only the simultaneous restitution of Gln and EAA (1x) restored mTOR activity (Fig. 23 upper). At variance with HepG2 cells, when Gln (4 mM) alone or EAA alone were restored to starved cells, a slight increase in the phosphorylated status of S6K1 was observed in HeLa cells. However, also in HeLa cells, like in HepG2, a complete mTOR activation was detected only when both Gln and EAA were simultaneously administered (Fig. 23 bottom).

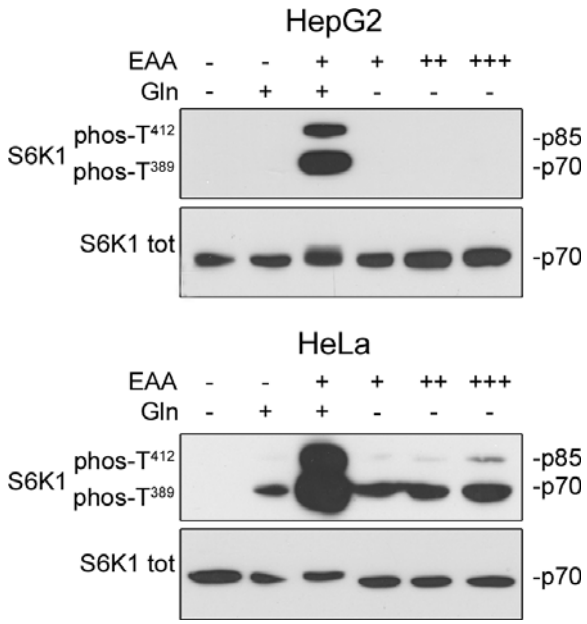

Fig. 23 ***Gln and EAA alone were not able to fully activate mTOR.*** *Western Blot of S6K1 (phospho T389 and T412) and S6K1 total was performed in HepG2 (upper) and HeLa (bottom) cells. Growth medium was washed and replaced with unsupplemented saline solution (EBSS) for 3 hours. Cells were then incubated in fresh EBSS or in EBSS supplemented with 4 mM Gln and/or Essential Amino Acids (EAA, 1x, + at the concentration present in DMEM) or at double (2x, ++) or triple (3x, +++) concentrations. The incubation was prolonged for 1 hour. The experiment was repeated three times with comparable results.*

By a parallel analysis of amino acid content in both cell lines, we found that the Leu content was comparable when EAA (1x) were added alone or in the presence of Gln (Fig. 24), confirming that the role of Gln in mTOR regulation is not restricted to favour Leu entry as previously reported [45]. Furthermore, when EAA were added at double or triple concentrations compared to those present in DMEM, an increased cell content of Leu was detected (Fig. 24), although mTOR activation was only sub-maximal.

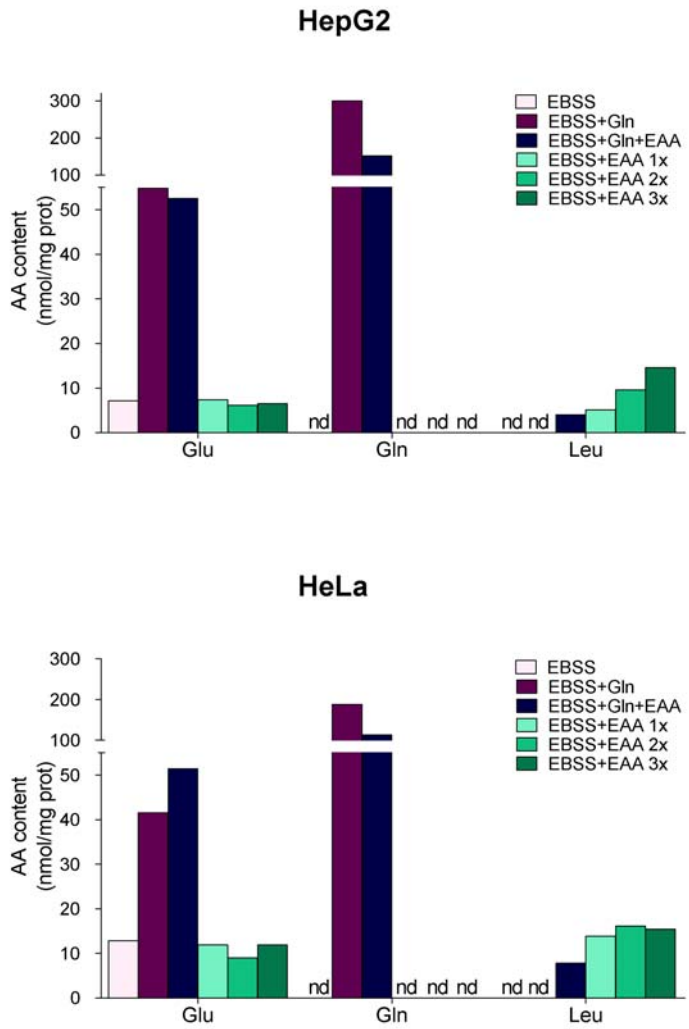

Fig. 24 ***Intracellular Leu content was not dependent on the presence of extracellular Gln.*** *Amino acid content was determined, as described in Methods, in HepG2 (upper) and HeLa (bottom) cells. Growth medium was washed and replaced with unsupplemented saline solution (EBSS) for 3 hours.Cells were then incubated in fresh EBSS or in EBSS supplemented with 4 mM Gln and/or Essential Amino Acids (EAA, 1x at the concentration present in DMEM) or at double, 2x, or triple, 3x concentrations). The incubation was prolonged for 1 hour. A single representative experiment is shown.*

These data, in accordance with previous reports [45, 146], confirms that Gln alone is not able to determine complete mTORC1 activation. However, the evidence that high extracellular Gln levels reduce EAA cell content in both HepG2 and HeLa cells suggests that the transport interaction between Gln and EAA is more complex that the tertiary transport proposed in previous reports [45, 147, 148]. In fact, in accordance to the tertiary transport theory, Leu and other EAA influx should be energized by the efflux of Gln previously accumulated through a secondary active transport. Instead, from these data it seems more likely that, at least in these models, Gln and Leu share, in a competitive manner, a secondary active transporter, endowed with a sufficient broad specificity. A potential candidate could be the ATB0+ carrier (see below), an active secondary transporter, encoded by the gene *SLC6A14*, able to mediate the uptake of 18 proteinogenic amino acids and, in particular, exhibiting high affinity for the most important mTOR stimulating amino acids, Leu and Gln [149]. However, considering that the recovery of mTOR activity started after 24 hours from Gln depletion, it cannot be excluded a role of the autophagic process in the increase of Leu and other EAA cell levels.

4.1.2 ATB0+ transporter may be involved in mTOR stimulation

To evaluate the involvement of ATB0+ in Gln and Leu competitive uptake, first we examined *SLC6A14* mRNA abundance in Gln deprived HepG2 cells. After 6 hours of Gln starvation, the transporter was 4-fold higher than in control cell (maintained with 4 mM Gln), and this induction persisted after 24 hours (Fig. 25).

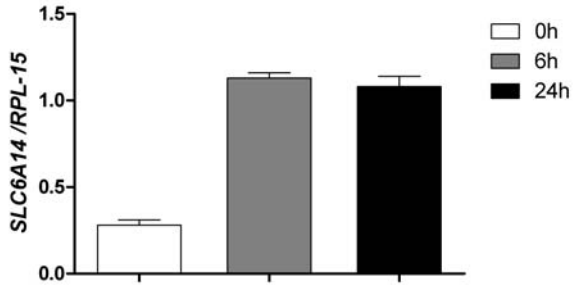

Fig. 25 ***ATB0+ was induced in Gln starved HepG2 cells.*** *SLC6A14 expression was analyzed by RT-qPCR. HepG2 cells were incubated in the absence of Gln for the indicated times. Relative SLC6A14 mRNA abundance was normalized to RPL-15 and expressed as Arbitrary Units.*

Considering that the tertiary transport theory should involve the system A carriers, such as SNAT2 transporter (encoded by *SLC38A2* gene), coupled with the exchanger ASCT2 transporter (encoded by *SLC1A5* gene), the expression of these two transporters was evaluated in Gln deprived HepG2 cells. RT-qPCR analysis revealed that both *SLC38A2* and *SLC1A5* doubled after Gln withdrawal (Fig. 26 A and B respectively). The induction of the system A transporter is not surprising since it was previously demonstrated that nutritional stress may induce this carrier [136, 150].

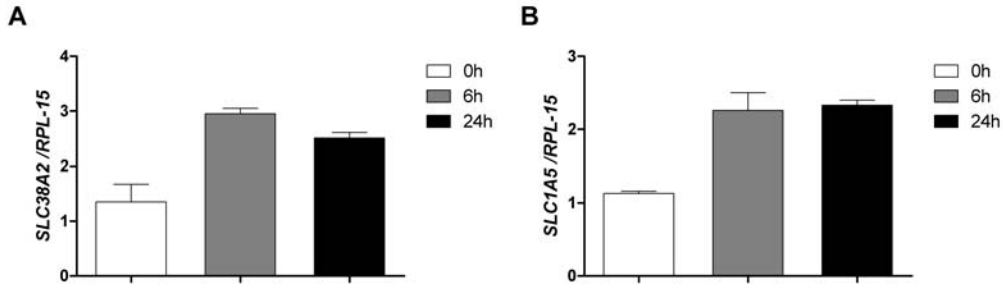

Fig. 26 ***SNAT2 and ASCT2 were induced after Gln withdrawal.*** *SLC38A2 (A) and SLC1A5 (B) mRNA levels were analyzed by RT-qPCR. HepG2 cells were incubated in the absence of Gln for the indicated times. Relative mRNA abundance was normalized to RPL-15 and expressed as Arbitrary Units.*

Then, to evaluate the transport system involved in Leu uptake in Gln starved cells, radio-labelled L-[4,5- ^{3}H]-leucine uptake was measured. The influx of 10 μM Leu, a concentration near to the K_m of ATB0+ and LAT transporters [151], was measured in the presence or in the absence of Na^+ in cells incubated in the presence (4 mM) or in the absence of Gln for 8 hours. Cells were washed and incubated for 1 hour in EBSS to cause amino acid efflux in order to empty the cells and minimize trans-effects that could modify carrier activities. Since EBSS incubation induces system A carriers [150], cycloheximide (5 μg/ml) was added to block protein synthesis during this further incubation.

In Gln-fed cells, Na^+-dependent transport was calculated subtracting the influx measured in the absence of Na^+ from that measured in the presence of the cation, and found to correspond to 180 pmol/mg prot/min (roughly the 27% of total). Saturating entry routes for leucine with high concentrations of the amino acid (2 mM), it was possible to estimate diffusion (18%).

Adding the ATB0+ inhibitors [149], α-methyl-DL-tryptophan (αMLT, 2.5 mM) or D-serine (D-Ser, 2.5 mM), the Na^+-dependent transport was inhibited, while the Na^+-independent component was inhibited by αMLT only (Fig 27).

Eventually, Leu transport was measured in the presence of a selective inhibitor of system A, N-methyl,α-methylaminoisobutyric acid (MeAIB, 2.5 mM). This condition did not produce any significant change in Na^+-dependent Leu uptake compared to control (Fig 27), suggesting that in Gln fed cell Leu Na^+-dependent uptake was referable to a MeAIB-resistant system.

Thus, in Gln-fed HepG2 cells Leu uptake is mainly mediated by diffusion (18%) and by the Na^+-independent system L (55%), however a small percentage of Leu uptake is effectively mediated by the Na^+-dependent system ATB0+ (27%).

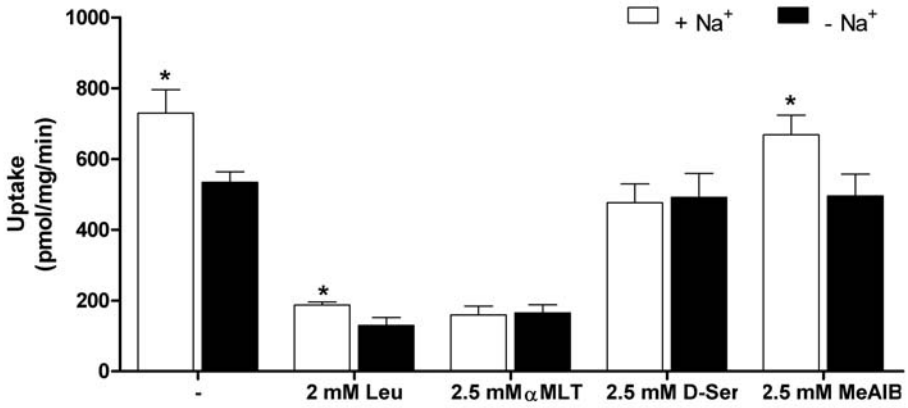

Fig 27 ***Leu uptake in Gln fed cells was attributable to Na+-dependent MeAIB-resistant systems.*** *Cells were incubated in DMEM with 4 mM Gln for 8 hours. DMEM was then replaced with EBSS supplemented with cycloheximide (5 µg/ml) for 1 hour. Then cells were incubated for 2 min in EBSS supplemented with L-[4,5-^{3}H] Leu (10 µM) with (white) or without (black) Na+, in the absence (control) or in the presence of the following inhibitors: 2 mM Leu, 2.5 mM αMLT, 2.5 mM D-Ser, 2.5 mM MeAIB. Values are the means of five independent determinations with SD shown. * p< 0.05 vs. cells incubated without Na+.*

Also in Gln deprived cells a Na^+-dependent uptake was observed (Fig. 28), which was doubled in relative terms compared with Gln-fed cells. However, in Gln deprived cells αMLT did not completely inhibit the Na^+-dependent transport, suggesting the involvement of another Na^+-dependent system in Leu uptake.

Consistently, a marked inhibition of Na^+-dependent transport was observed in the presence of MeAIB, suggesting that, under Gln deprivation, an induction of system A had occurred.

Hence, in Gln-deprived HepG2 cells Leu uptake is still mediated by diffusion (18%), but the contribution of Na^+-independent system L decrease (35%) and on the other hand there is an increase of the uptake by Na^+-dependent systems ATB0+ (38%) and A (6%).

These data confirm the hypothesis that Gln and Leu may compete for ATB0+ mediated uptake, explaining why, in the absence of extracellular Gln, the cell content of Leu increased. Yet, it was not possible to discriminate if the increased Na^+-dependent uptake observed in Gln starved cells was referable only to the induction of system A or of both systems A and ATB0+. However, due to the low affinity of system A for Leu, the increase in amino acid content observed in Gln deprived cells is likely still referable to the ATB0+ transporter, which has high affinity for Leu (K_m= 12 μM [151]). Thus, the system may be involved in mTOR activation.

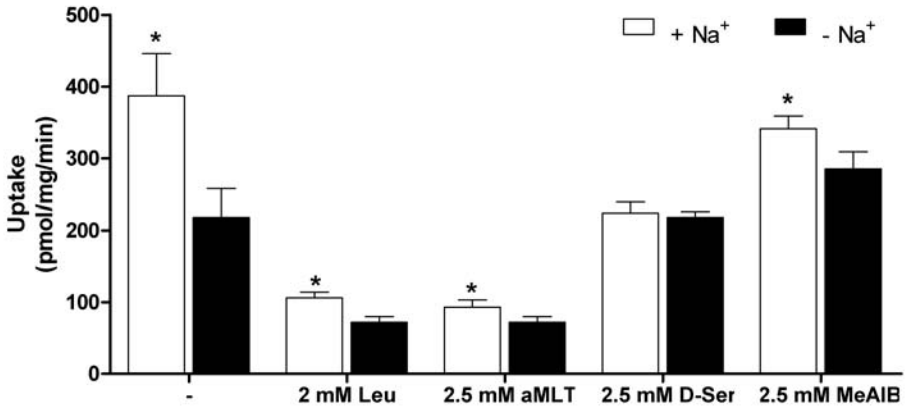

Fig. 28 ***Leu Na+-dependent uptake in Gln deprived cells.*** *Cells were incubated in DMEM without Gln for 8 hours; DMEM was then replaced with EBSS supplemented with cycloheximide (5 µg/ml) for 1 hour. Then cells were incubated for 2 min in EBSS supplemented with L-[4,5-^{3}H] Leu (10 µM) with (white) or without (black) Na+, in the absence (control) or in the presence of the following inhibitors: 2 mM Leu, 2.5 mM αMLT, 2.5 mM D-Ser, 2.5 mM MeAIB. Values are means of five independent determinations with SD shown. * p< 0.05 vs. cells incubated without Na+.*

4.1.3 Glutamine Synthetase inhibitors activate mTORC1

4.1.3.1 GS inhibitors activate mTOR in a dose dependent manner

Due to the importance of mTOR in cell growth and protein synthesis regulation it is not surprising that a large amount of studies and papers are focused on understanding how the kinase senses amino acids. A recent paper [152] confirmed the paradoxical observation that we made while studying the effects of Gln depletion on hepatocellular carcinoma cell lines [136]: the irreversible Glutamine Synthetase (GS) inhibitor, methionine-L-sulfoximine (MSO), while further depleted cell Gln, stimulated mTOR.

To discriminate if the GS inhibitor was directly involved in the kinase activation, HepG2 cells were treated for 6 hours with MSO or with another GS inhibitor, DL-phosphinothricin (PPT), in the absence of Gln. As shown in Fig. 29, both MSO and PPT were able to activate mTOR in a dose-dependent manner.

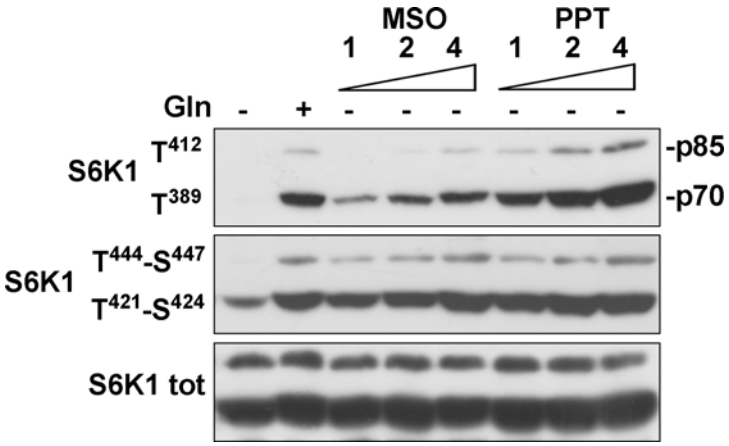

Fig. 29 ***MSO and PPT stimulated mTOR in Gln deprived cells.*** *Western Blot of p70S6K1 (phospho T389 and T421/S424), p85S6K1 (phospho T412 and T444/S447) was performed in HepG2 cells incubated for 6 hours in DMEM without Gln in the presence of increasing concentration (1, 2, 4 mM) of MSO or PPT. Control cells were maintained in presence of 4 mM Gln (+). Total S6K1 was used as a loading control. The experiment was repeated three times with comparable results.*

The phosphorylated fraction of S6K1 was even higher when PPT (4 mM) was added instead of Gln (4 mM) (Fig. 29). Furthermore PPT (4 mM) was also able to further activate mTOR in Gln fed cells, while MSO did not show any supra-stimulatory effects in the presence of extracellular Gln (Fig. 30).

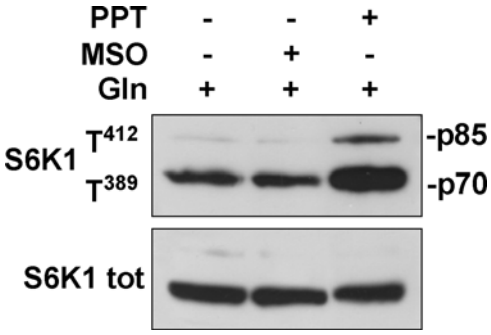

Fig. 30 ***PPT stimulated mTOR in Gln fed cells.*** *Western Blot of S6K1 (phospho T389 and T412) was performed in HepG2 cells incubated for 6 hours in DMEM in the presence of 4 mM Gln and/or 4 mM MSO or 4mM PPT. S6K1 total was used as a loading control. The experiment was repeated three times with comparable results.*

The functional consequences of mTOR activation were directly investigated measuring the rate of protein synthesis. MSO and PPT did not produce any changes in protein synthesis, when added in presence of Gln (Fig. 31); however protein synthesis rate was significantly hindered by Gln starvation and GS inhibitors caused a further decrease of Leu incorporation, suggesting that, despite mTOR activation, cell Gln availability was further decreased in the presence of GS inhibitors.

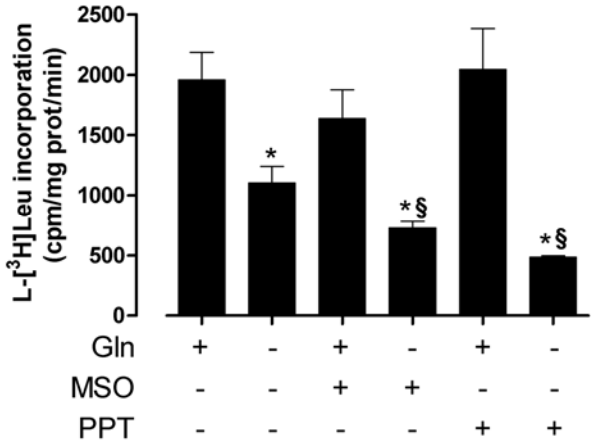

Fig. 31 ***MSO and PPT affected protein synthesis rate in Gln starved cells.*** *HepG2 cells incubated for 6 hours in DMEM with or without 4 mM Gln alone or in combination with 4 mM MSO or 4mM PPT. Protein synthesis rate was measured as described in Methods. A single representative experiment is shown. * p<0.05 vs. Gln fed cells, § p<0.05 vs. Gln starved cells.*

4.1.3.2 MSO prevents mTOR inactivation caused by Gln and EAA depletion

To asses if GS inhibitors synergized with essential amino acids (EAA) to stimulate mTOR, HepG2 cells were incubated in an unsupplemented saline solution (EBSS) for 6 hours, in the absence or in the presence of Gln and EAA (for control) or of MSO or PPT alone or in combination with EAA. When added alone, MSO produced an increase in phosphorylation of S6K1, which was further raised by adding EAA simultaneously (Fig. 32).

Instead, while PPT alone was not able to prevent the dephosphorylation of S6K1, a powerful mTOR activation was detected upon EAA supplementation, reaching control levels (Gln + EAA).

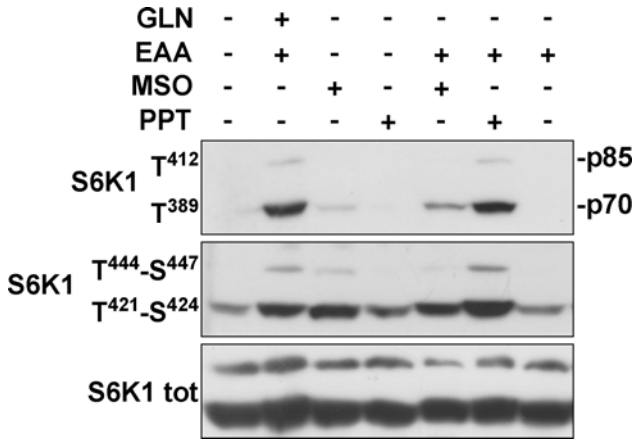

Fig. 32 ***MSO prevented mTOR inactivation.*** *Western Blot of p70S6K1 (phospho T389 and T421/S424), p85S6K1 (phospho T412 and T444/S447) was performed in HepG2 cells incubated for 6 hours in EBSS supplemented with the indicated compounds, alone or in combination: Gln (4 mM), EAA (1x, at the concentration present in DMEM), MSO (4 mM), PPT (4 mM). Total S6K1 was used as a loading control. The experiment was repeated three times with comparable results.*

Given the amino acidic structure of MSO and PPT (see Fig. 8), it was possible to verify their uptake by HPLC. Amino acid analysis revealed that MSO cell content was higher when added alone then when combined with EAA (Fig. 33), suggesting a competition in membrane transport. Instead, PPT content was higher when combined with EAA (Fig. 33) rather than given alone, suggesting that the higher effect on S6K1 phosphorylation may be due not only to the presence of EAA, since cell EAA were comparable to those measured in cells treated with MSO and EAA (not shown, see [153]), but to the increased amount of PPT.

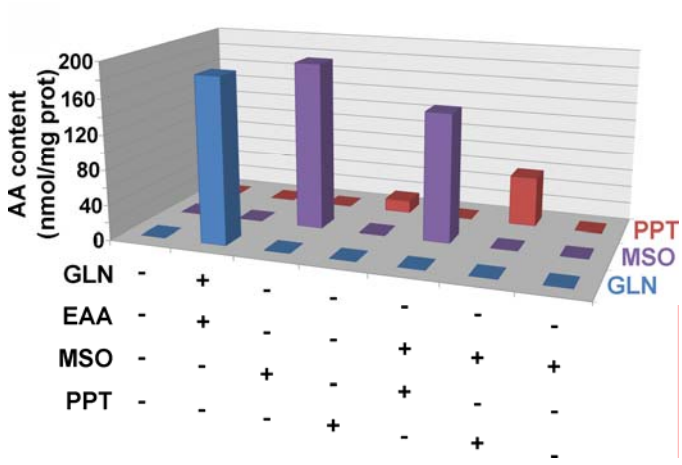

Fig. 33 ***PPT and MSO uptake.*** *Amino acids content was determined as described in HepG2 cells. The incubation medium was EBSS for 6 hours with or without Gln, MSO, PPT (all at 4 mM), Essential Amino Acids (EAA, at the concentration present in DMEM).*

Although it is not possible to identify the amino acid sensor upstream of mTOR, from these results, two important observations have emerged.

First, Gln is not only involved in Leu uptake but it really seems to have a direct effect on mTOR stimulation. Furthermore, the relationship between Gln and Leu uptake seems to be more complex than previously proposed [45]. It should be stressed that, if Gln activates mTOR, mTOR activation is known to promote Gln metabolism [47].

Second, two GS inhibitors, the non-proteinogenic amino acids MSO and PPT, besides further depleting cell Gln, activate mTOR. It has been proposed that this effect should be referable to the inhibition of GS activity [152, 154]; however considering the dose dependence and the affinity of GS for MSO and PPT [155], it is more likely that these two amino acids deceive sensors upstream of mTOR mimicking Gln and/ or Leu. Interestingly, MSO and PPT together were able, in the absence of Gln and EAA, to fully activate mTOR (data not shown). Hence, they could be

considered useful tools for assessing how amino acids are sensed by mTOR.

Thus, it is possible to conclude that not only EAA stimulate mTOR; however, further studies are needed to understand the basis of this activation, which is also involved in supporting uncontrolled cell growth in several cancer models.

4.2 Glutamine depletion is a potential therapeutic tool against selected types of cancer

Metabolic rewiring is now effectively considered a hallmark of cancer [1]. The metabolic relevance of Gln and the effects of Gln depletion are still objects of several studies. As described in Introduction (see 1.1.2 “Glutamine Addiction”: a new concept in cancer metabolism) Gln is the most abundant amino acid in serum and it is involved is several roles: nucleotides and protein synthesis, essential amino acids uptake (as described above), synthesis of other non essential amino acids (i.e. glutamate, asparagine, serine, praline). Moreover Gln is used as an anaplerotic substrate in different kind of cancers to fuel cell growth [35]. For this reason, targeting glutamine metabolism may prove a useful tool for cancer control.

4.2.1 “GS positive” human hepatocellular carcinoma (HCC) cell lines are sensitive to glutamine starvation

Gln is synthesized from glutamate and ammonium through the enzyme Glutamine Synthetase (GS). GS activity is regulated at both transcriptional and post-transcriptional levels [52, 53]. However, it has been demonstrated that the expression of *GLUL*, the gene coding for GS, is under β-catenin control. β-catenin, a cytoskeleton protein, when mutated, may act as a monogenic transcription factor in several human tumors and, in particular, in HCC. Therefore, the effects of Gln depletion, obtained with the antitumor glutamine-depleting enzyme L-asparaginase (ASNase), from *E. chrysanthemi*, alone or in combination with the irreversible GS inhibitor (MSO), were evaluated on HCC cell lines, both *in vitro* and *in vivo*.

4.2.1.1 Glutamine starvation affects human HCC cell viability

4.2.1.1.1 ASNase depletes cell glutamine and inactivates mTOR

The β-catenin mutated HepG2 cell line and the β-catenin wild type Huh7 cell line were incubated in the presence of ASNase (1 U/ml) with or without 1 mM MSO for 24 hours. Amino acid analysis revealed that ASNase caused a clear cut decrease in Gln content in both cell lines, while MSO presence during ASNase treatment caused a further decrease of Gln content which fell under analytical detection limits (< 1 nmol). Moreover HepG2 cells showed higher Gln content compared to Huh7 and accumulated more GS inhibitor (Fig. 34). We have indeed demonstrated that MSO uptake is mediated by system A transport [136] which is more expressed in HepG2 cells (not shown).

As a consequence of the intracellular Gln decrease caused by ASNase treatment, mTOR activity, evaluated from the phosphorylated status of S6K1, was severely decreased 6 hours after treatment in HepG2 cells and, at later times, in Huh7.

One of the consequences of the nutritional stress caused by amino acid shortage, is the phosphorylation, at residue S51, of the *eukaryotic initiation translation factor 2α* (eIF2α) [156] operated by the *general control non repressed 2* (GCN2), a serine/threonine kinase that senses amino acid deficiency through binding to uncharged tRNA. Consistently, in ASNase treated cells it was observed an increase in the phosphorylated fraction of eIF2α, more evident in HepG2 cells (Fig. 35). However, MSO caused paradoxical effect not only in mTOR activation (see 4.1.3 Glutamine Synthetase inhibitors activate mTORC1) but also in the inactivation of eIF2α (Fig. 35), confirming the hypothesis that it deceives cellular amino acid sensors.

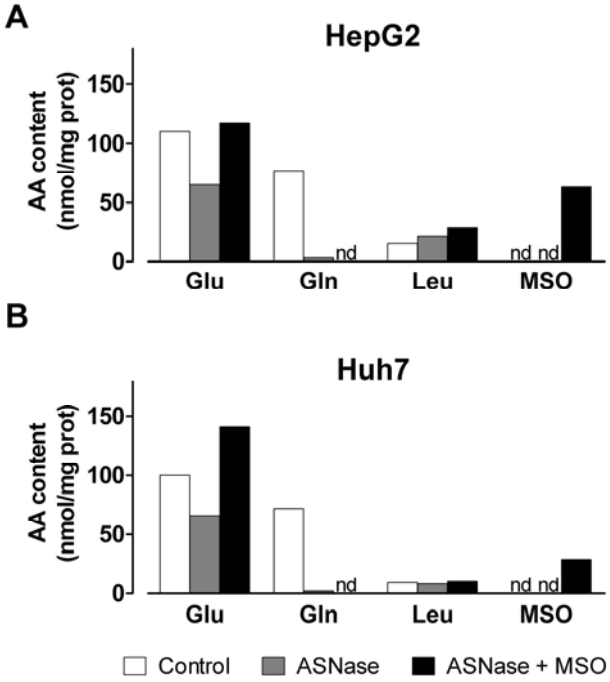

Fig. 34 ***ASNase lowered Gln intracellular content in HCC cells.*** *Amino acid content was determined as described in HepG2 (A) and Huh7 (B) cells incubated for 24 hours in DMEM supplemented with 1 U/ml ASNase (A) or 1 U/ml ASNase with 1 mM MSO (AM). A single representative experiment is shown.*

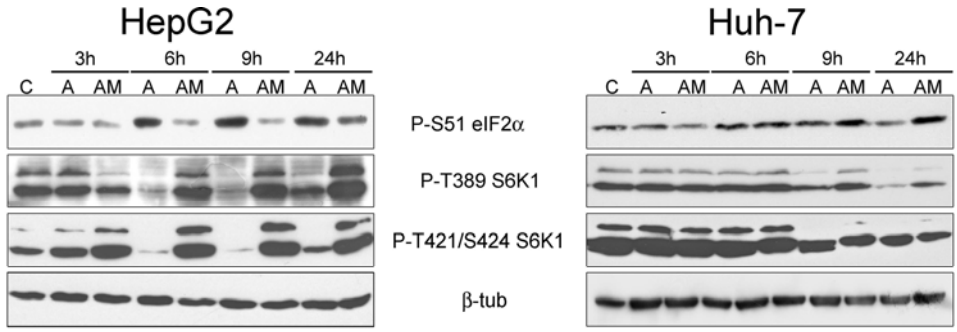

Fig. 35 ***ASNase lowered mTOR activity and caused the phosphorylation of eIF2α.*** *Western Blot of p70S6K1 (phospho T389 and T421/S424), eIF2α (phospho S51) was performed in HepG2 and Huh7cells incubated, for the indicated times, in DMEM with 1 U/ml ASNase (A) or 1 U/ml ASNase with 1 mM MSO (AM). β-tubulin was used as a loading control. The experiment was repeated three times with comparable results.*

4.2.1.1.2 β-catenin-mutated HepG2 and Huh6 cell lines are extremely sensitive to Gln starvation.

β-catenin-mutated HepG2 (HCC) and Huh6 (HB) cells and β-catenin wild type Huh7 (HCC) cells were incubated in DMEM for 72 hours with decreasing Gln concentrations. Cell count revealed that β-catenin mutated cells were more dependent on the extracellular Gln concentration than Huh7 (Fig. 36).

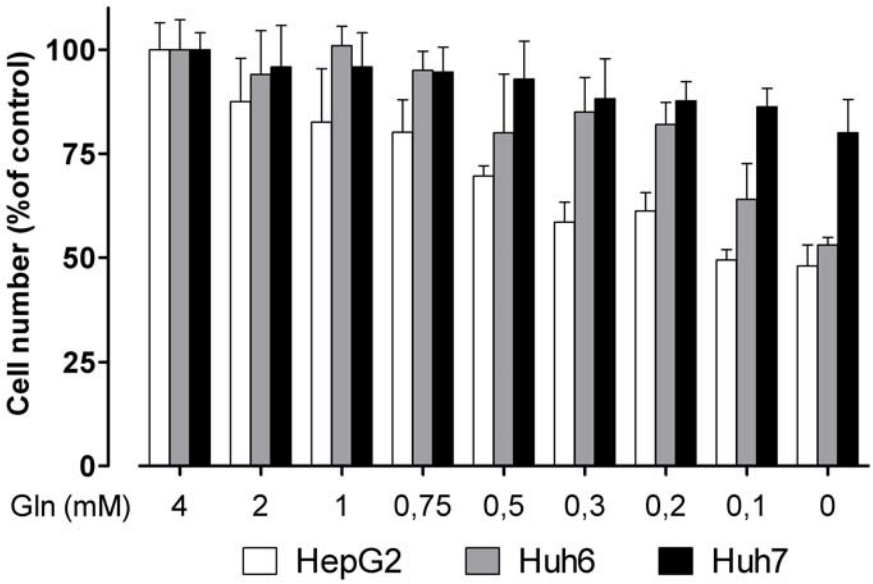

Fig. 36 β-*catenin-mutated cell number was affected by Gln shortage.* *HepG2, Huh6 and Huh7 cells were incubated in DMEM supplemented with 10% dialyzed FBS and the indicated concentrations of Gln. After 72 hours, cells were rinsed and counted. Data are expressed in % of each control (4 mM fed cells). Means of five determinations ± SD are shown.*

Then, HepG2, Huh6 and Huh7 cells were incubated with ASNase, ASNase and MSO or MSO alone. Cell count confirmed the higher sensitivity of β-catenin mutated cells to Gln starvation, obtained with ASNase. Furthermore, the incubation in the presence of both ASNase and the GS inhibitor caused a dramatic fall in the cell number of β-catenin-mutated cell population (Fig. 37 and Fig. 38). Also Huh7 cell population was affected when MSO was added to the glutamine-depleting enzyme. However MSO alone, *in vitro*, had no effect in all the cell lines tested (Fig. 37), suggesting that GS activity is critical only during Gln deprivation. Nevertheless, since MSO competes with Gln for system A transport, it cannot be excluded that in the presence of 4 mM Gln, MSO uptake could be partially inhibited.

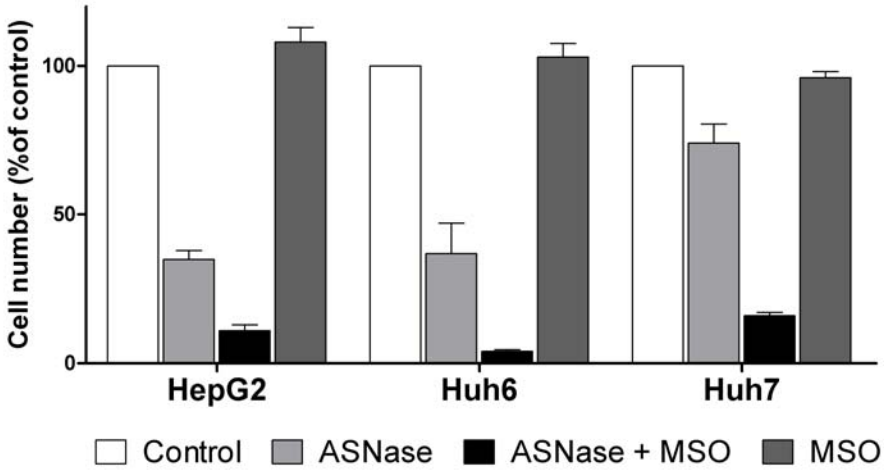

Fig. 37 ***ASNase severely affected β-catenin-mutated cell population.*** *HepG2, Huh6 and Huh7 cells were incubated in DMEM in the presence of ASNase (1 U/ml) or MSO (1 mM) or with the two compounds together. Control cells were incubated in standard growth medium. After 72 hours, cells were counted. Data are expressed in % of each control (4mM fed cells). Means of five determinations ± SD are shown.*

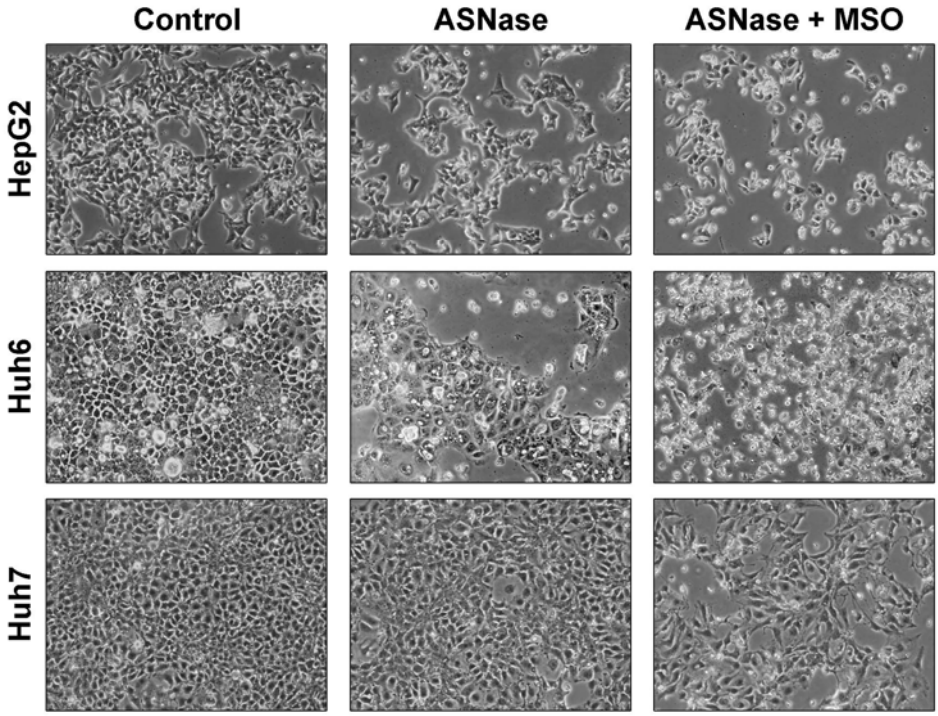

Fig. 38 ***ASNase severely affected β-catenin-mutated cell population.*** *HepG2, Huh6 and Huh7 cells were incubated in DMEM in the presence of ASNase (1 U/ml) or MSO (1 mM) or with the two compounds together. Control cells were incubated in standard growth medium. After 72 hours, cells were photographed. Single representative fields of each condition are shown, 100x.*

Furthermore, it should be noticed that the effect of ASNase, compared with that obtained just incubating cells in the absence of extracellular Gln, was higher; indeed, in HepG2 cells ASNase caused a 65% cell loss while the incubation in the absence of Gln caused only a 52% loss of cell population. It is likely that the ASNase treatment is more severe since the enzyme maintains a very high transmembrane gradient of Gln thus causing a fast efflux of the amino acid from the intracellular compartment.

4.2.1.1.3 In HepG2 cells Gln is utilized as an anaplerotic substrate.

Gln can enter Krebs cycle through a first deamidation operated by glutaminase (GLS1 and GLS2); subsequent deamination by glutamate dehydrogenase (GDH) or transamination, eventually produces the α-ketoglutaric acid (αKG, 2-oxo-glutarate) from Gln. In HepG2 cells, but not in Huh7 cells, other anaplerotic substrates, such as pyruvate and αKG, mitigate ASNase effects (Fig. 39), confirming that Gln fuel Krebs cycle in this model.

Consistently with these data, it was observed by another research group that HepG2 cells utilize Gln as predominant anaplerotic precursor [157], confirming that HepG2 cells is effectively a “glutamine addicted” model.

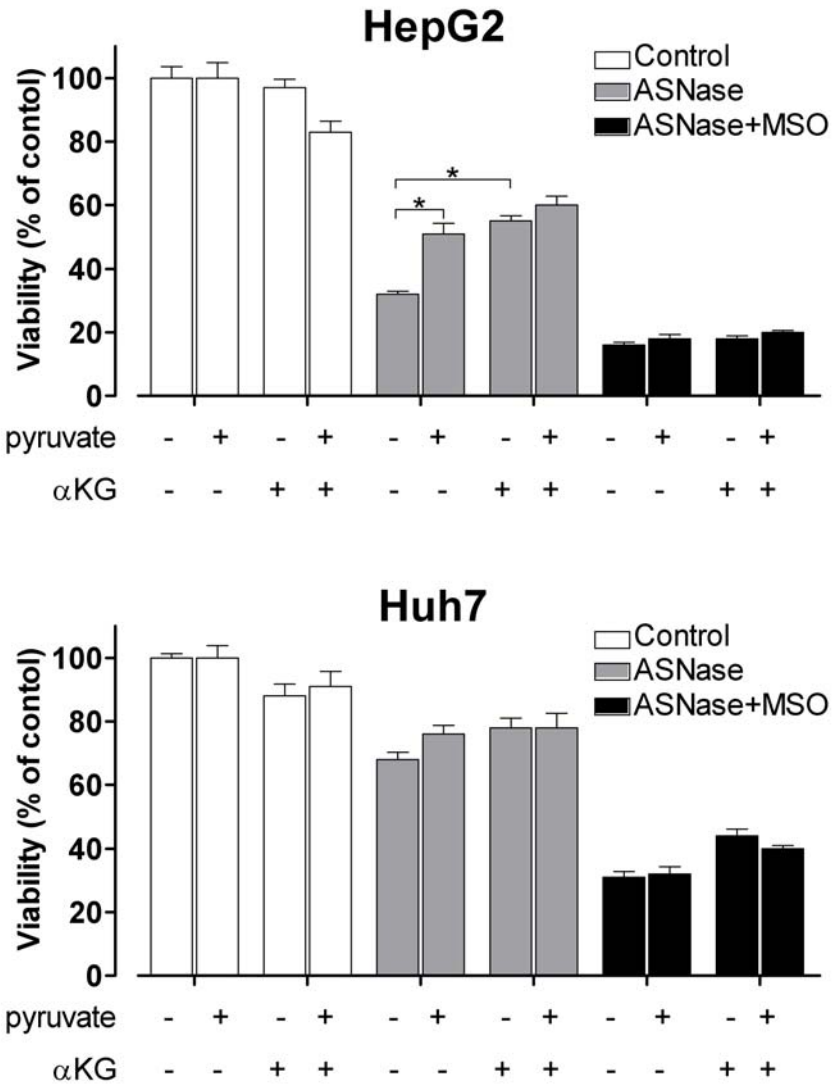

Fig. 39 ***Pyruvate and αKG mitigated ASNase antiproliferative effects.*** *HepG2 and Huh7 cells were incubated in DMEM (pyruvate-free) with ASNase (1 U/ml) and ASNase + MSO (1 mM) in the absence or in the presence of pyruvate (1 mM) and/or dimethyl α-ketoglutaric acid (αKG, 8 mM). Data are expressed as % of control (cells incubated in standard growth medium). Means of two experiments with four determinations each, ± SD are shown. * $p < 0.05$ compared with ASNase-treated cells.*

4.2.1.1.4 Notch pathways are not involved in ASNase sensitivity

Notch and β-catenin pathways are known to overlap often. It has been demonstrated that in some kind of cancers (i.e. colon cancer), the membrane bound Notch physically associates with the active (unphosphorylated) form of β-catenin, reducing the WNT/ β-catenin signal independent of GS3Kβ activity [158]. Conversely, it has also been proven that in colorectal cancers, exhibiting an uncontrolled β-catenin due to APC mutations, a downstream Notch activation occurs. This activation is due to a β-catenin-dependent overexpression of the Notch ligand Jagged 1 [159]. Taking into account the interaction between Notch and β-catenin pathways and the fact that many HCC cells do express Notch, which is, in addition, correlated to a poor prognosis [160], we evaluated the effects of Notch inhibition in our models. Since Notch activation is mediated by γ-secretase, HCC cells were incubated with DAPT, a γ-secretase inhibitor, in the absence or in the presence of ASNase (1 U/ml).

Cell count revealed that not all the cell lines were sensitive to DAPT, with a maximal anti-proliferative effect of 20% at the highest DAPT dose (75 μM) obtained in HepG2 cells (Fig. 40). Moreover no effect of DAPT was observed in ASNase treated Huh6 cells and only a partial addition of the highest dose (75 μM) of DAPT with ASNase was observed in HepG2 cells (Fig. 40). In Huh7 cells ASNase did not affect cell proliferation and DAPT effects were similar in ASNase-treated and untreated cells (Fig. 40).

However, measuring in parallel experiments the mRNA abundance of HES-1, a direct Notch target, it was evident that in all the cell lines an inhibition of Notch had effectively occurred (Fig. 41). HES-1 decrease was higher in HepG2 cells, consistent with the larger effects of the γ-secretase inhibitor on cell proliferation in this cell line.

Moreover the expression of c-myc, another downstream target of Notch, was evaluated. Unlike HES-1, c-myc behaved differently depending on cell

type. In fact, c-myc expression in Huh7 cells did not change, in HepG2 halved, and in Huh6 almost doubled (Fig. 42).

This behaviour does not negate the effects of Notch inhibition, since c-myc is also a direct β-catenin target. So, considering the complex mutual relationship linking these oncogenic signals [158, 159], it is possible that, as a consequence of Notch inhibition, changes in β-catenin status may occur.

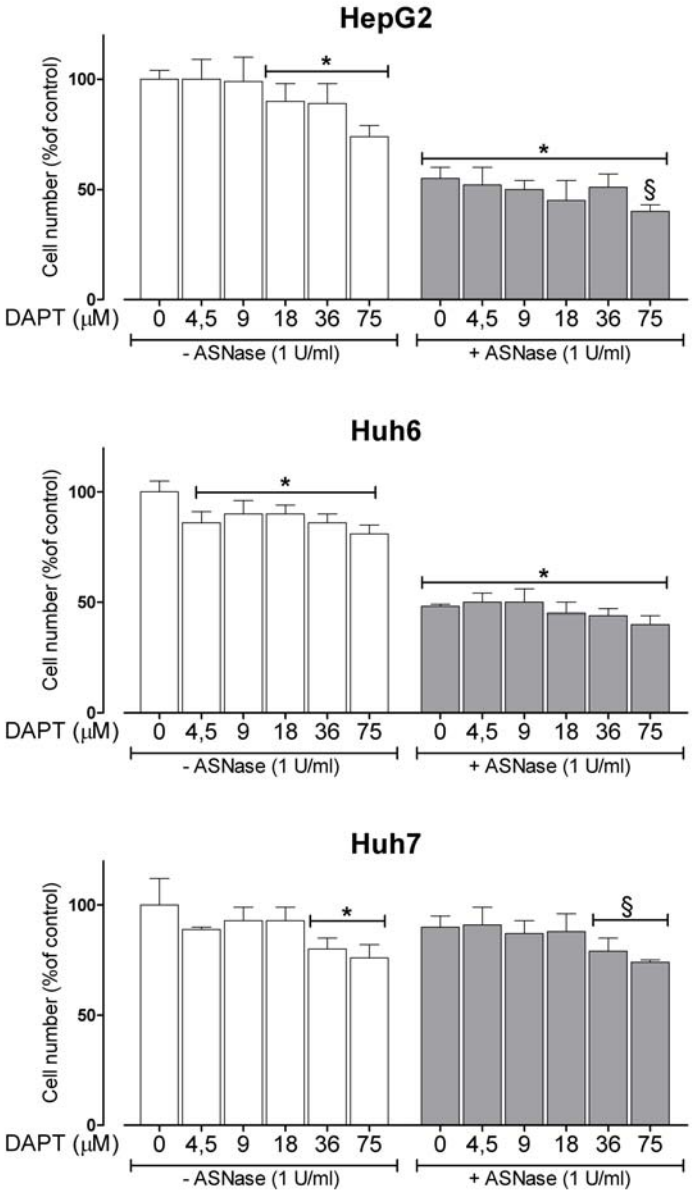

Fig. 40 ***Notch inhibitors did not synergize ASNase.*** *HepG2, Huh6 and Huh7 cells were incubated in DMEM in presence of the indicated concentrations of DAPT in the absence or in the presence of ASNase (1 U/ml). Control cells were incubated in standard growth medium. After 72 hours, cells were counted. Data are expressed in % of the corresponding control. Means of three experiments with six determinations each ± SD are shown. * p< 0.05 vs. control cell, § p< 0.05 vs. ASNase-treated cells.*

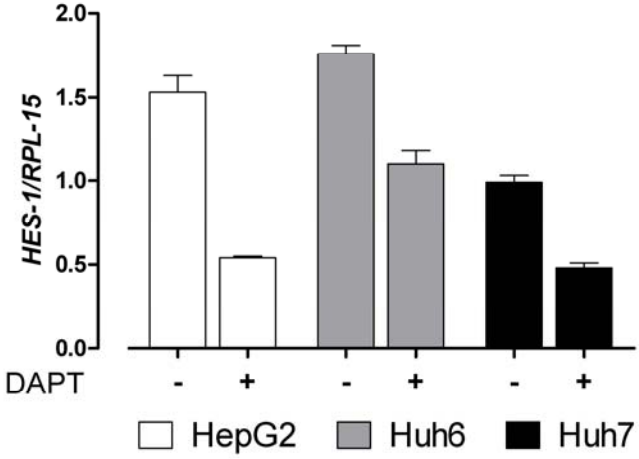

Fig. 41 ***DAPT lowered HES-1 expression.*** *HES-1 expression was analyzed by RT-qPCR. HepG2, Huh6 and Huh7 cells were incubated in DMEM with DAPT (+, 75 µM) or in standard growth medium (-). Relative HES-1 mRNA abundance was normalized to RPL-15 and expressed as Arbitrary Units.*

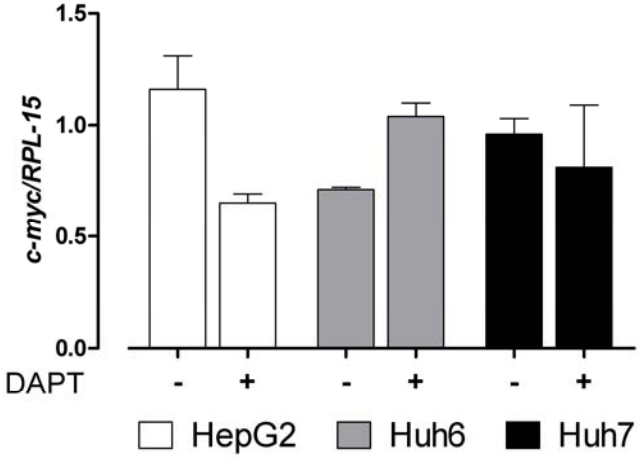

Fig. 42 ***c-myc expression showed different dependency on DAPT depending on the cell model.*** *HepG2, Huh6 and Huh7 cells were incubated in DMEM with DAPT (75 μM) or in standard growth medium (-). Relative c-myc mRNA abundance was normalized to RPL-15 and expressed as Arbitrary Units.*

4.2.1.1.5 β-catenin silencing mitigates ASNase effects

Given that Notch inhibition did not modify ASNase effects on all the cell lines tested (see above), a direct involvement of this pathways on "glutamine addicted" cancer phenotype is unlikely. Furthermore it is known that β-catenin controls the expression of GS and c-myc, which in turn regulates the expression of GLS1 [75]. Thus, two key enzymes of Gln metabolism seems to be under direct or indirect β-catenin control, suggesting a straight involvement of this oncogene in leading to a "glutamine addicted" HCC.

To confirm this hypothesis, the effects of ASNase were evaluated on β-catenin- silenced HepG2 and Huh6 cells. The silencing procedure determined a clear cut fall in β-catenin (*CTNNB1*) mRNA content (> 70%) in both cells lines (Fig. 43). Furthermore, compared with scramble-

transfected cells, β-catenin was still heavily down-regulated 6 days after transfection in *CTNNB1*-silenced cells (Fig. 43).

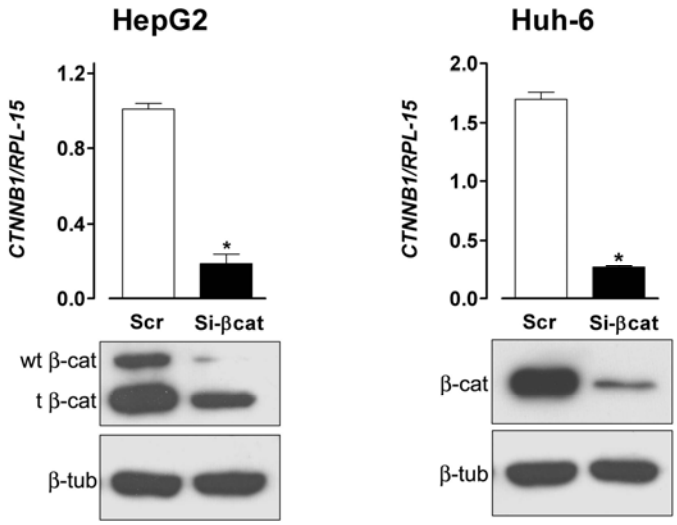

Fig. 43 ***β-catenin was still down-regulated 6 days after gene silencing.*** *CTNNB1expression was analyzed by RT-qPCR in HepG2 and Huh6 cells 2 days after transfection (upper). Relative CTNNB1 mRNA abundance was normalized to RPL-15 and expressed as Arbitrary Units. β-catenin protein expression was evaluated by Western blot in parallel cultures 6 days after transfection (bottom). β-tubulin was used as a loading control. For PCR means of four different experiments with SD are shown. *p < 0.05. For Western blot, a representative experiment of three is shown.*

To verify that the silencing procedure reduced not only β-catenin protein levels but also its activity, the expression of the β-catenin downstream targets, cyclin D1 (*CCND1*) and c-myc, was monitored. In addition, the c-myc-downstream target GLS1 was also evaluated. As shown in Fig. 44, both cyclin D1 and c-myc expression decreased (60% and 40% respectively). Moreover also the c-myc downstream target GLS1 mRNA expression decreased (about 30%), strengthening the link between β-catenin and Gln metabolism.

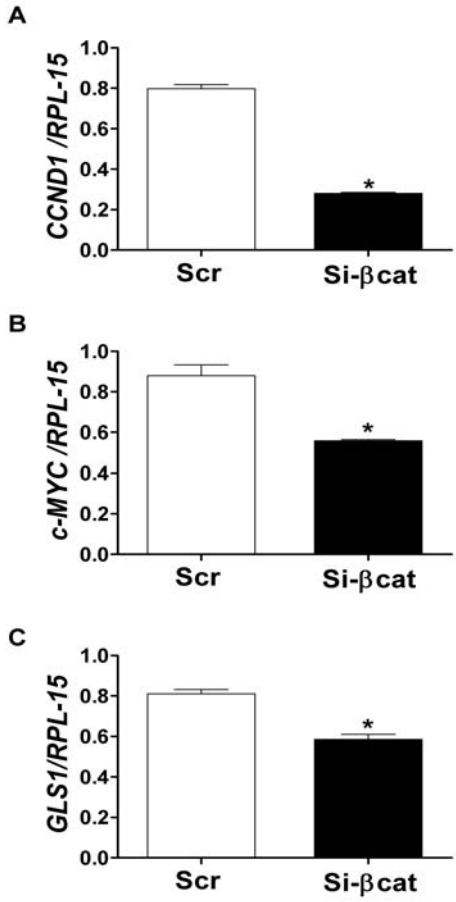

Fig. 44 ***β-catenin downstream target expression was lowered in silenced cells.*** *CCND1 (A), c-MYC (B) and GLS1 (C) expression in HepG2 silenced cells was analyzed by RT-qPCR. Relative CCND1 (A), c-MYC (B) and GLS1 (C) mRNA abundance was normalized to RPL-15 and expressed as Arbitrary Units. Data are means ± SD of three independent experiments.*

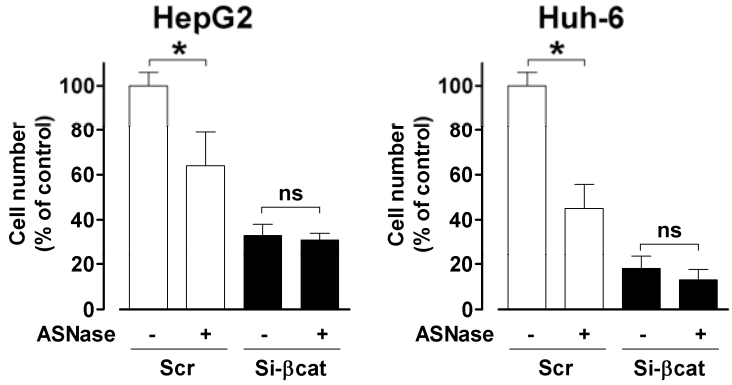

Fig. 45 ***ASNase did not affect β-catenin-silenced cell viability.*** *3 days after transfection, scramble- (Scr) and β-catenin- (Si-β-cat) silenced HepG2 and Huh6 cells were incubated in the absence or in the presence of ASNase (1 U/ml). After 72 hours cells were counted. Data represent the means ± SD of three independent experiments whit four determinations each. * p< 0.05; ns, not significant.*

In β-catenin silenced cells, a 3-day treatment with ASNase (from day 3 to day 6 after transfection) significantly lowered the number of HepG2 and Huh-6 cells transfected with scrambled siRNA but had no significant effect in β-catenin-silenced cells (Fig. 45). However, it should be also noticed that β-catenin downregulation itself severely hindered cell proliferation.
These data support the involvement of β-catenin in the enhanced sensitivity to ASNase of HCC mutated cell lines.

4.2.1.1.6 Glutamine availability seems to influence β-catenin activity

We have demonstrated that β-catenin influences Gln metabolism, yet it is unknown if, conversely, Gln availability may influence β-catenin activity.
ASNase effects on β-catenin activity were assessed with the TOPflash reporter assay, which is a direct and reliable measure of the β-catenin/Tcf-dependent transcriptional activity [161].

In ASNase-treated Huh6 cells, a significant increase of luciferase activity was observed (Fig. 46). Also in HepG2 cells a slight increase of the reporter activity occurred in the same experimental condition but it did not reach a statistical significance. Interestingly the luciferase activity was 20-fold higher in HepG2 cells than in Huh6 (Fig. 46), suggesting that in the former cell model the deletion of exon-3 of *CTNNB1* gene leads to a more active β-catenin than the point mutated *CTNNB1* gene of the latter.

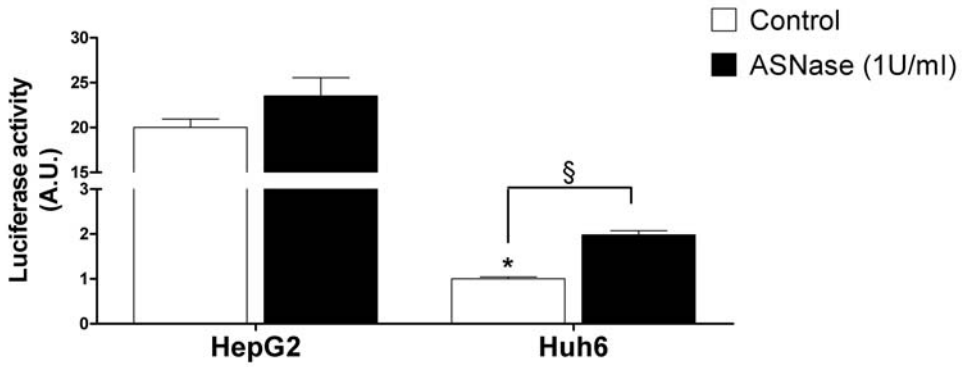

Fig. 46 ***ASNase increased luciferase activity in Huh6 cells.*** *HepG2 and Huh6 cells were incubated in presence of ASNase (1 U/ml) or in standard growth medium for control. After 6 hours cells were transfected with both Firefly luciferase, under the control of a TCF enhancer, and Renilla luciferase, used as internal control for transfection efficiency. After 24 hours, luciferase assay was performed. Data are expressed as relative Firefly/Renilla luciferase activity. Results are mean ± SD of two independent experiments with two determination each. § p<0.05 referred to control; * p<0.05 compared to HepG2 control luciferase activity.*

However, the same experiment performed in Gln-deprived cells yielded inconsistent results. It should be noted that, since ASNase and Gln deprivation causes a strong nutritional stress, followed by protein synthesis attenuation and loss in cell viability it cannot be excluded that the effects of the treatments on luciferase activity might be confused by different translational rates.

In conclusion, ASNase caused a clear cut decrease of Gln intracellular content in all the cell lines tested, which, in turn, determined a decrease in mTOR activity and the phosphorylation of eIF2α. This condition affected the viability of β-catenin-mutated HCC and HB cell lines, but not that of β-catenin wild type Huh7 HCC line. MSO alone, which *in vitro* did not produce changes either in Gln content (not shown, see [136]) or in cell proliferation rate, further depleted cell Gln by inhibiting GS activity (see [136]) and deceived amino acid sensors. This condition led to a marked cell viability loss in all the cell lines tested, even in the ASNase-resistant line. Anaplerotic substrates mitigated ASNase effects in the β-catenin mutated HepG2 cell line, suggesting that mutated β-catenin leads to a Gln-addicted phenotype. This hypothesis is strengthened by two observations:

1. β-catenin-silenced HepG2 and Huh6 cells no longer responded to ASNase;
2. the inhibition of other pathways (at least Notch) did not produce any changes in the cell response to ASNase.

These results prompted us to evaluate the effects of Gln depletion on HCC xenografts models.

4.2.1.2 ASNase and MSO affect the growth of HCC xenografts

4.2.1.2.2 ASNase and MSO treatment is well tolerated

Before establish HCC xenografts, the toxicity of the combined treatment with ASNase (5 U/g) and MSO (10 mg/kg) was assessed in nude mice.

The combined treatment, administered three times a week for three weeks, was well tolerated by athymic nude mice, with no significant alteration in body and liver weights (Fig. 47 A, B).

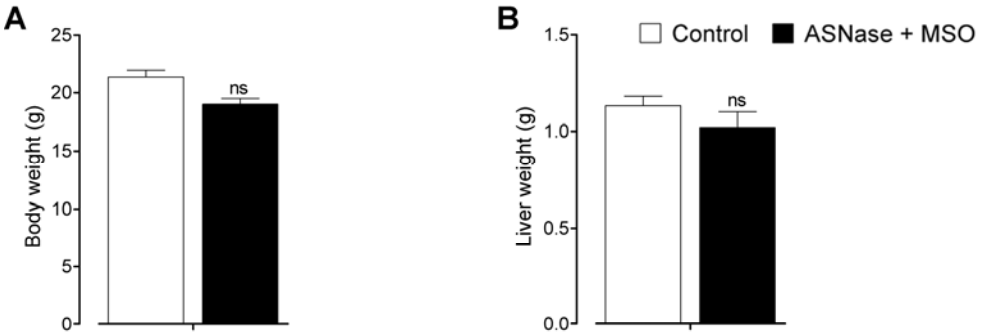

Fig. 47 ***ASNase and MSO was not toxic for nude mice.*** *Male athymic nude mice were treated by intraperitoneal (i.p.) injection of ASNase and MSO three times a week for three weeks. At the end, body (A) and liver weight (B) were determined. Data represent means ± SD of a single experiment with three mice for each group.This experiment was performed at LIGeMa by the group of Prof. Arcangeli.*

To evaluate the biochemical effect of the treatment, serum and liver amino acids were determined in control and treated mice. In serum, major changes were observed for asparagine (Asn) and Gln, which disappeared in the serum of treated animals, whereas aspartate (Asp) and glutamate (Glu) levels markedly increased (Fig. 48). MSO was also detected.

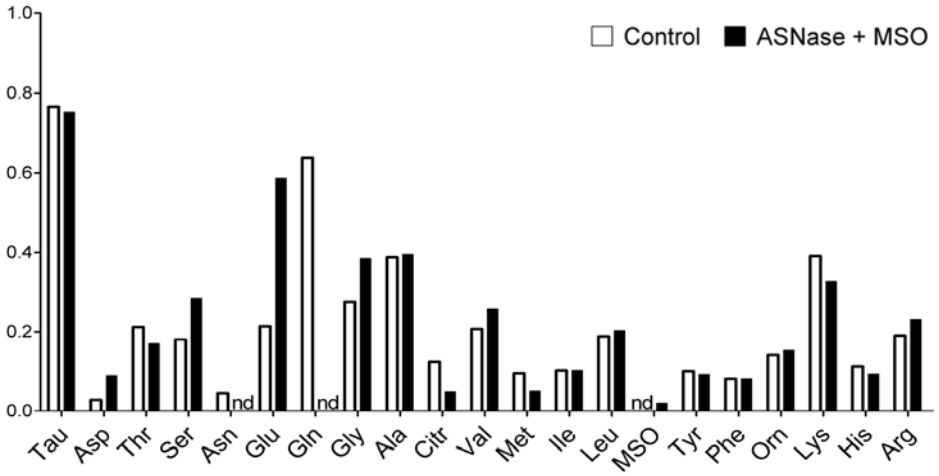

Fig. 48 ***ASNase and MSO depleted serum Gln in mice.*** *Male athymic nude mice were treated with ASNase and MSO for three weeks. At sacrifice, peripheral blood was collected, serum extracted and amino acid content analyzed by HPLC. A representative experiment is shown.*

Moreover ASNase and MSO treatment caused a significant decrease in liver Gln content; in liver homogenates of treated animals a small amount of MSO was detected (Fig. 49 A), demonstrating the tissue uptake of the inhibitor. Consistently, the activity of Glutamine Synthetase (GS), determined in parallel in the same samples, was lowered by more than 97% in treated animals compared with control (Fig. 49 B).

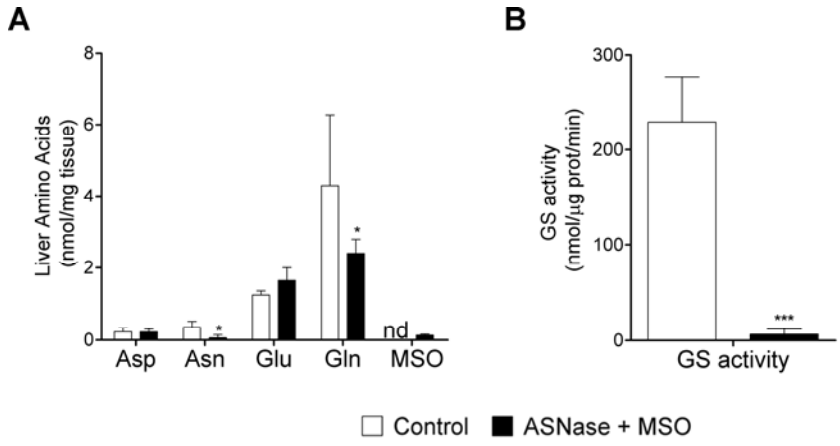

Fig. 49 ***MSO entered liver and inhibited liver GS.*** *Male athymic nude mice were treated with intraperitoneal (i.p.) injections of ASNase and MSO. At sacrifice, liver was explanted and analyzed. A. Amino acid content was analyzed by HPLC. Means (n=3) ± SD are shown. * p<0.05 B. Liver GS activity was measured as described in Methods. Means (n=3) ± SD are shown. ***p<0.001.*

4.2.1.2.2 ASNase and MSO treatment suppresses HepG2 xenografts.

2.5 million cells were subcutaneously (s.c.) injected in athymic nude mice. After 8 days, tumors were palpable and treatment started. Five mice per group (four for MSO group) were treated with ASNase or MSO, with both drugs together or with vehicle for control.

After 19 days of treatment, at sacrifice, the growth of HepG2 xenografts resulted suppressed in mice undergone the combined treatment, while it was significantly hindered (by 51% and 60%, respectively) in animals treated with ASNase or MSO alone. Consistently, the weight of the explanted masses was significantly lower in animals treated with ASNase or MSO alone (34% and 61% respectively), while no tumor mass was dissectable in animals treated with ASNase and MSO together (Fig. 51). The effects of the different treatments on tumor growth were consistent with the macroscopic inspection of the xenografted animals (Fig. 52).

As shown in the picture, both single treatments caused a variable effect on tumor growth, while no mass can be noticed in mice receiving the combined treatment ASNase and MSO.

From histological evaluation, it was observed that, while β-catenin showed a normal membrane positivity in livers of mice, the protein signal was diffused and mainly into the nucleus in xenografts (Fig. 53), a clear indicator of its activated status.

Furthermore, HepG2 tumors were also positive for GS (Fig. 54 upper, top left) and the expression of the enzyme was appreciably increased by neither ASNase (Fig. 54, upper, top right) nor MSO (Fig. 54, upper, bottom left); no GS-positive cell was detected from animals treated with ASNase and MSO (Fig. 54, upper, bottom right) in tissue samples deriving from xenograft injection site. GS expression in the liver (Fig. 54, bottom) had the typical perivenous pattern of expression and was induced by ASNase, MSO or ASNase and MSO, with an extension of the expression to several rows of hepatocytes.

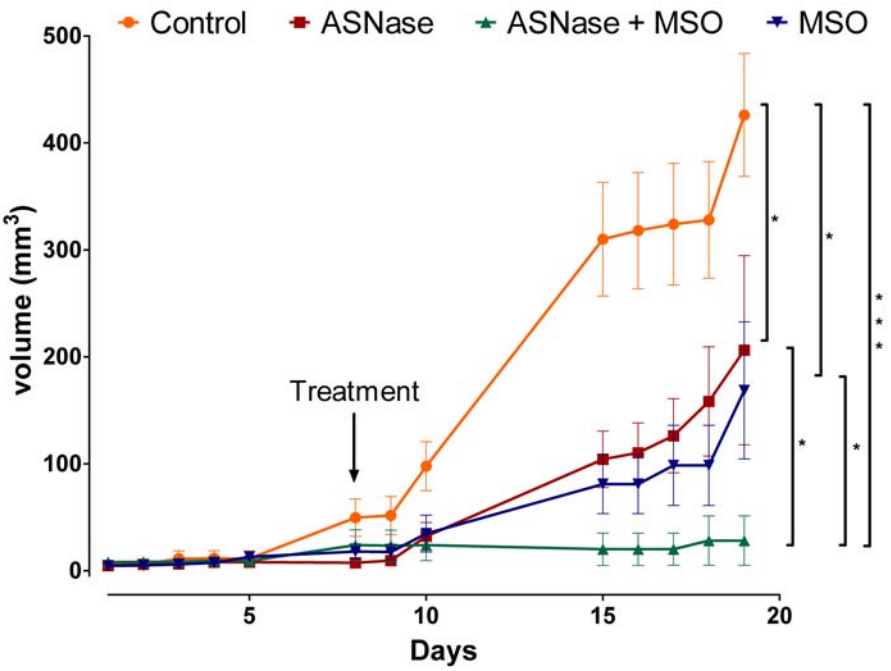

Fig. 50 ***ASNase and MSO suppressed HepG2 tumor growth.*** *8 days after HepG2 s.c. injection mice were treated i.p. with ASNase (5 U/g) or MSO (10 mg/kg), alone or together, or with vehicle, 3 times a week for 19 days. Tumor growth was measured with caliper. Means ± SD is shown (n=5, n=4 for MSO group). * p < 0.05; *** p < 0.001 assessed with two-tail Student's t test for unpaired data. This experiment was performed at LIGeMa by the group of Prof. Arcangeli.*

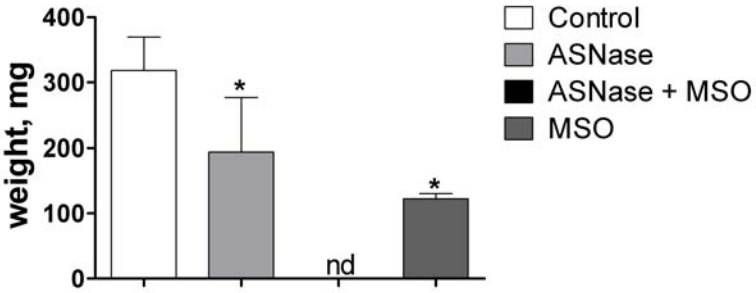

Fig. 51 ***No tumor was found in ASNase and MSO treated mice.*** *8 days after HepG2 s.c. injection mice were treated i.p. with ASNase (5 U/g) or MSO (10 mg/kg), alone or together, or with vehicle three times a week for 19 days. At the end, tumors were dissected and weighted. Means ± SD are shown (n=5, n=4 for MSO group). This experiment was performed at LIGeMa by the group of Prof. Arcangeli.*

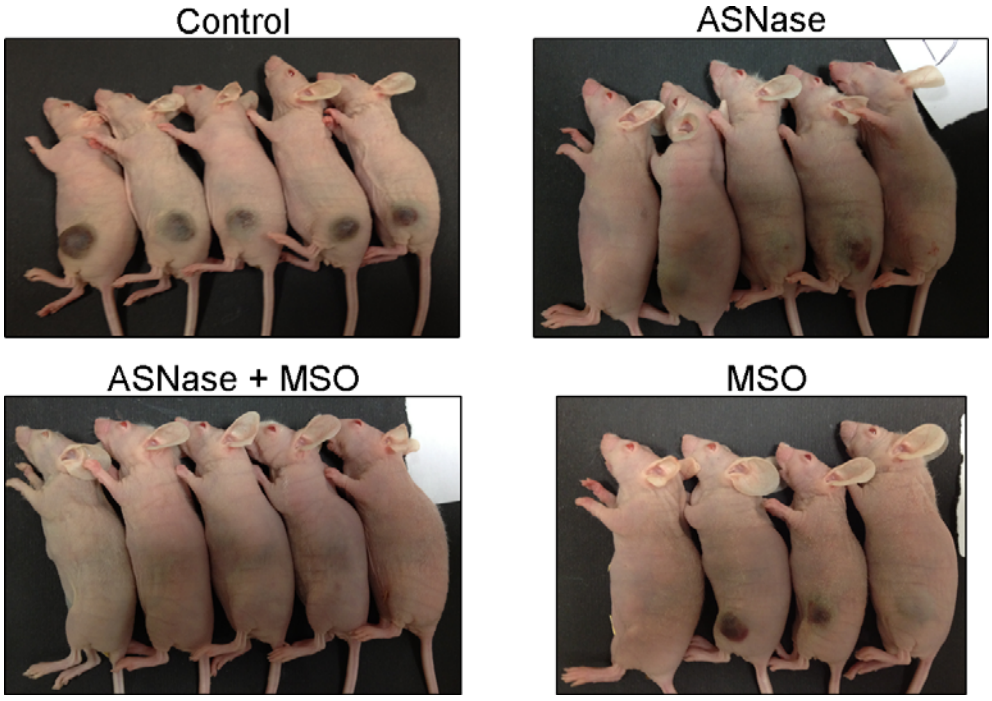

Fig. 52 ***HepG2 xenografts in mice.*** *Eight days after HepG2 s.c. injection mice were treated i.p. with ASNase (5 U/g) or MSO (10 mg/kg), alone or together, or with vehicle three times a week for 19 days. At the end, animals were anesthetized and photographed. This experiment was performed at LIGeMa by the group of Prof. Arcangeli.*

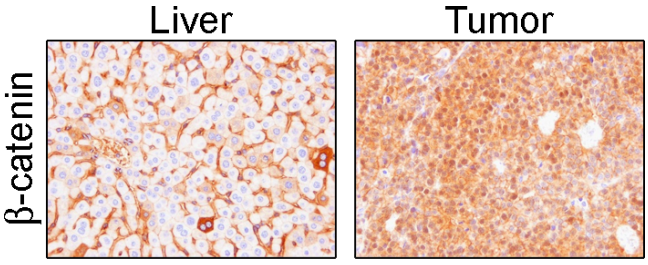

Fig. 53 ***β-catenin signal was diffuse in tumors.*** *Histochemical analysis of β-catenin expression in liver and HepG2 xenografts. A single representative field is shown, x40. This analysis was performed by the group of Prof. Silini.*

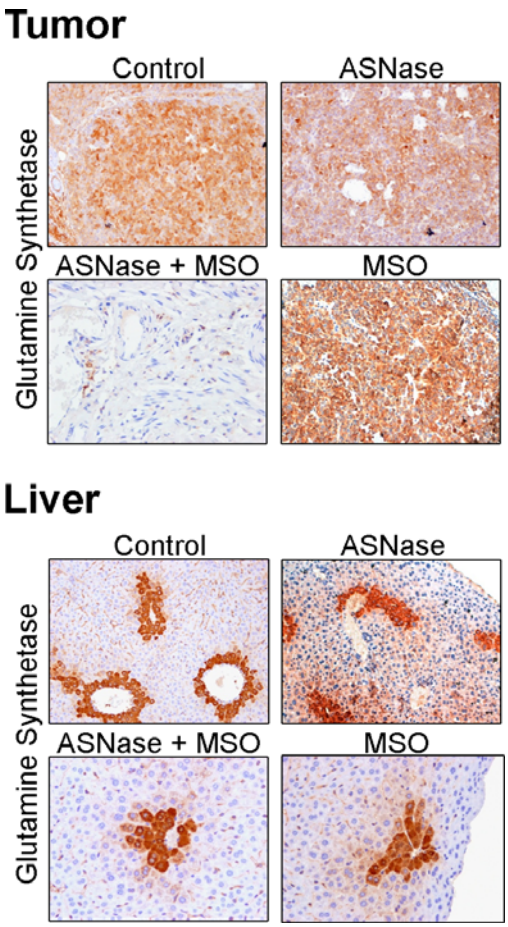

Fig. 54 ***GS was induced in liver of treated mice.*** *Histochemical analysis of Glutamine Synthetase (GS) expression in HepG2 xenografts (upper) and in liver (bottom). A single representative field for each condition is shown, x40. This analysis was performed by the group of Prof. Silini.*

From a biochemical point of view, both ASNase and ASNase and MSO treatment caused a marked depletion of Asn and Gln in serum with a consisted increase of Asp and Glu. MSO was detected in mice treated with ASNase and MSO or MSO alone (Fig. 55 A). The decrease of Asn and Gln in serum was also detected in tumor tissue of ASNase treated mice (Fig. 55 B). However, in these samples a fall in Glu content was also detected (Fig. 55 B), pointing to an attempt to synthesize *de novo* Gln through GS. For ASNase and MSO treated mice, no tumor was dissected, and it was not possible to evaluate amino acids.

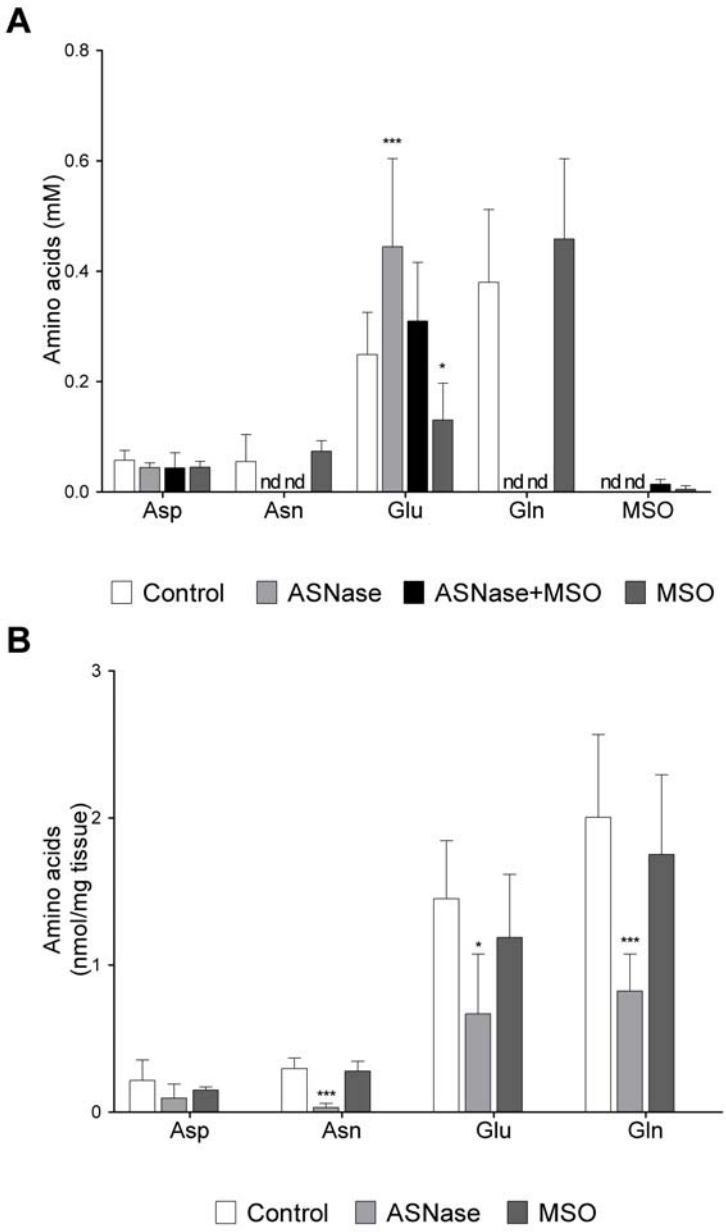

Fig. 55 ***ASNase lowered serum and tumor Asn and Gln content.*** *Eight days after HepG2 s.c. injection mice were treated i.p. with ASNase (5 U/g) or MSO (10 mg/kg), alone or together, or with vehicle three times a week for 19 days. At the end, amino acids were extracted as described in Methods and analyzed by HPLC. Means ± SD are shown (n= 5, n=4 for MSO group). *p<0.05; *** p<0.001*

4.2.1.2.3 The combined treatment ASNase and MSO is effective also in Huh7 xenografts.

To understand if the sensibility to the combined (ASNase and MSO) treatment was limited to β-catenin-mutated tumors, athymic nude mice were s.c. injected with HepG2 and Huh7 cells on each flank. After 2 weeks, both tumors were palpable and treatment started. After 3 weeks, a massive effect of the treatment on HepG2 xenografts was observed, confirming what previously demonstrated. However also Huh7 tumor growth was significantly impaired by the treatment (Fig. 56).

Determination of tumor volumes at sacrifice confirmed a marked inhibition of cancer cell growth in both HepG2 (- 91%) and Huh7 xenografts (- 46%), as shown in Fig. 57.

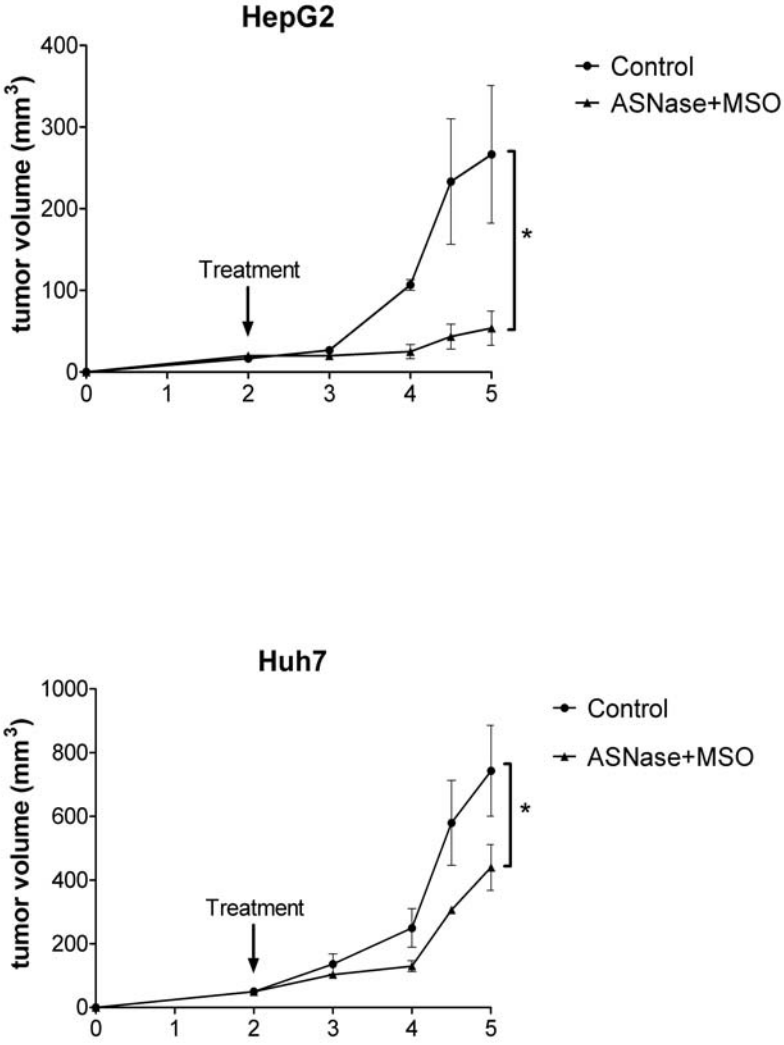

Fig. 56 ***The combined treatment (ASNase and MSO) is effective also in Huh7 xenografts.*** *HepG2 and Huh7 were simultaneously s.c. injected on the left and right flank of animals. After 2 weeks mice were treated i.p. with ASNase (5 U/g) and MSO (10 mg/kg) or with vehicle for control three times a week for three weeks. Tumor growth was monitored with caliper. Means ± SD are shown (n=3 each group). *p<0.05, assessed with two-tail Student's t test for unpaired data. This experiment was performed at LIGeMa by the group of Prof. Arcangeli.*

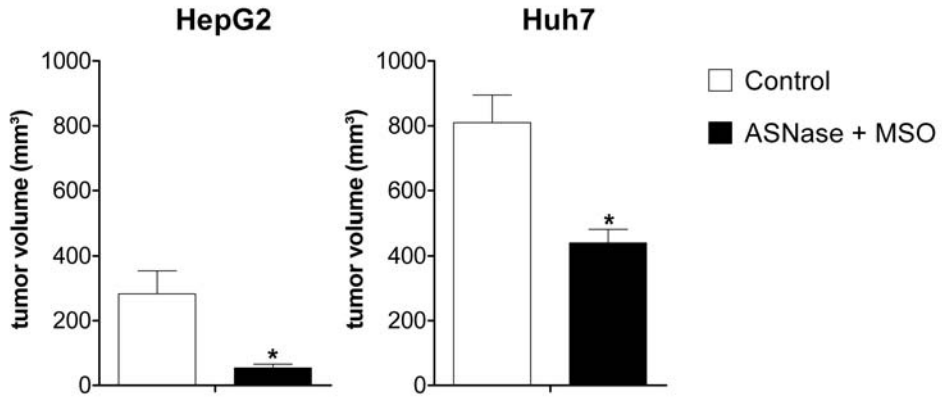

Fig. 57 ***The combined treatment affected Huh7 tumors.*** *HepG2 and Huh7 cells were simultaneously s.c. injected on the left and right flank of nude mice. After 2 weeks, mice were treated i.p. with ASNase (5 U/ml) and MSO (10 mg/kg), or with vehicle for control, three times a week for three weeks. At the end, masses were dissected and weighted. Means ± SD are shown (n=3). *p<0.05. This experiment was performed at LIGeMa by the group of Prof. Arcangeli.*

From these results, it is evident that depleting extracellular Gln (with ASNase) and inhibiting *de novo* Gln synthesis (with MSO) significantly affected HCC tumor growth. Yet, given the limited number of mice used (3 for each group) in this experiment, it has not been possible to evaluate if significant differences exist in the sensitivity of the two xenografts to the combined treatment.

4.2.1.3 β-catenin mutated HC-AFW1 cell line is ASNase-resistant in vitro but ASNase-sensitive in vivo.

4.2.1.3.1 HC-AFW1 cells over-express GS and resist to ASNase treatment

β-catenin-mutated paediatric HC-AFW1 HCC cells showed the classical nuclear localization of β-catenin, as demonstrated with immunofluorescence (Fig. 58). However, unlike HepG2 and Huh6 ASNase-sensitive cells, the viability of this model was not affected by ASNase alone (Fig. 59 and Fig. 60). In fact, only the combined treatment was able to severely hinder HC-AFW1 growth (Fig. 59 and Fig. 60).

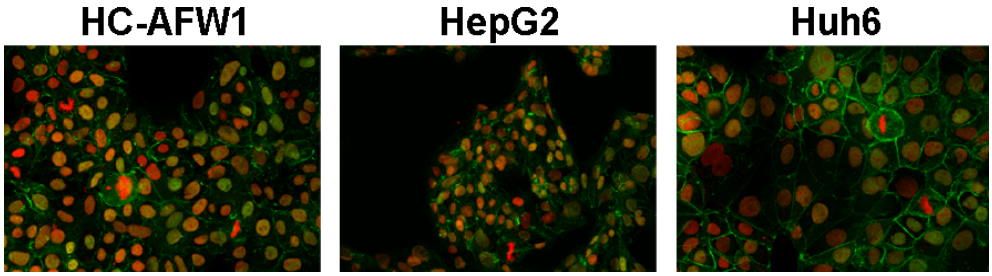

Fig. 58 ***β-catenin localization.*** *Merged immunofluorescence of β-catenin in HC-AFW1, HepG2 and Huh6. Nuclei, red; β-catenin, green. A single confocal section is shown.*

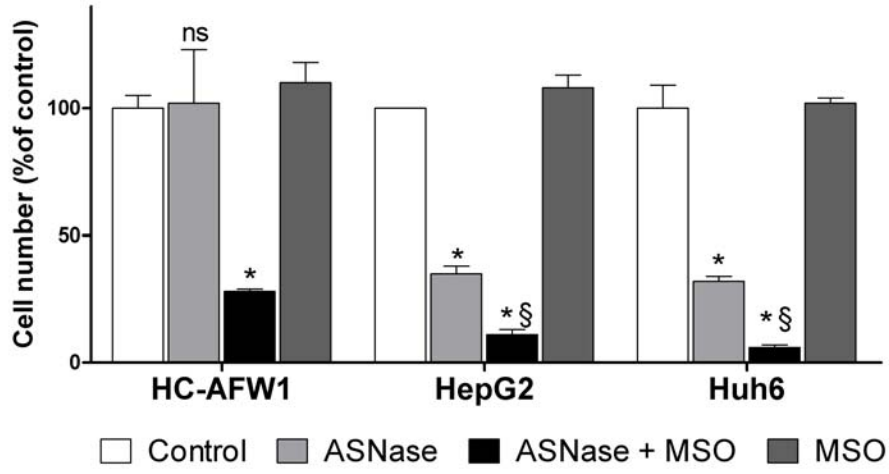

Fig. 59 ***HC-AFW1 cells were not affected by ASNase in vitro.*** *HC-AFW1, Huh6, and HepG2 cells were incubated in DMEM in the presence of ASNase (1 U/ml), with or without MSO (1 mM), or with MSO (1 mM) alone. Control cells were incubated in standard growth medium. After 72 hours, cells were counted. Data are expressed in % of the corresponding control, maintained in growth medium with 4 mM Gln. Means of two experiments with five independent determinations each ± SD are shown. *p < 0.05 compared with control; § p < 0.05 compared with ASNase treated cells; ns, not significant.*

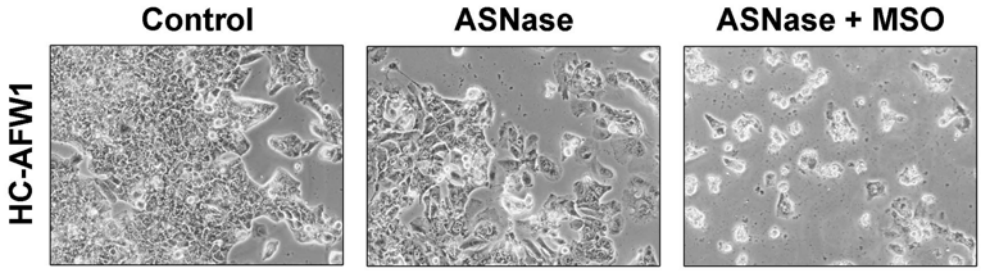

Fig. 60 ***HC-AFW1 cells were not affected by ASNase.*** *HC-AFW1cells were incubated in DMEM in the presence of ASNase (1 U/ml) with or without MSO (1 mM). Control cells were incubated in standard growth medium. After 72 hours, cells were photographed. Magnification 100x.*

HC-AFW1 cells expressed the highest level of GS, both at mRNA and protein level (Fig. 61, Fig. 62), compared with Huh6 and HepG2 cells. Furthermore HC-AFW1 cells showed lower levels of asparagine synthetase (*ASNS*) and of *SLC38A2* and *SLC1A5* (for the SNAT2 and ASCT2 transporters, Fig. 61) mRNAs compared with HepG2.

ASNase treatment decreased mTOR activity only in HepG2 and Huh6 cells, while it did not affected kinase activity in HC-AFW1 (Fig. 62), suggesting that a not completely fall of Gln intracellular content occurred in this cell model. The activation of mTOR in ASNase and MSO treated cells was not surprising (see paragraph 4.1.3 Glutamine Synthetase inhibitors activate mTORC1). GS protein abundance, which is regulated also by Gln availability [52, 53], clearly rose in HepG2 and Huh6 cells after 6 hours of ASNase treatment and, even further, after 24 hours, but in HC-AFW1 cells a slight increase was detected only 24 hours after ASNase administration.

Consistently, amino acid analysis revealed that, while in HepG2 and Huh6 cells ASNase completely depleted cell Gln, in HC-AFW1 cells intracellular Gln was still detectable (30% compared to control values) after 24 hours of ASNase treatment (Fig. 63).

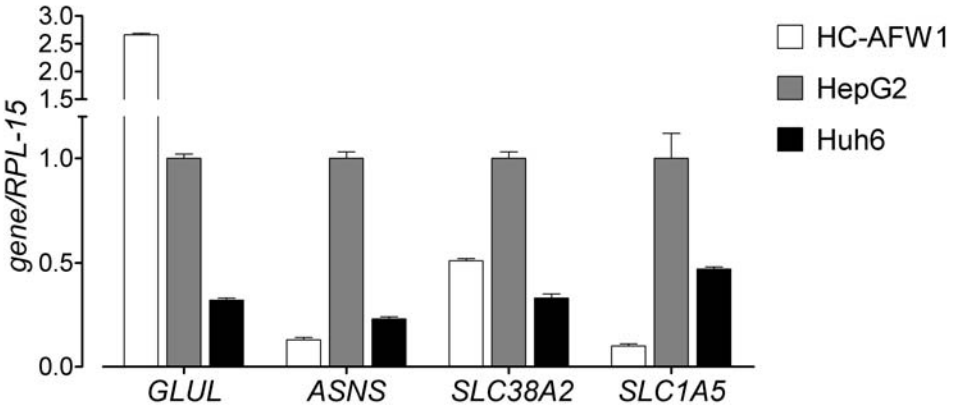

Fig. 61 ***HC-AFW1 cells expressed higher GLUL levels.*** *GLUL, ASNS, SLC38A2, and SLC1A5 expression levels were analyzed by RT-qPCR. Cells were incubated in standard growth medium. Relative gene mRNA abundances were normalized to RPL-15 and expressed as Arbitrary Units.*

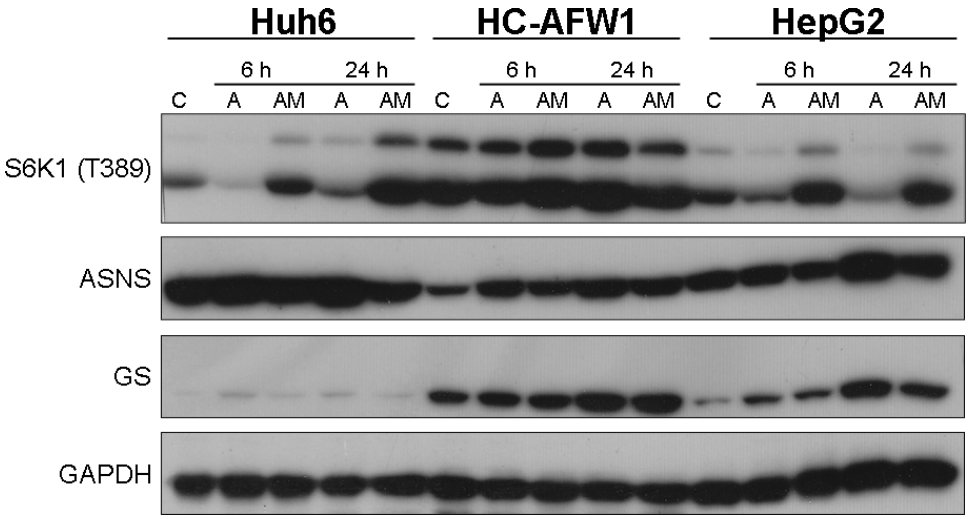

Fig. 62 ***ASNase did not inactivate mTOR in HC-AFW1 cells.*** *Western Blot of S6K1 (phospho T389), ASNS, and GS was performed in Huh6, HC-AFW1, and HepG2 cells incubated, for the indicated times, in DMEM with 1 U/ml ASNase (A) or 1 U/ml ASNase with 1 mM MSO (AM). GAPDH was used as a loading control. The experiment was repeated three times with comparable results.*

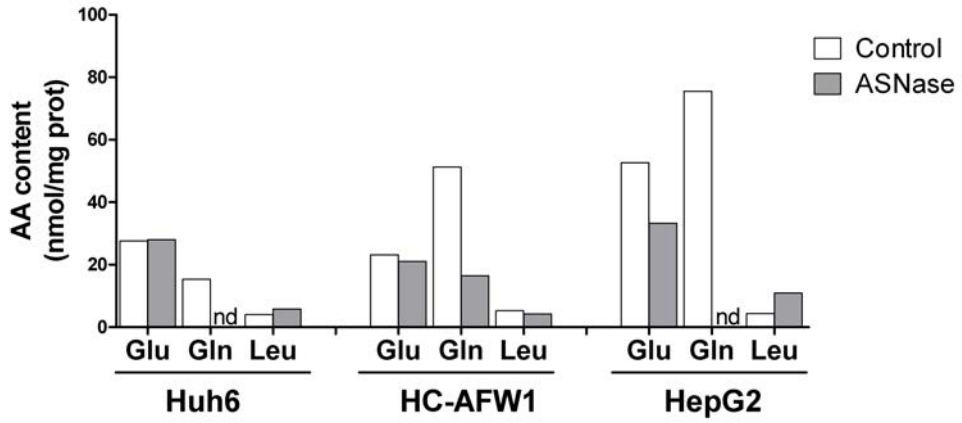

Fig. 63 ***ASNase did not completely deplete HC-AFW1 cell Gln.*** *Amino acid content was determined, as described in Methods, in Huh6, HC-AFW1, and HepG2 cells incubated for 24 hours in DMEM with 1U/ml ASNase or in standard growth medium for control. A single representative experiment is shown.*

This result is consistent with the behaviour of mTOR and GS described above and may be caused by the low expression of the exchange transporter ASCT2, which limits Gln efflux, and the high expression of GS, which refills cell Gln. In fact, adding the GS inhibitor, MSO, to ASNase completely depleted intracellular Gln also in HC-AFW1 cells (not shown), thus leading to a severe decrease in cell viability (see above).

Moreover, HC-AFW1 expressed very low levels of ASNS, which increased after ASNase treatment. This observation contradicts the hypothesis that low asparagine synthetase levels are symptoms of ASNase sensitivity as recently proposed for HCC [162], and strengthens the idea that the metabolic stress caused by ASNase is more dependent on intracellular Gln content and Gln-related enzymes levels. However, ASNase resistance is more likely a multifactor phenomenon [163], possibly due to different mechanisms in different biological models.

4.2.1.3.2 HC-AFW1 ASNase resistant model is sensitive to the combined (ASNase and MSO) treatment in vivo.

HC-AFW1 cells were s.c. injected in NGS mice. After 2 weeks animals were treated with ASNase (5 U/g) and MSO (10 mg/kg), with either drug alone, or with vehicle for control. After 10 days animals were sacrificed and tumor masses were dissected and weighted. At explantation time, only the combined treatment with ASNase and MSO produced a significant decrease (60%) in the mean weight of tumors at sacrifice, while the mean weight of tumors in mice treated with ASNase or MSO was smaller than control without reaching statistical significance (Fig. 64 and 65). However, when the starting tumor volume was considered, all treatments caused a significant delay in tumor growth in terms of relative volume increase (Fig. 66). Furthermore, the Ki67 index, an indicator of proliferative activity of the tumor, was significantly lowered either by ASNase, alone or in combination, but not by MSO alone (Fig. 67).

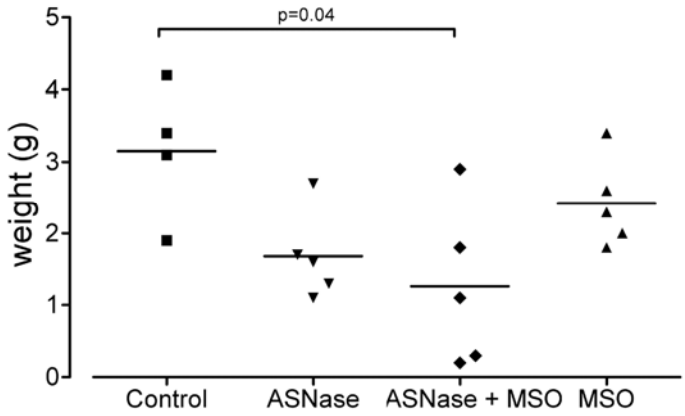

Fig. 64 ***ASNase and MSO reduced HC-AFW1 tumor mass.*** *NSG mice were s.c. engrafted with HC-AFW1 cells. After 2 weeks, mice (n=5 for treated groups; n = 4 for controls) were i.p. injected with ASNase and/or MSO. After 10 days of treatment, mice were sacrificed, and tumors were explanted and weighted. One-way ANOVA analysis was performed and p values are shown. This experiment was performed at Univesity of Tübingen by the group of Prof. Armeanu-Ebinger.*

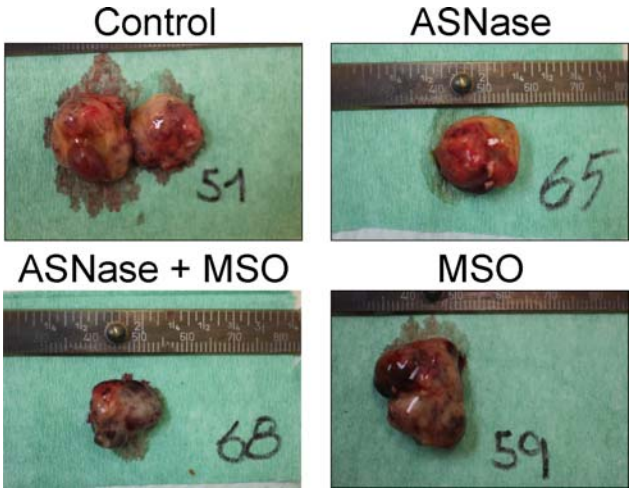

Fig. 65 ***Explanted HC-AFW1 tumors.*** *Representative pictures of dissected tumors. For each group, the tumor with the weight closest to the group mean is shown. This experiment was performed at Univesity of Tübingen by the group of Prof. Armeanu-Ebinger.*

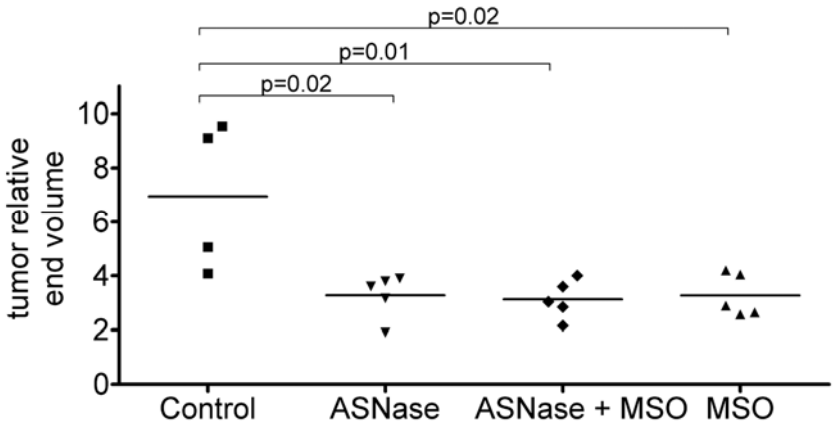

Fig. 66 ***ASNase and MSO delayed the growth of HC-AFW1 xenografts.*** *NSG mice were s.c. engrafted with HC-AFW1 cells. After 2 weeks, mice (n=5 for treated groups; n = 4 for controls) were i.p. injected with ASNase and/or MSO. After 10 days of treatment, mice were sacrificed, and tumors were explanted. Relative tumor volume was calculated as the ratio between the volume at sacrifice and the volume at the beginning of treatments. One-way ANOVA analysis was performed and p values are shown. This experiment was performed at Univesity of Tübingen by the group of Prof. Armeanu-Ebinger.*

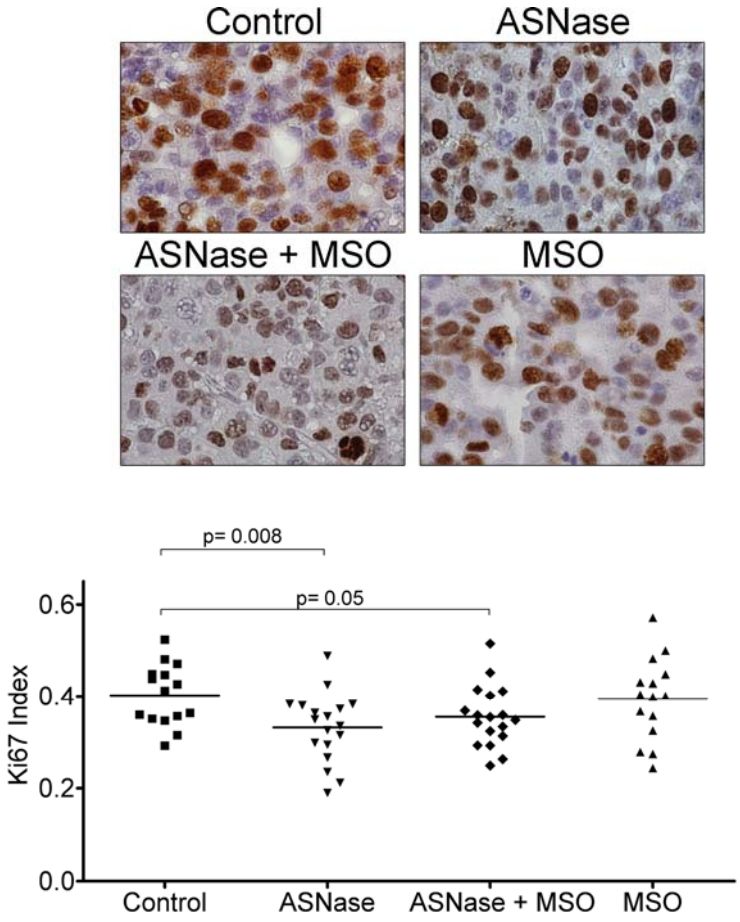

Fig. 67 ***ASNase alone or in combination lowered Ki76 index.*** *NSG mice were s.c. engrafted with HC-AFW1 cells. After 2 weeks, mice (n=5 for treated groups; n = 4 for controls) were i.p. injected with ASNase and/or MSO. After 10 days of treatment, mice were sacrificed, tumors were explanted, and Ki67 positivity of tumors was assessed as described in Methods. A single representative field for each condition is shown (40x). Ki67 index was calculated as described in Methods. One-way ANOVA analysis was performed and p values are shown. This experiment was performed at Univesity of Tübingen by the group of Prof. Armeanu-Ebinger.*

These results clearly show that, when assayed *in vivo*, HC-AFW1 ASNase-resistant HC-AFW1 cells are sensitive to Gln depletion achieved with the combined treatment (ASNase and MSO), which substantially reduced tumor growth. Interestingly, when tumor volume at sacrifice (Fig. 66) was matched and normalized to the tumor size at the beginning of the treatments, both drugs used alone also showed significant effects on tumor growth. Thus, apparently, HC-AFW1 cells seem more sensitive to Gln depletion *in vivo* than *in vitro*. This paradox may be explained considering that the extracellular concentration of glutamine is markedly higher in the culture medium (2 mM for HC-AFW1 cells) than in serum (about 0.6 mM, unpublished observation).

In conclusion, we demonstrated that glutaminoytic treatment may be considered a useful tool for the control of HCC, a pathology characterized by poor prognosis, low sensitivity to chemotherapy, and high recurrence. Since the β-catenin-mutated HC-AFW1 HCC cells, which are resistant to ASNase *in vitro*, are sensitive to ASNase and, even more, to ASNase and MSO *in vivo*, it is possible to conclude that, at least in β-catenin-mutated tumor, this treatment is effective under experimental set. Given that ASNase is a drug already in use in clinic, being one of the keystones of acute lymphoblastic leukaemia treatment, these results may open the path to assess ASNase use in HCC in clinical trials.

4.2.2 "GS negative" human oligodendroglioma (OD) cell lines are extremely sensitive to glutamine depletion

We have demonstrated that GS-expressing HCC lines are sensitive to ASNase treatment. Moreover, the line HC-AFW1, which expresses the highest GS expression, is resistant to ASNase *in vitro*. This result points to a protective role for GS expression/activity in ASNase-treated cells. If this is the case, *a fortiori* the drug should be effective in tumors which express low levels of Glutamine Synthetase.

Oligodendroglioma (OD) is a rare form of glioma originating from oligodendrocytes. *In vivo*, OD is characterized by low expression of GS, which is a distinctive trait for discriminate OD from astrocytoma [164]. Therefore, we decided to test ASNase effects also in OD cell lines.

4.2.2.1 In Hs683 and HOG, two OD lines, GS is under detection limits

First of all, *GLUL* mRNA expression and GS protein abundance were measured in Hs683 and HOG, two human OD cell lines. For positive control the human glioma cell line U87 was used. We observed that, compared to U87, OD cell lines expressed much lower *GLUL* levels (Fig. 68). Furthermore at protein level GS, although it was under detection limits in all the cell lines, was stabilized only in ASNase treated U87 cells, but not in HOG or in Hs683 cells (Fig. 69), thus confirming that these models can be considered "GS negative".

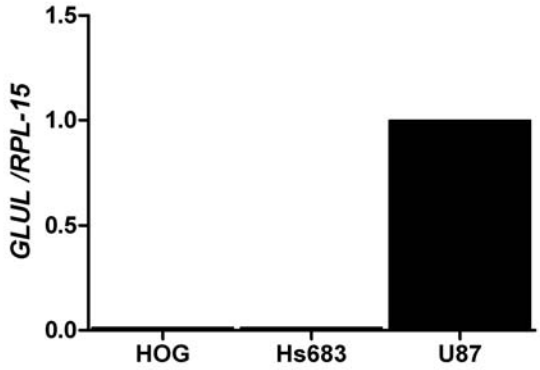

Fig. 68 ***HOG and Hs683 cells express very low levels of GLUL.*** *GLUL expression was analyzed by RT-qPCR. Cells were incubated in standard growth medium. Relative GLUL mRNA abundance was normalized to RPL-15 and expressed as Arbitrary Units.*

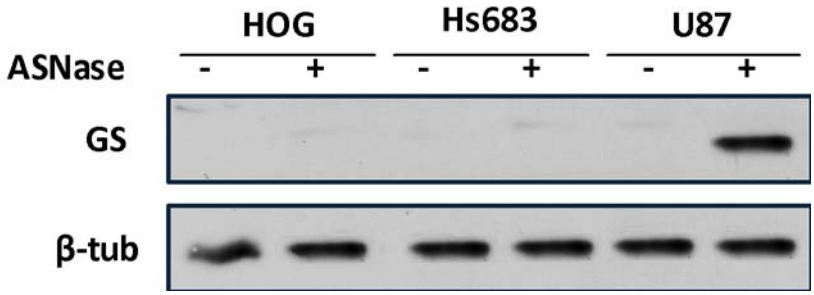

Fig. 69 ***"GS-negative" OD cell lines did not induce GS after ASNase treatment.*** *Western Blot of GS was performed in HOG, Hs683, and U87 cells incubated with 1 U/ml ASNase (+) or in standard growth medium (-). β-tubulin was used as a loading control. The experiment was repeated three times with comparable results.*

4.2.2.2 "GS-negative" OD cell lines are extremely sensitive to glutamine depletion.

HOG, Hs683 and U87 cells were incubated with decreasing concentration of ASNase (from 1 to 0.001 U/ml) in the absence or in the presence of 1 mM MSO. From the dose-response curve it was possible to notice that both the OD cell lines were extremely sensitive to Gln depletion caused by ASNase, with an IC_{50} of, approximately, 0.03 U/ml (Fig. 70), lower than 0.1 U/ml, which is considered the threshold sensibility concentration in leukaemia cells. In OD cells, MSO did not cause an increase in toxicity, as expected for cells lacking GS activity. Instead, in U87 cells IC_{50} for ASNase was about 0.2 U/ml, thus higher than 0.1 U/ml, and MSO supplementation lowered ASNase IC_{50} to 0.06 U/ml (Fig. 70).

Consistently, the microscopic observation of HOG, Hs683 and U87 cells revealed massive cell death in OD cells treated with the ASNase (1 U/ml) and no difference between ASNase alone or in combination with MSO (Fig. 71), while in U87 cells MSO clearly enhances ASNase effects. These results support the hypothesis that GS is involved in the adaptation to ASNase treatment.

ASNase treatment, hydrolyzing Gln produces equimolar Glu and ammonium. Given that it has been demonstrated that Glu may cause excitotoxicity and, consequently, oligodendrocyte cell death [165], HOG, Hs683 and U87 were treated with 2 mM of Glu, so as to ascertain if Glu is involved in ASNase effects. No toxic effects of Glu in cell viability was detected in all the cell lines (Fig. 72), confirming that the toxicity of ASNase is not attributable to elevated extracellular Glu concentration.

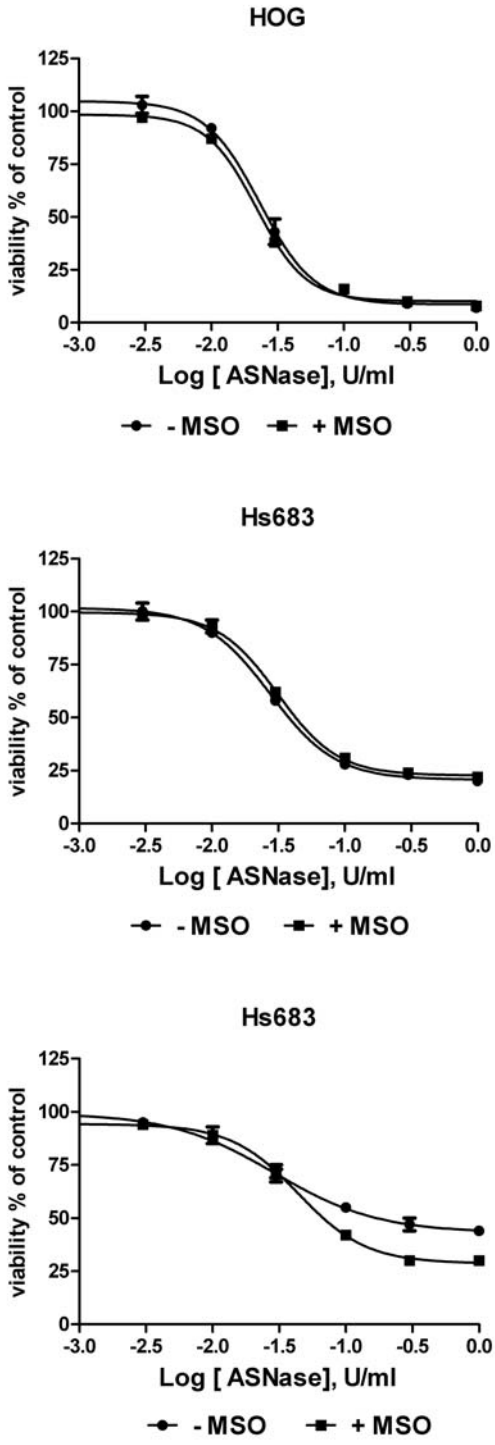

Fig. 70 ***MSO synergized ASNase effects only in GS expressing cells.*** *HOG, Hs683, and U87 cells were incubated with different ASNase concentrations (1, 0.3, 0.1, 0.03, 0.01, 0.003, 0.001 U/ml) in the absence or in the presence of 1 mM MSO. After 48 hours cells were incubated with resazurin and viability was assessed. Data are expressed as % of viability determined in untreated cells. Means ± SD of three experiments with four determinations each, are shown.* IC_{50} *was calculated with non-linear regression curve fit software.*

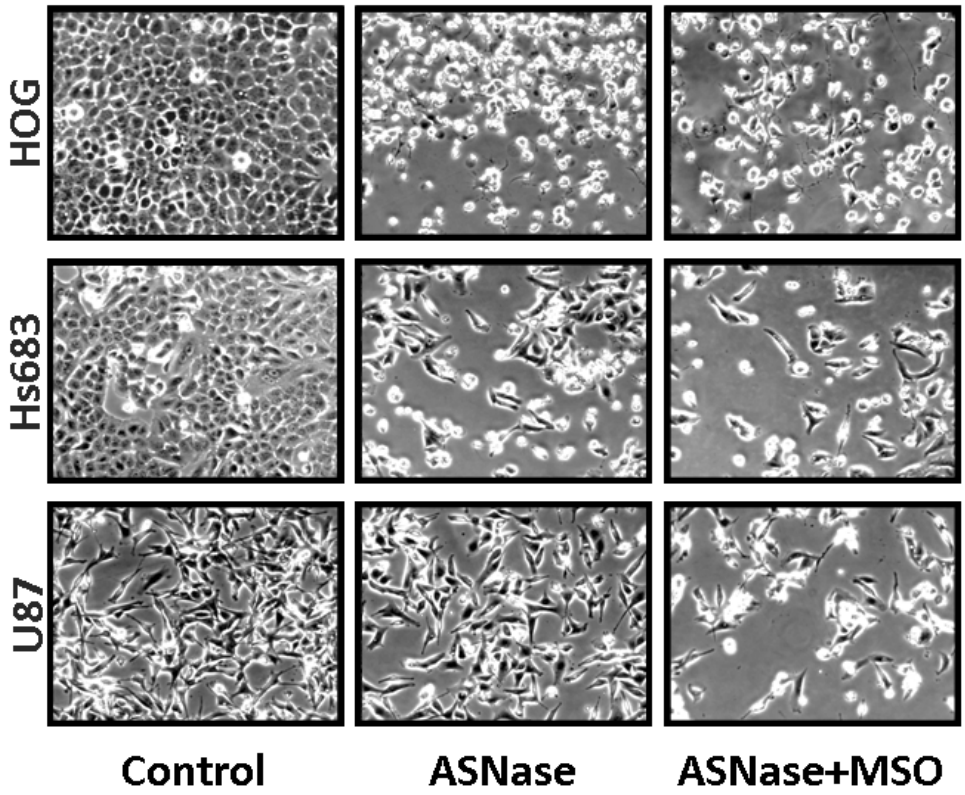

Fig. 71 ***MSO synergized ASNase effects only in GS expressing cells.*** *Microscopic observation of HOG, Hs683 and U87 cells treated with ASNase (1 U/ml) alone or in combination with MSO (1 mM). A single representative field is shown for each condition. Magnification 200x.*

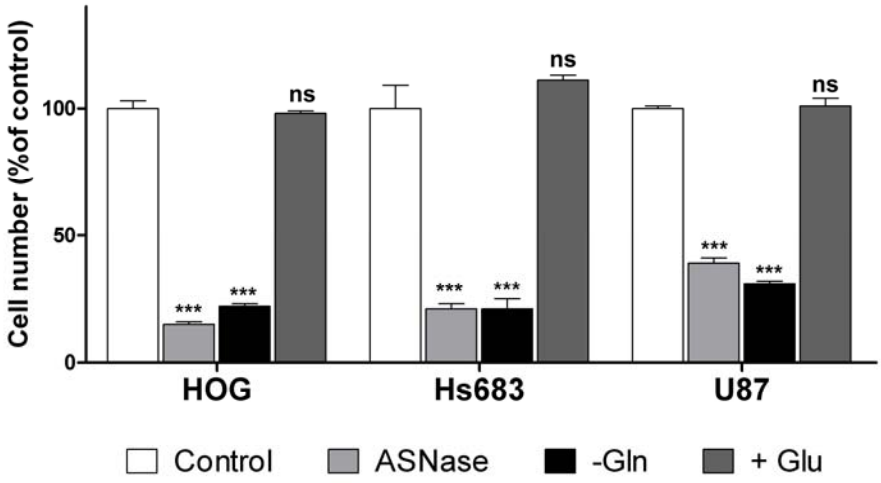

Fig. 72 ***No glutamate toxicity effect was detected.*** *HOG, Hs683 and U87 cells were treated with ASNase (1 U/ml) or in absence of Gln (-Gln) or in presence of both Gln and 2 mM Glu (+Glu). After 48 hours viability was assessed and data expressed as % of cells incubated in standard growth medium. Means ± SD of four independent determinations are shown. *** p < 0.001 vs. control.*

Oligodendrogliomas, although rare and slow-growing cancers, are generally more sensitive to chemotherapy than other gliomas, but recurrences are possible [166].

The translational impact of these findings fully deserves, therefore, further investigations.

4.2.3 Mesenchymal stem cells are involved in ASNase resistance

L-Asparaginases of bacterial origin have been used in acute lymphoblastic leukaemia (ALL) treatment since early 70s and have dramatically improved the prognosis of this form of infantile cancer. Although survival in childhood ALL is now approaching 90%, some subsets still have an adverse prognosis [128], and resistance-associated relapse, usually due to immune- and non-immune mechanisms, is frequently observed.

It has been demonstrated that, after multiple ASNase administrations, patients develop antibodies against ASNase [167]. To circumvent the immune response, ASNase is changed from the *E. coli* native product to its pegylated form or, eventually, to *E. chysantemi* enzyme. Relapse, however, may be exacerbated and correlated with the up-regulation of the Gln-dependent enzyme ASNS [62], while the role of GS has not been yet evaluated. However, if Gln depletion plays a role in ASNase anti-leukemic effect, the *E. chysantemi* enzyme is to be preferred since it has an higher glutaminase activity than *E. coli* ASNase [61].

Recently it has been proposed that a trophic role of bone marrow mesenchymal stem cells (MSC) may be involved in ASNase resistance and leukaemia relapse in ALL [66, 71]. According to this theory, bone marrow MSC form a niche and release Asn to feed the leukemic blasts, thus preserving them from ASNase effects. However, no data are yet available on ASNase effects on MSC themselves.

4.2.3.1 MSC are relatively insensitive to ASNase treatment

A time course experiment showed that MSC, obtained from the bone marrow of two donors, initially arrested proliferation in the presence of ASNase or of ASNase and MSO (Fig. 73). However, a partial restoration of viability was observed in cells treated with ASNase after 72 hours. On the

contrary, no rescue of viability was observed with ASNase and MSO (Fig. 73) suggesting that GS plays a role in counteracting ASNase effects. MSO alone was without significant effects. Results were corroborated by microscopic observation (Fig. 74).

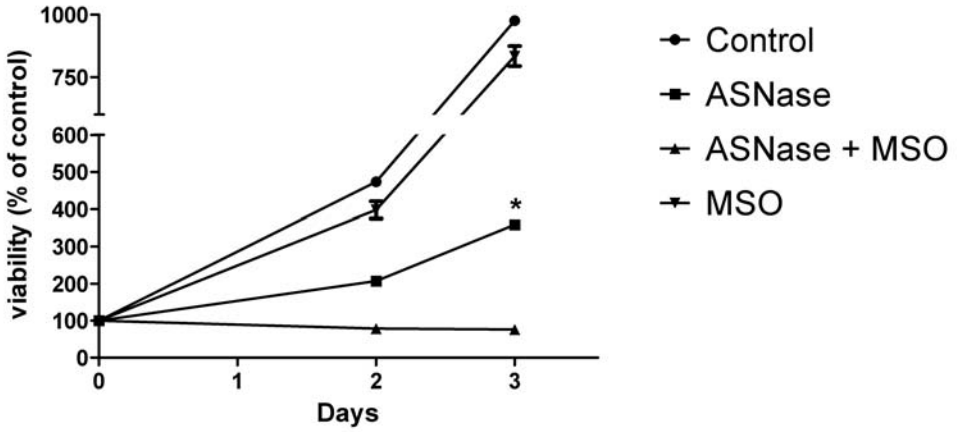

Fig. 73 ***MSC rescue proliferation two days after ASNase administration.*** *MSC were incubated in DMEM with ASNase (1 U/ml, alone or in presence of 1 mM MSO) or MSO alone. Control cells were maintained in standard growth medium. Viability was assessed with resazurin at t=0 and after 2 and 3 days of treatments. Data are expressed as % of t=0 for each condition. Means of four independent determinations ± SD are shown. *p<0.05 vs. 2d-ASNase-treated cells.*

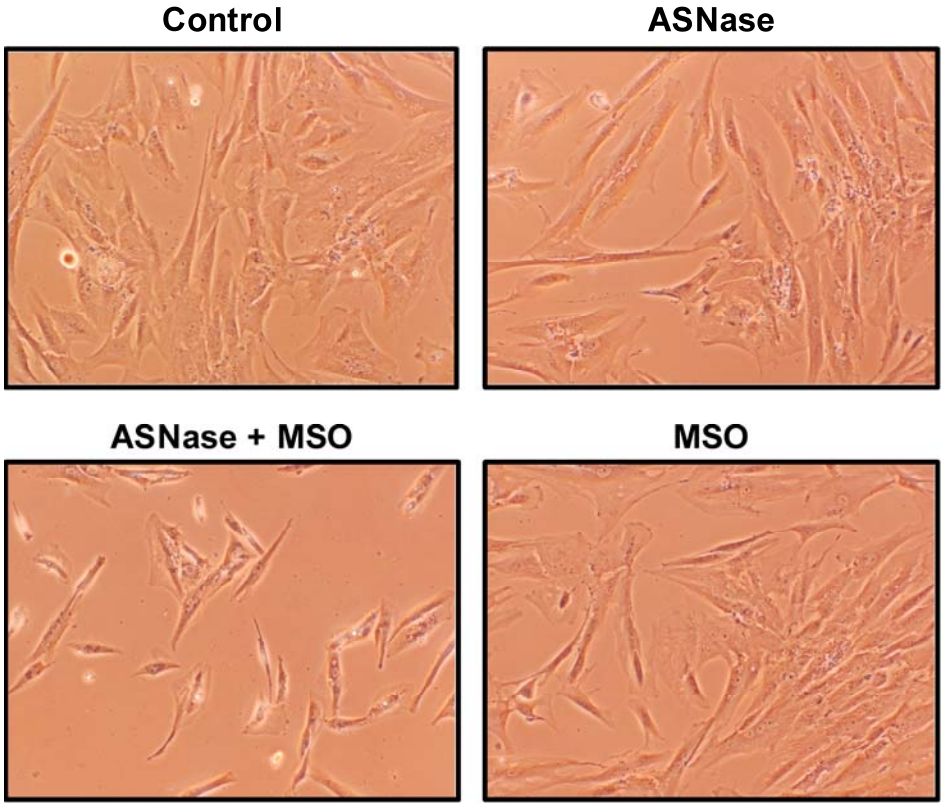

Fig. 74 ***ASNase delays MSC cell proliferation.*** *MSC were incubated in DMEM with ASNase (1 U/ml, alone or in the presence of 1 mM MSO) or MSO alone. Control cells were maintained in standard growth medium. Cells were photographed after 72 hours treatments. Magnification 100x.*

Consistently, the IC_{50} of ASNase in MSC was higher than 10 U/ml (Fig. 75) and adding MSO to ASNase, although decreased ASNase IC_{50} to 0.25 ± 0.04, did not severely affect cell viability. Comparable results were obtained from the two different donors (Fig. 75), and therefore intrinsic biological variability could be excluded. Moreover, when MSC were incubated in media supplemented with different Gln concentrations, they confirm their limited sensitivity to Gln depletion. Significant changes are observed only when cells were cultivated in absence of Gln (not shown). Furthermore, when the time course experiment was prolonged to 6 days, it was clearly

evident that ASNase treated cell population had significantly grown (Fig. 76), suggesting that MSC are able to successfully adapt to Gln starvation. MSO prevented MSC adaptation and, in fact, cell number decreased (Fig. 76), suggesting that this condition caused cell death and that GS may be directly involved in the adaptation process.

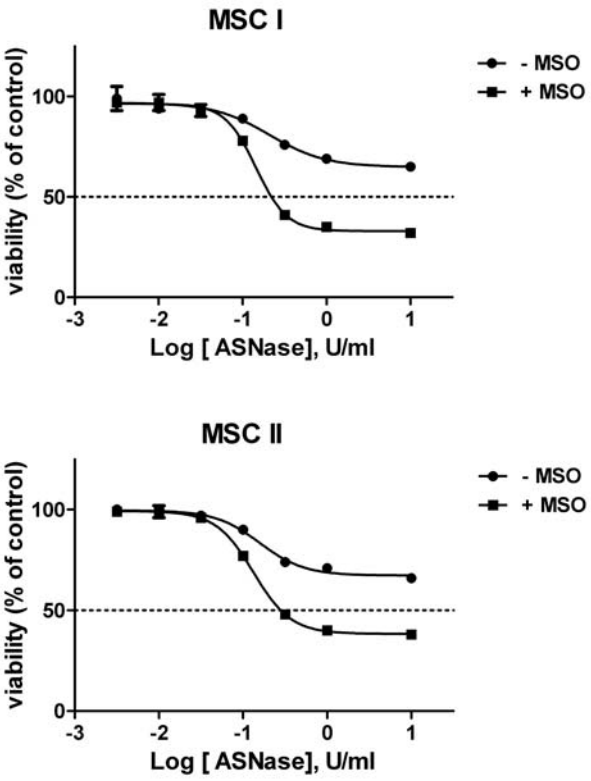

Fig. 75 ***MSC were not sensitive to ASNase.*** *MSC from two different donors (MSC I and MSC II) were incubated in DMEM with decreasing concentrations of ASNase (from 10 to 0.003 U/ml) alone or in the presence of MSO (1 mM). Control cells were maintained in standard growth medium. After 48 hours viability was assessed with resazurin. Data are expressed as % of control. Means ± SD are shown. IC_{50} was calculated with a non-linear regression curve fit.*

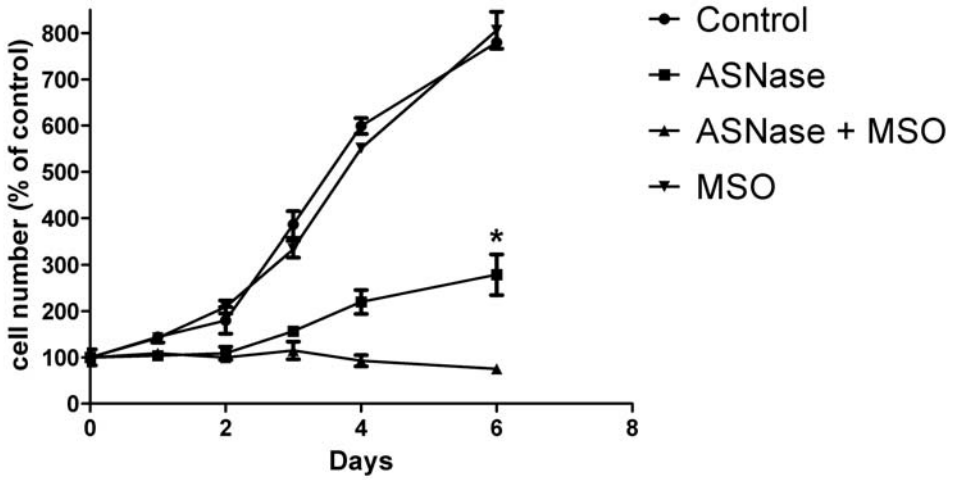

Fig. 76 ***MSC successfully adapt to ASNase.*** *MSC were incubated in DMEM with ASNase (1U/ml, in the presence or in the absence of 1 mM MSO) or with MSO alone. Control cells were maintained in unsupplemented growth medium. Cells were counted at t=0 on every day of treatment. Data are expressed as % of cell number at t=0. Means ± SD are shown. *p<0.05 compared to t=0.*

4.2.3.2 MSC adapt to ASNase through the induction of GS and autophagy

What are the molecular mechanisms involved in adaptation to ASNase-imposed nutritional stress in MSC cells? A 2-fold transient induction of *ASNS* and *SLC38A2* (encoding for the transporter SNAT2) genes was observed in both ASNase and ASNase and MSO treated cells (Fig. 77), while no statistical difference in *GLUL* or in *SLC1A5* (encoding for the transporter ASCT2) mRNA expression was detected. These results suggest that Gln depletion caused the phosphorylation of eIF2α (as confirmed by Western blot analysis, see Fig. 78) with the activation of *activating transcription factor* (ATF4) and, subsequently, the expression of its downstream targets ASNS and SNAT2 [150, 156].

Furthermore mTORC1 activity, assessed as the phosphorylation of the downstream target S6K1 at residue T389, was decreased by ASNase at earlier times (from 3 to 9 hours of treatment), but increased, reaching levels even higher than control, after 48 hours of ASNase treatment. Consistently, autophagy, a catabolic process directly down-regulated by mTOR [45] and assessed through the accumulation of the lipidated LC3 protein (LC3 II), was induced after 6 hours, reached the maximum at 24 hours, and decreased after 48 hours of ASNase treatment (Fig. 78).

MSO yielded apparently paradoxical results, which, however, are fully consistent with the results described in 4.1.3 Glutamine Synthetase inhibitors activate mTORC1 paragraph. Moreover, GS protein was stabilized by treatments in a time-dependent manner (Fig. 78). Similar results were obtained in cells incubated in the absence of Gln (not shown).

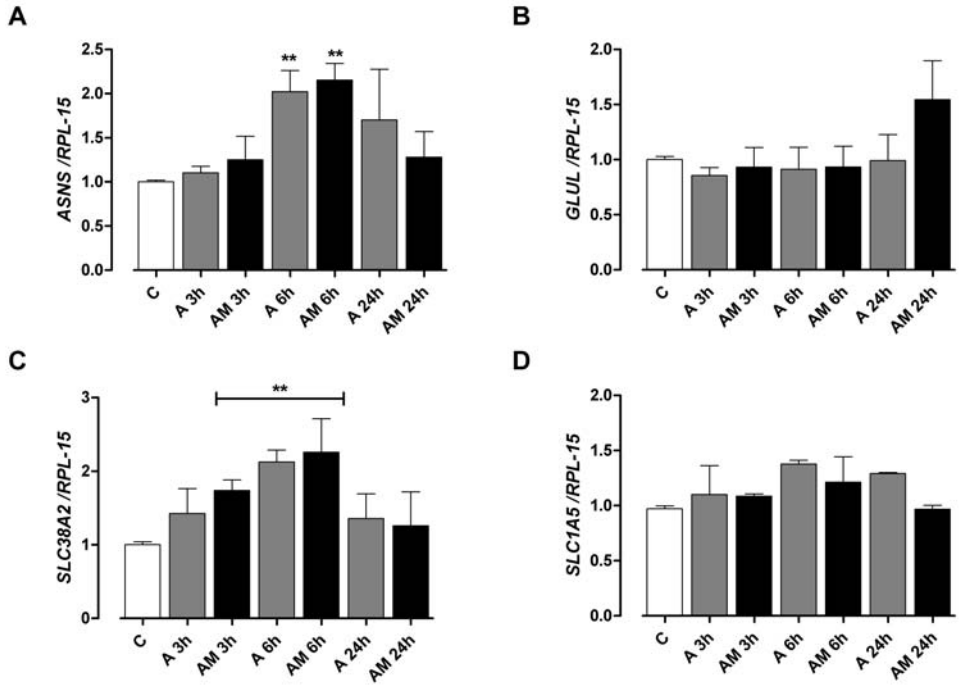

Fig. 77 ***MSC induced ASNS and the SNAT2 transporter after treatments.*** *ASNS (A), GLUL (B), SLC38A2 (C), and SLC1A5 (D) expression was analyzed by RT-qPCR. MSC (from two donors) were incubated with ASNase (A) or ASNase and MSO (AM) for the indicated times. Control cells were maintained in standard growth medium. ASNS (A), GLUL (B), SLC38A2 (C) and SLC1A5 (D) mRNA abundance was normalized to RPL-15 and expressed as Arbitrary Units. Means ± SD of three experiments with two determinations each are shown. **p<0.01*

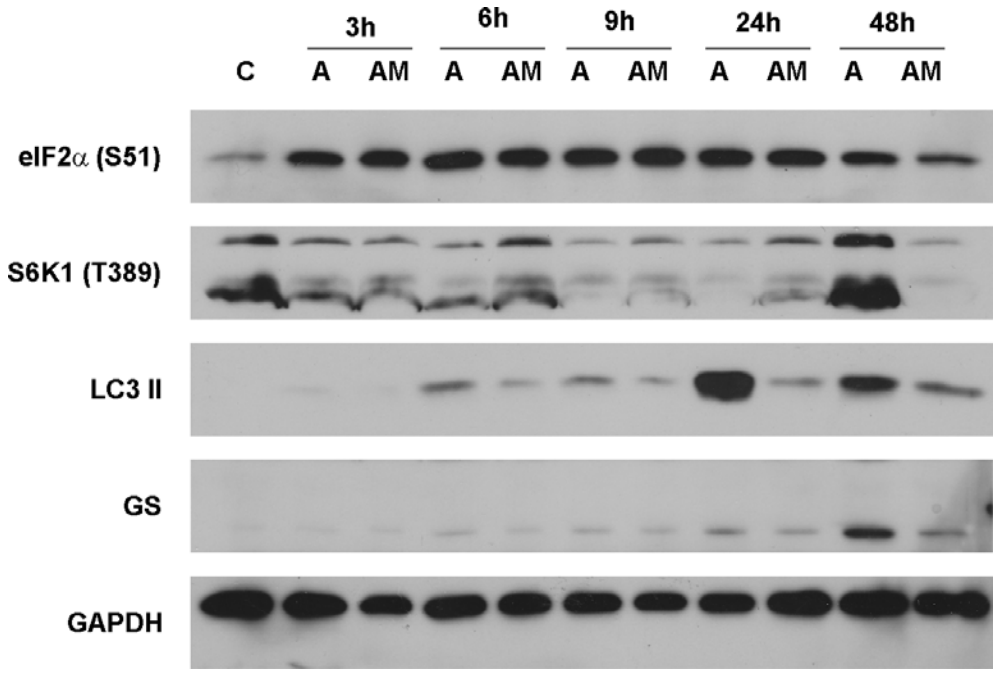

Fig. 78 ***Autophagy and GS induction were responsible of ASNase-induced Gln depletion.*** *Western Blot of eIF2α (phospho S51), S6K1 (phospho T389), LC3 II, and GS was performed in MSC incubated with ASNase (A), ASNase and MSO (AM) or in standard growth medium for control (C). GAPDH was used as a loading control. The experiment was repeated three times with MSC from two donors with comparable results.*

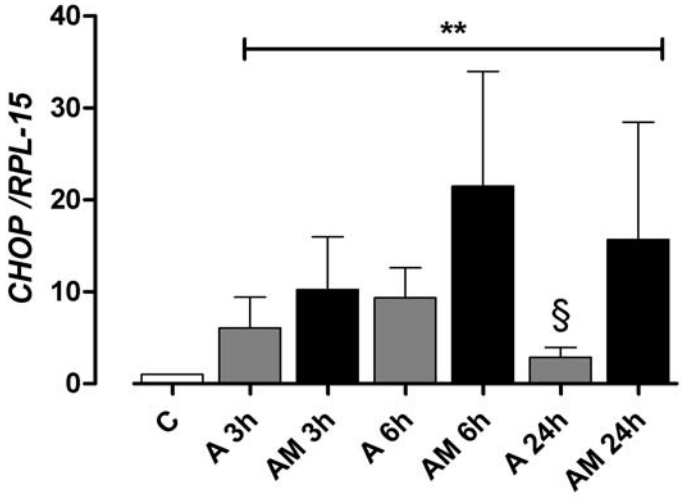

Fig. 79 ***CHOP induction is transient in ASNase treated MSC.*** *CHOP expression was analyzed by RT-qPCR. MSC were incubated with ASNase (A) or ASNase and MSO (AM) for the indicated times. CHOP mRNA abundance was normalized to RPL-15 and expressed as Arbitrary Units. Means ± SD of three experiments with two determinations each are shown. **p<0.01 vs. control, § p<0.05 v cells treated with ASNase for 6 hours*

The expression of the mRNA for the pro-apoptotic protein CHOP was also evaluated by qPCR. As shown in Fig. 79, *CHOP* mRNA was already significantly increased after 3 hours treatment. However, while in ASNase and MSO treated cells *CHOP* induction was sustained up to 24 hours, without MSO was transient (Fig. 79), consistently with the successful adaptation to the Gln-depleting agent.

Thus, since MSO inhibits GS but also causes abnormal mTOR activation with a consequent delay of the autophagic response, both GS and autophagy may contribute to MSC adaptation to ASNase. These results may strengthen the hypothesis that a release of Asn and Gln by MSC feed leukemic blasts in a confined *niche* in the bone marrow compartment during ASNase treatment.

4.2.3.3 MSC protect ALL blast from ASNase treatment

To verify the protective role of MSC, ALL cell lines RS4;11, REH, and Nalm6 were treated with decreasing ASNase concentration. Viability assay revealed the extreme sensitivity of these cells to ASNase with IC_{50} of $3.21*10^{-04}$ ± $3,35*10^{-05}$ U/ml for RS4;11, 0.008 ± 0.002 U/ml for REH and 0.04 ± 0.02 U/ml for Nalm6 (Fig. 80). This different sensitivity seems to be correlated to *ASNS* gene expression which is barely detectable in RS4;11 and highest in Nalm6 (not shown), although it has been demonstrated that low *ASNS* expression does not always predict high ASNase sensitivity [168].

Incubating ALL cells in the absence of Gln revealed only a partial sensitivity to Gln starvation in REH and RS4;11, while Nalm6 cells viability was not affected at all (Fig. 81). Thus, it is likely that the loss of viability caused by ASNase in these cell lines is mainly due to the lack of Asn.

Then, a preliminary co-culture experiment was set. The most sensitive RS4;11 and REH cells were treated with ASNase (at the IC_{50} concentration each) alone or in combination with 1 mM MSO, in the presence of a feeder layer of MSC. After 48 hours of treatment it was clear that MSC protected ALL cells from ASNase treatment (Fig. 82). The protective effect of MSC was still detectable in the presence of MSO (Fig. 82).

From these results it is possible to conclude that mesenchymal stem cells do adapt to ASNase and effectively protect ALL blast from this drug.

Indeed while MSO prevents MSC adaptation to ASNase, through the inhibition of both GS and autophagy, it do not avoid MSC trophic interaction with ALL blasts, suggesting that other mechanisms are involved. However, further experiments need to unveil the complex interaction between MSC and ALL blasts.

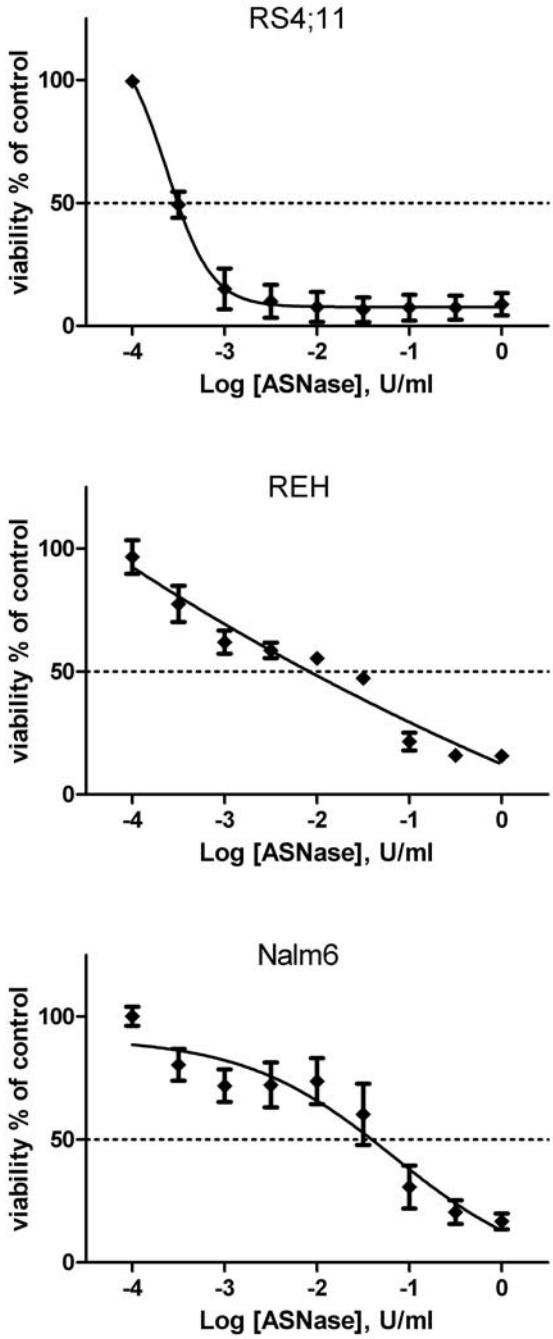

Fig. 80 ***ALL cell lines were extremely sensitive to ASNase.*** *RS4;11, REH, and Nalm6 were incubated in RPMI with different concentrations of ASNase (from 1 to 0.0001 U/ml). Control cells were maintained in standard growth medium. After 48 hours viability was assessed with resazurin. Data are expressed as % of control. Means of three different experiments with six independent determinations each ± SD are shown.* IC_{50} *was calculated with a non-linear regression curve fit.*

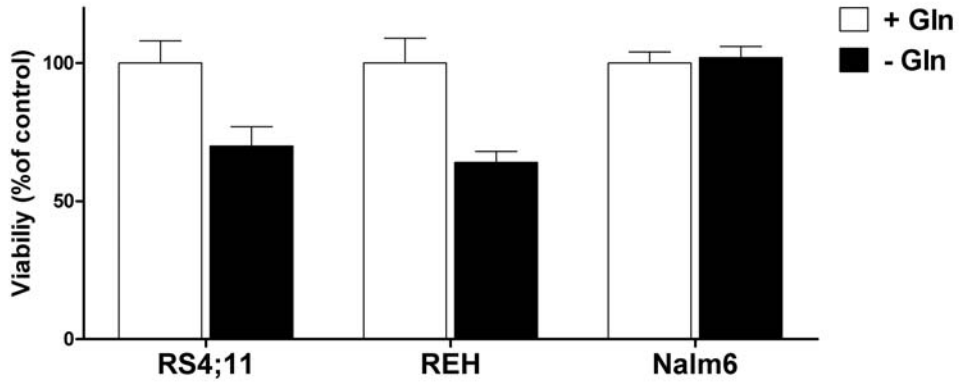

Fig. 81 ***Gln starvation only partially affects ALL cell line viability.*** *RS4;11, REH, and Nalm6 were incubated in RPMI with or without 2 mM Gln. After 48 hours viability was assessed with resazurin. Data are expressed as % of control. Means of six independent determinations in a single experiment are shown ± SD.*

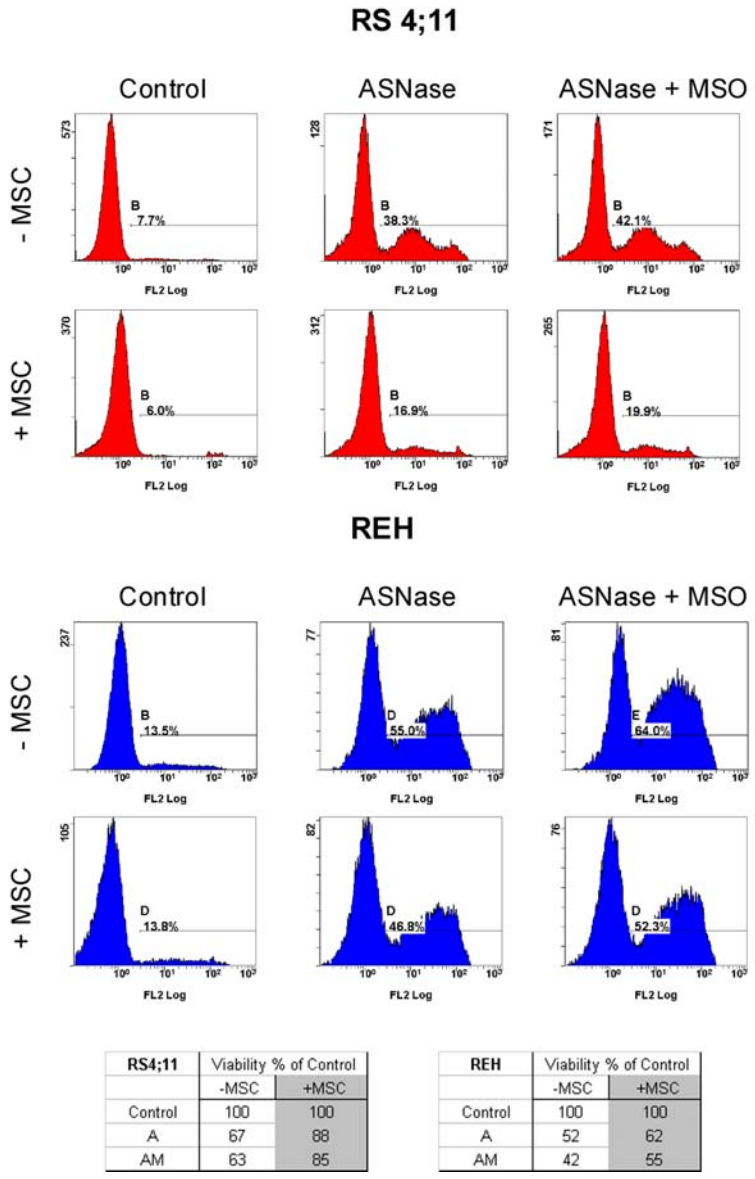

RS4;11	Viability % of Control	
	-MSC	+MSC
Control	100	100
A	67	88
AM	63	85

REH	Viability % of Control	
	-MSC	+MSC
Control	100	100
A	52	62
AM	42	55

Fig. 82 ***MSC protected ALL lines from ASNase and ASNase and MSO.*** *MSC were seeded and incubated in standard growth medium for 48 hours. RS4;11 and REH were added to the feeder layer or on plastic and incubated in RPMI with ASNase (A) or ASNase and MSO (AM). ASNase was used at the IC_{50} of each cell lines. After 48 hours cells were stained for PI and flow cytometry was assessed. Data are expressed as viability in % of each control. A single preliminary experiment is shown.*

CHAPTER 5

CONCLUSIONS

In conclusion, the results obtained show that glutamine plays an important role in promoting both cell growth and mTOR activation. Moreover, non proteinogenic amino acids, which are analogs of glutamine and inhibitors of Glutamine Synthetase (GS), are also able to activate mTOR, indicating that not only essential amino acids regulate the kinase.

As far as the possibility of targeting glutamine metabolism in human hepatocellular carcinoma (HCC) is concerned, we have demonstrated that pharmacologically-induced glutamine depletion, obtained with the bacterial enzyme L-asparaginase (ASNase) and the GS inhibitor MSO, markedly hinder β-catenin-mutated HCC cell proliferation not only *in vitro* but also in xenograft models.

These results suggest that the combination of extracellular Gln depletion with the inhibition of intracellular glutamine synthesis causes a severe metabolic stress, which leads to liver cancer cell death (Fig. 83). Moreover, this is the first evidence of antitumor activity of a GS inhibitor and suggests that a glutamine-depleting treatment may be relevant for the therapy of hepatocellualar carcinoma, a cancer which still has a poor prognosis.

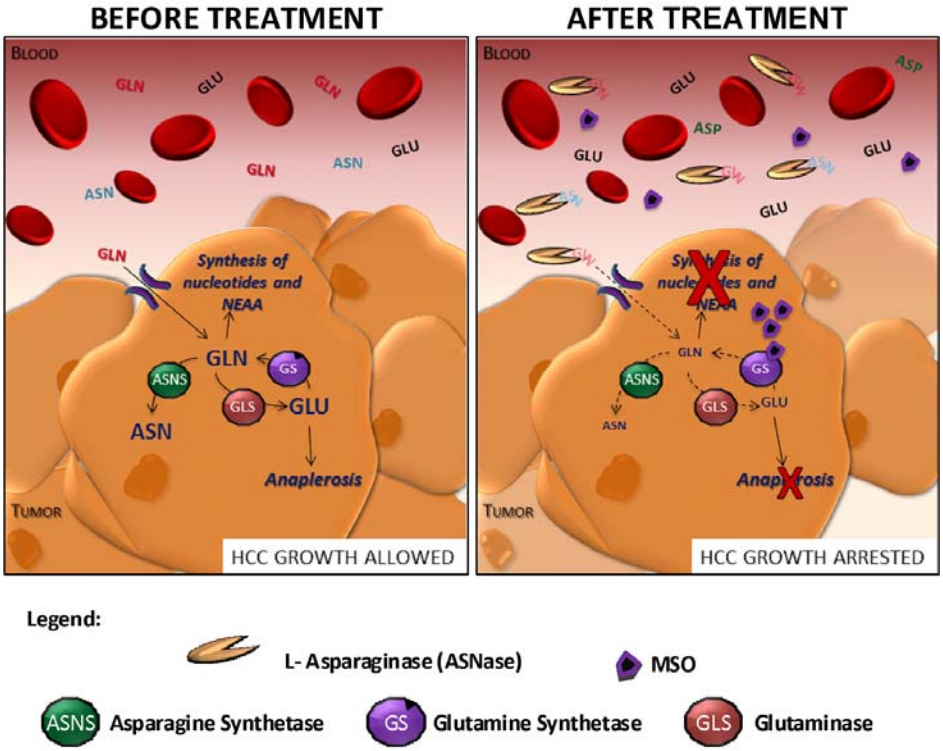

Fig. 83 ***ASNase and MSO mechanism of action.***

However, the hyper-expression of GS may be considered a defense against glutamine shortage, as demonstrated *a contrariis* by the synthetic lethality observed in ASNase-treated GS-negative human oligodendroglioma *in vitro*, a result worthy of a confirmation with *in vivo* models. Lastly, the combination of ASNase and MSO may also hinder the recently described nutritional interaction between bone marrow stromal cells and leukemic blasts. Indeed, stromal cells adapt to ASNase through GS induction and autophagy triggering, mechanisms both prevented by MSO.

In summary, interference with Gln metabolism and, in particular, with GS activity may constitute a useful approach for the control of selected human cancers.

REFERENCES

1. Hanahan, D. and R.A. Weinberg, Hallmarks of cancer: the next generation. Cell, 2011. 144(5): p. 646-74.
2. Vander Heiden, M.G., Exploiting tumor metabolism: challenges for clinical translation. J Clin Invest, 2013. 123(9): p. 3648-51.
3. Mullen, A.R. and R.J. DeBerardinis, Genetically-defined metabolic reprogramming in cancer. Trends Endocrinol Metab, 2012. 23(11): p. 552-9.
4. Warburg, O., F. Wind, and E. Negelein, The Metabolism of Tumors in the Body. J Gen Physiol, 1927. 8(6): p. 519-30.
5. Vander Heiden, M.G., L.C. Cantley, and C.B. Thompson, Understanding the Warburg effect: the metabolic requirements of cell proliferation. Science, 2009. 324(5930): p. 1029-33.
6. Mankoff, D.A. and J.R. Bellon, Positron-emission tomographic imaging of cancer: glucose metabolism and beyond. Semin Radiat Oncol, 2001. 11(1): p. 16-27.
7. Parks, S.K., J. Chiche, and J. Pouyssegur, pH control mechanisms of tumor survival and growth. J Cell Physiol, 2011. 226(2): p. 299-308.
8. Chiu, M., L. Ottaviani, M.G. Bianchi, R. Franchi-Gazzola, and O. Bussolati, Towards a metabolic therapy of cancer? Acta Biomed, 2012. 83(3): p. 168-76.
9. Pastorino, J.G., J.B. Hoek, and N. Shulga, Activation of glycogen synthase kinase 3beta disrupts the binding of hexokinase II to mitochondria by phosphorylating voltage-dependent anion channel and potentiates chemotherapy-induced cytotoxicity. Cancer Res, 2005. 65(22): p. 10545-54.

10. Hamanaka, R.B. and N.S. Chandel, Cell biology. Warburg effect and redox balance. Science, 2011. 334(6060): p. 1219-20.
11. Yang, M., T. Soga, and P.J. Pollard, Oncometabolites: linking altered metabolism with cancer. J Clin Invest, 2013. 123(9): p. 3652-8.
12. Schwartzenberg-Bar-Yoseph, F., M. Armoni, and E. Karnieli, The tumor suppressor p53 down-regulates glucose transporters GLUT1 and GLUT4 gene expression. Cancer Res, 2004. 64(7): p. 2627-33.
13. Kawauchi, K., K. Araki, K. Tobiume, and N. Tanaka, p53 regulates glucose metabolism through an IKK-NF-kappaB pathway and inhibits cell transformation. Nat Cell Biol, 2008. 10(5): p. 611-8.
14. Maddocks, O.D. and K.H. Vousden, Metabolic regulation by p53. J Mol Med (Berl), 2011. 89(3): p. 237-45.
15. Baysal, B.E., R.E. Ferrell, J.E. Willett-Brozick, E.C. Lawrence, D. Myssiorek, A. Bosch, A. van der Mey, P.E. Taschner, W.S. Rubinstein, E.N. Myers, C.W. Richard, 3rd, C.J. Cornelisse, P. Devilee, and B. Devlin, Mutations in SDHD, a mitochondrial complex II gene, in hereditary paraganglioma. Science, 2000. 287(5454): p. 848-51.
16. Bayley, J.P. and P. Devilee, Warburg tumours and the mechanisms of mitochondrial tumour suppressor genes. Barking up the right tree? Curr Opin Genet Dev, 2010. 20(3): p. 324-9.
17. Alam, N.A., E. Barclay, A.J. Rowan, J.P. Tyrer, E. Calonje, S. Manek, D. Kelsell, I. Leigh, S. Olpin, and I.P. Tomlinson, Clinical features of multiple cutaneous and uterine leiomyomatosis: an underdiagnosed tumor syndrome. Arch Dermatol, 2005. 141(2): p. 199-206.
18. Pollard, P.J., J.J. Briere, N.A. Alam, J. Barwell, E. Barclay, N.C. Wortham, T. Hunt, M. Mitchell, S. Olpin, S.J. Moat, I.P.

Hargreaves, S.J. Heales, Y.L. Chung, J.R. Griffiths, A. Dalgleish, J.A. McGrath, M.J. Gleeson, S.V. Hodgson, R. Poulsom, P. Rustin, and I.P. Tomlinson, Accumulation of Krebs cycle intermediates and over-expression of HIF1alpha in tumours which result from germline FH and SDH mutations. Hum Mol Genet, 2005. 14(15): p. 2231-9.

19. Willam, C., L.G. Nicholls, P.J. Ratcliffe, C.W. Pugh, and P.H. Maxwell, The prolyl hydroxylase enzymes that act as oxygen sensors regulating destruction of hypoxia-inducible factor alpha. Adv Enzyme Regul, 2004. 44: p. 75-92.
20. Dang, L., D.W. White, S. Gross, B.D. Bennett, M.A. Bittinger, E.M. Driggers, V.R. Fantin, H.G. Jang, S. Jin, M.C. Keenan, K.M. Marks, R.M. Prins, P.S. Ward, K.E. Yen, L.M. Liau, J.D. Rabinowitz, L.C. Cantley, C.B. Thompson, M.G. Vander Heiden, and S.M. Su, Cancer-associated IDH1 mutations produce 2-hydroxyglutarate. Nature, 2009. 462(7274): p. 739-44.
21. Locasale, J.W., A.R. Grassian, T. Melman, C.A. Lyssiotis, K.R. Mattaini, A.J. Bass, G. Heffron, C.M. Metallo, T. Muranen, H. Sharfi, A.T. Sasaki, D. Anastasiou, E. Mullarky, N.I. Vokes, M. Sasaki, R. Beroukhim, G. Stephanopoulos, A.H. Ligon, M. Meyerson, A.L. Richardson, L. Chin, G. Wagner, J.M. Asara, J.S. Brugge, L.C. Cantley, and M.G. Vander Heiden, Phosphoglycerate dehydrogenase diverts glycolytic flux and contributes to oncogenesis. Nat Genet, 2011. 43(9): p. 869-74.
22. Possemato, R., K.M. Marks, Y.D. Shaul, M.E. Pacold, D. Kim, K. Birsoy, S. Sethumadhavan, H.K. Woo, H.G. Jang, A.K. Jha, W.W. Chen, F.G. Barrett, N. Stransky, Z.Y. Tsun, G.S. Cowley, J. Barretina, N.Y. Kalaany, P.P. Hsu, K. Ottina, A.M. Chan, B. Yuan, L.A. Garraway, D.E. Root, M. Mino-Kenudson, E.F. Brachtel, E.M. Driggers, and D.M. Sabatini, Functional genomics reveal that the

serine synthesis pathway is essential in breast cancer. Nature, 2011. 476(7360): p. 346-50.
23. Zhao, Y., E.B. Butler, and M. Tan, Targeting cellular metabolism to improve cancer therapeutics. Cell Death Dis, 2013. 4: p. e532.
24. Dwarakanath, B. and V. Jain, Targeting glucose metabolism with 2-deoxy-D-glucose for improving cancer therapy. Future Oncol, 2009. 5(5): p. 581-5.
25. Fantin, V.R., J. St-Pierre, and P. Leder, Attenuation of LDH-A expression uncovers a link between glycolysis, mitochondrial physiology, and tumor maintenance. Cancer Cell, 2006. 9(6): p. 425-34.
26. Flavin, R., S. Peluso, P.L. Nguyen, and M. Loda, Fatty acid synthase as a potential therapeutic target in cancer. Future Oncol, 2010. 6(4): p. 551-62.
27. Seyfried, T.N., J. Marsh, L.M. Shelton, L.C. Huysentruyt, and P. Mukherjee, Is the restricted ketogenic diet a viable alternative to the standard of care for managing malignant brain cancer? Epilepsy Res, 2012. 100(3): p. 310-26.
28. Tennant, D.A., R.V. Duran, and E. Gottlieb, Targeting metabolic transformation for cancer therapy. Nat Rev Cancer, 2010. 10(4): p. 267-77.
29. DeBerardinis, R.J., J.J. Lum, G. Hatzivassiliou, and C.B. Thompson, The biology of cancer: metabolic reprogramming fuels cell growth and proliferation. Cell Metab, 2008. 7(1): p. 11-20.
30. DeBerardinis, R.J. and T. Cheng, Q's next: the diverse functions of glutamine in metabolism, cell biology and cancer. Oncogene, 2010. 29(3): p. 313-24.
31. Divino Filho, J.C., S.J. Hazel, P. Furst, J. Bergstrom, and K. Hall, Glutamate concentration in plasma, erythrocyte and muscle in relation to plasma levels of insulin-like growth factor (IGF)-I, IGF

binding protein-1 and insulin in patients on haemodialysis. J Endocrinol, 1998. 156(3): p. 519-27.

32. Gao, P., I. Tchernyshyov, T.C. Chang, Y.S. Lee, K. Kita, T. Ochi, K.I. Zeller, A.M. De Marzo, J.E. Van Eyk, J.T. Mendell, and C.V. Dang, c-Myc suppression of miR-23a/b enhances mitochondrial glutaminase expression and glutamine metabolism. Nature, 2009. 458(7239): p. 762-5.
33. Suzuki, S., T. Tanaka, M.V. Poyurovsky, H. Nagano, T. Mayama, S. Ohkubo, M. Lokshin, H. Hosokawa, T. Nakayama, Y. Suzuki, S. Sugano, E. Sato, T. Nagao, K. Yokote, I. Tatsuno, and C. Prives, Phosphate-activated glutaminase (GLS2), a p53-inducible regulator of glutamine metabolism and reactive oxygen species. Proc Natl Acad Sci U S A, 2010. 107(16): p. 7461-6.
34. Hensley, C.T., A.T. Wasti, and R.J. Deberardinis, Glutamine and cancer: cell biology, physiology, and clinical opportunities. J Clin Invest, 2013. 123(9): p. 3678-84.
35. DeBerardinis, R.J., A. Mancuso, E. Daikhin, I. Nissim, M. Yudkoff, S. Wehrli, and C.B. Thompson, Beyond aerobic glycolysis: transformed cells can engage in glutamine metabolism that exceeds the requirement for protein and nucleotide synthesis. Proc Natl Acad Sci U S A, 2007. 104(49): p. 19345-50.
36. Yuneva, M., N. Zamboni, P. Oefner, R. Sachidanandam, and Y. Lazebnik, Deficiency in glutamine but not glucose induces MYC-dependent apoptosis in human cells. J Cell Biol, 2007. 178(1): p. 93-105.
37. Morita, M., S.P. Gravel, V. Chenard, K. Sikstrom, L. Zheng, T. Alain, V. Gandin, D. Avizonis, M. Arguello, C. Zakaria, S. McLaughlan, Y. Nouet, A. Pause, M. Pollak, E. Gottlieb, O. Larsson, J. St-Pierre, I. Topisirovic, and N. Sonenberg, mTORC1 Controls Mitochondrial Activity and Biogenesis through 4E-BP-

Dependent Translational Regulation. Cell Metab, 2013. 18(5): p. 698-711.
38. Schmelzle, T. and M.N. Hall, TOR, a central controller of cell growth. Cell, 2000. 103(2): p. 253-62.
39. Kim, S.G., G.R. Buel, and J. Blenis, Nutrient regulation of the mTOR complex 1 signaling pathway. Mol Cells, 2013. 35(6): p. 463-73.
40. Smith, E.M., S.G. Finn, A.R. Tee, G.J. Browne, and C.G. Proud, The tuberous sclerosis protein TSC2 is not required for the regulation of the mammalian target of rapamycin by amino acids and certain cellular stresses. J Biol Chem, 2005. 280(19): p. 18717-27.
41. Sancak, Y., L. Bar-Peled, R. Zoncu, A.L. Markhard, S. Nada, and D.M. Sabatini, Ragulator-Rag complex targets mTORC1 to the lysosomal surface and is necessary for its activation by amino acids. Cell, 2010. 141(2): p. 290-303.
42. Zoncu, R., L. Bar-Peled, A. Efeyan, S. Wang, Y. Sancak, and D.M. Sabatini, mTORC1 senses lysosomal amino acids through an inside-out mechanism that requires the vacuolar H(+)-ATPase. Science, 2011. 334(6056): p. 678-83.
43. Bar-Peled, L., L. Chantranupong, A.D. Cherniack, W.W. Chen, K.A. Ottina, B.C. Grabiner, E.D. Spear, S.L. Carter, M. Meyerson, and D.M. Sabatini, A Tumor suppressor complex with GAP activity for the Rag GTPases that signal amino acid sufficiency to mTORC1. Science, 2013. 340(6136): p. 1100-6.
44. Han, J.M., S.J. Jeong, M.C. Park, G. Kim, N.H. Kwon, H.K. Kim, S.H. Ha, S.H. Ryu, and S. Kim, Leucyl-tRNA synthetase is an intracellular leucine sensor for the mTORC1-signaling pathway. Cell, 2012. 149(2): p. 410-24.

45. Nicklin, P., P. Bergman, B. Zhang, E. Triantafellow, H. Wang, B. Nyfeler, H. Yang, M. Hild, C. Kung, C. Wilson, V.E. Myer, J.P. MacKeigan, J.A. Porter, Y.K. Wang, L.C. Cantley, P.M. Finan, and L.O. Murphy, Bidirectional transport of amino acids regulates mTOR and autophagy. Cell, 2009. 136(3): p. 521-34.
46. Duran, R.V., W. Oppliger, A.M. Robitaille, L. Heiserich, R. Skendaj, E. Gottlieb, and M.N. Hall, Glutaminolysis activates Rag-mTORC1 signaling. Mol Cell, 2012. 47(3): p. 349-58.
47. Csibi, A., S.M. Fendt, C. Li, G. Poulogiannis, A.Y. Choo, D.J. Chapski, S.M. Jeong, J.M. Dempsey, A. Parkhitko, T. Morrison, E.P. Henske, M.C. Haigis, L.C. Cantley, G. Stephanopoulos, J. Yu, and J. Blenis, The mTORC1 pathway stimulates glutamine metabolism and cell proliferation by repressing SIRT4. Cell, 2013. 153(4): p. 840-54.
48. Pinilla, J., J.C. Aledo, E. Cwiklinski, R. Hyde, P.M. Taylor, and H.S. Hundal, SNAT2 transceptor signalling via mTOR: a role in cell growth and proliferation? Front Biosci (Elite Ed), 2011. 3: p. 1289-99.
49. Seltzer, M.J., B.D. Bennett, A.D. Joshi, P. Gao, A.G. Thomas, D.V. Ferraris, T. Tsukamoto, C.J. Rojas, B.S. Slusher, J.D. Rabinowitz, C.V. Dang, and G.J. Riggins, Inhibition of glutaminase preferentially slows growth of glioma cells with mutant IDH1. Cancer Res, 2010. 70(22): p. 8981-7.
50. Wang, J.B., J.W. Erickson, R. Fuji, S. Ramachandran, P. Gao, R. Dinavahi, K.F. Wilson, A.L. Ambrosio, S.M. Dias, C.V. Dang, and R.A. Cerione, Targeting mitochondrial glutaminase activity inhibits oncogenic transformation. Cancer Cell, 2010. 18(3): p. 207-19.
51. Willems, L., N. Jacque, A. Jacquel, N. Neveux, T. Trovati Maciel, M. Lambert, A. Schmitt, L. Poulain, A.S. Green, M. Uzunov, O. Kosmider, I. Radford-Weiss, I.C. Moura, P. Auberger, N. Ifrah, V.

Bardet, N. Chapuis, C. Lacombe, P. Mayeux, J. Tamburini, and D. Bouscary, Inhibiting glutamine uptake represents an attractive new strategy for treating acute myeloid leukemia. Blood, 2013.

52. Labow, B.I., S.F. Abcouwer, C.M. Lin, and W.W. Souba, Glutamine synthetase expression in rat lung is regulated by protein stability. Am J Physiol, 1998. 275(5 Pt 1): p. L877-86.
53. Labow, B.I., W.W. Souba, and S.F. Abcouwer, Glutamine synthetase expression in muscle is regulated by transcriptional and posttranscriptional mechanisms. Am J Physiol, 1999. 276(6 Pt 1): p. E1136-45.
54. Rotoli, B.M., J. Uggeri, V. Dall'Asta, R. Visigalli, A. Barilli, R. Gatti, G. Orlandini, G.C. Gazzola, and O. Bussolati, Inhibition of glutamine synthetase triggers apoptosis in asparaginase-resistant cells. Cell Physiol Biochem, 2005. 15(6): p. 281-92.
55. Tardito, S., J. Uggeri, C. Bozzetti, M.G. Bianchi, B.M. Rotoli, R. Franchi-Gazzola, G.C. Gazzola, R. Gatti, and O. Bussolati, The inhibition of glutamine synthetase sensitizes human sarcoma cells to L-asparaginase. Cancer Chemother Pharmacol, 2007. 60(5): p. 751-8.
56. Wise, D.R. and C.B. Thompson, Glutamine addiction: a new therapeutic target in cancer. Trends Biochem Sci, 2010. 35(8): p. 427-33.
57. Broome, J.D., Evidence that the L-asparaginase of guinea pig serum is responsible for its antilymphoma effects. II. Lymphoma 6C3HED cells cultured in a medium devoid of L-asparagine lose their susceptibility to the effects of guinea pig serum in vivo. J Exp Med, 1963. 118: p. 121-48.
58. Panosyan, E.H., R.S. Grigoryan, I.A. Avramis, N.L. Seibel, P.S. Gaynon, S.E. Siegel, H.J. Fingert, and V.I. Avramis, Deamination of glutamine is a prerequisite for optimal asparagine deamination

by asparaginases in vivo (CCG-1961). Anticancer Res, 2004. 24(2C): p. 1121-5.
59. Avramis, V.I. and P.N. Tiwari, Asparaginase (native ASNase or pegylated ASNase) in the treatment of acute lymphoblastic leukemia. Int J Nanomedicine, 2006. 1(3): p. 241-54.
60. Avramis, V.I., Asparaginases: a successful class of drugs against leukemias and lymphomas. J Pediatr Hematol Oncol, 2011. 33(8): p. 573-9.
61. Aghaiypour, K., A. Wlodawer, and J. Lubkowski, Structural basis for the activity and substrate specificity of Erwinia chrysanthemi L-asparaginase. Biochemistry, 2001. 40(19): p. 5655-64.
62. Avramis, V.I., Asparaginases: biochemical pharmacology and modes of drug resistance. Anticancer Res, 2012. 32(7): p. 2423-37.
63. Narta, U.K., S.S. Kanwar, and W. Azmi, Pharmacological and clinical evaluation of L-asparaginase in the treatment of leukemia. Crit Rev Oncol Hematol, 2007. 61(3): p. 208-21.
64. Lorenzi, P.L., J. Llamas, M. Gunsior, L. Ozbun, W.C. Reinhold, S. Varma, H. Ji, H. Kim, A.A. Hutchinson, E.C. Kohn, P.K. Goldsmith, M.J. Birrer, and J.N. Weinstein, Asparagine synthetase is a predictive biomarker of L-asparaginase activity in ovarian cancer cell lines. Mol Cancer Ther, 2008. 7(10): p. 3123-8.
65. Timmerman, L.A., T. Holton, M. Yuneva, R.J. Louie, M. Padro, A. Daemen, M. Hu, D.A. Chan, S.P. Ethier, L.J. van 't Veer, K. Polyak, F. McCormick, and J.W. Gray, Glutamine Sensitivity Analysis Identifies the xCT Antiporter as a Common Triple-Negative Breast Tumor Therapeutic Target. Cancer Cell, 2013.
66. Iwamoto, S., K. Mihara, J.R. Downing, C.H. Pui, and D. Campana, Mesenchymal cells regulate the response of acute lymphoblastic leukemia cells to asparaginase. J Clin Invest, 2007. 117(4): p. 1049-57.

67. Zhang, W., D. Trachootham, J. Liu, G. Chen, H. Pelicano, C. Garcia-Prieto, W. Lu, J.A. Burger, C.M. Croce, W. Plunkett, M.J. Keating, and P. Huang, Stromal control of cystine metabolism promotes cancer cell survival in chronic lymphocytic leukaemia. Nat Cell Biol, 2012. 14(3): p. 276-86.
68. Tong, W.H., R. Pieters, W.C. Hop, C. Lanvers-Kaminsky, J. Boos, and I.M. van der Sluis, No evidence of increased asparagine levels in the bone marrow of patients with acute lymphoblastic leukemia during asparaginase therapy. Pediatr Blood Cancer, 2013. 60(2): p. 258-61.
69. Steiner, M., D. Hochreiter, D.C. Kasper, R. Kornmuller, H. Pichler, O.A. Haas, U. Potschger, C. Hutter, M.N. Dworzak, G. Mann, and A. Attarbaschi, Asparagine and aspartic acid concentrations in bone marrow versus peripheral blood during Berlin-Frankfurt-Munster-based induction therapy for childhood acute lymphoblastic leukemia. Leuk Lymphoma, 2012. 53(9): p. 1682-7.
70. Ehsanipour, E.A., X. Sheng, J.W. Behan, X. Wang, A. Butturini, V.I. Avramis, and S.D. Mittelman, Adipocytes cause leukemia cell resistance to L-asparaginase via release of glutamine. Cancer Res, 2013. 73(10): p. 2998-3006.
71. Williams, D.A., A new mechanism of leukemia drug resistance? N Engl J Med, 2007. 357(1): p. 77-8.
72. Garnick, M.B. and P.R. Larsen, Acute deficiency of thyroxine-binding globulin during L-asparaginase therapy. N Engl J Med, 1979. 301(5): p. 252-3.
73. Bartalena, L., E. Martino, A. Pacchiarotti, S. Balzano, M. Falcone, V. Sica, P. Biddau, and A. Pinchera, Effects of the antileukemic drug L-asparaginase on sex hormone-binding globulin: studies in vivo and in vitro. J Endocrinol Invest, 1989. 12(7): p. 489-93.

74. Land, V.J., W.W. Sutow, D.J. Fernbach, D.M. Lane, and T.E. Williams, Toxicity of L-asparginase in children with advanced leukemia. Cancer, 1972. 30(2): p. 339-47.
75. Yuneva, M.O., T.W. Fan, T.D. Allen, R.M. Higashi, D.V. Ferraris, T. Tsukamoto, J.M. Mates, F.J. Alonso, C. Wang, Y. Seo, X. Chen, and J.M. Bishop, The metabolic profile of tumors depends on both the responsible genetic lesion and tissue type. Cell Metab, 2012. 15(2): p. 157-70.
76. Ferlay, J., H.R. Shin, F. Bray, D. Forman, C. Mathers, and D.M. Parkin, Estimates of worldwide burden of cancer in 2008: GLOBOCAN 2008. Int J Cancer, 2010. 127(12): p. 2893-917.
77. El-Serag, H.B., Hepatocellular carcinoma. N Engl J Med, 2011. 365(12): p. 1118-27.
78. Imbeaud, S., Y. Ladeiro, and J. Zucman-Rossi, Identification of novel oncogenes and tumor suppressors in hepatocellular carcinoma. Semin Liver Dis, 2010. 30(1): p. 75-86.
79. Ayub, A., U.A. Ashfaq, and A. Haque, HBV induced HCC: major risk factors from genetic to molecular level. Biomed Res Int, 2013. 2013: p. 810461.
80. Jeong, S.W., J.Y. Jang, and R.T. Chung, Hepatitis C virus and hepatocarcinogenesis. Clin Mol Hepatol, 2012. 18(4): p. 347-56.
81. Wu, H.C. and R. Santella, The role of aflatoxins in hepatocellular carcinoma. Hepat Mon, 2012. 12(10 HCC): p. e7238.
82. Moudgil, V., D. Redhu, S. Dhanda, and J. Singh, A review of molecular mechanisms in the development of hepatocellular carcinoma by aflatoxin and hepatitis B and C viruses. J Environ Pathol Toxicol Oncol, 2013. 32(2): p. 165-75.
83. Ekstrom, G. and M. Ingelman-Sundberg, Rat liver microsomal NADPH-supported oxidase activity and lipid peroxidation

dependent on ethanol-inducible cytochrome P-450 (P-450IIE1). Biochem Pharmacol, 1989. 38(8): p. 1313-9.
84. Alzahrani, B., T.J. Iseli, and L.W. Hebbard, Non-viral causes of liver cancer: Does obesity led inflammation play a role? Cancer Lett, 2013.
85. Mazzaferro, V., E. Regalia, R. Doci, S. Andreola, A. Pulvirenti, F. Bozzetti, F. Montalto, M. Ammatuna, A. Morabito, and L. Gennari, Liver transplantation for the treatment of small hepatocellular carcinomas in patients with cirrhosis. N Engl J Med, 1996. 334(11): p. 693-9.
86. Maluccio, M. and A. Covey, Recent progress in understanding, diagnosing, and treating hepatocellular carcinoma. CA Cancer J Clin, 2012. 62(6): p. 394-9.
87. Marrero, J.A., Multidisciplinary management of hepatocellular carcinoma: where are we today? Semin Liver Dis, 2013. 33 Suppl 1: p. S3-10.
88. Kuang, M., X.Y. Xie, C. Huang, Y. Wang, M.X. Lin, Z.F. Xu, G.J. Liu, and M.D. Lu, Long-term outcome of percutaneous ablation in very early-stage hepatocellular carcinoma. J Gastrointest Surg, 2011. 15(12): p. 2165-71.
89. Farazi, P.A. and R.A. DePinho, Hepatocellular carcinoma pathogenesis: from genes to environment. Nat Rev Cancer, 2006. 6(9): p. 674-87.
90. Shiraha, H., K. Yamamoto, and M. Namba, Human hepatocyte carcinogenesis (review). Int J Oncol, 2013. 42(4): p. 1133-8.
91. Minguez, B., V. Tovar, D. Chiang, A. Villanueva, and J.M. Llovet, Pathogenesis of hepatocellular carcinoma and molecular therapies. Curr Opin Gastroenterol, 2009. 25(3): p. 186-94.
92. Wang, Y., M.C. Wu, J.S. Sham, W. Zhang, W.Q. Wu, and X.Y. Guan, Prognostic significance of c-myc and AIB1 amplification in

hepatocellular carcinoma. A broad survey using high-throughput tissue microarray. Cancer, 2002. 95(11): p. 2346-52.
93. Zheng, X., W. Zeng, X. Gai, Q. Xu, C. Li, Z. Liang, H. Tuo, and Q. Liu, Role of the Hedgehog pathway in hepatocellular carcinoma (review). Oncol Rep, 2013. 30(5): p. 2020-6.
94. Lee, C.M., C.Y. Hsu, H.L. Eng, W.S. Huang, S.N. Lu, C.S. Changchien, C.L. Chen, and C.L. Cho, Telomerase activity and telomerase catalytic subunit in hepatocellular carcinoma. Hepatogastroenterology, 2004. 51(57): p. 796-800.
95. Gougelet, A. and S. Colnot, A Complex Interplay between Wnt/beta-Catenin Signalling and the Cell Cycle in the Adult Liver. Int J Hepatol, 2012. 2012: p. 816125.
96. Clevers, H., Wnt/beta-catenin signaling in development and disease. Cell, 2006. 127(3): p. 469-80.
97. Nejak-Bowen, K.N. and S.P. Monga, Beta-catenin signaling, liver regeneration and hepatocellular cancer: sorting the good from the bad. Semin Cancer Biol, 2011. 21(1): p. 44-58.
98. Moon, R.T., A.D. Kohn, G.V. De Ferrari, and A. Kaykas, WNT and beta-catenin signalling: diseases and therapies. Nat Rev Genet, 2004. 5(9): p. 691-701.
99. Benhamouche, S., T. Decaens, C. Godard, R. Chambrey, D.S. Rickman, C. Moinard, M. Vasseur-Cognet, C.J. Kuo, A. Kahn, C. Perret, and S. Colnot, Apc tumor suppressor gene is the "zonation-keeper" of mouse liver. Dev Cell, 2006. 10(6): p. 759-70.
100. Gumbiner, B.M., Regulation of cadherin-mediated adhesion in morphogenesis. Nat Rev Mol Cell Biol, 2005. 6(8): p. 622-34.
101. Monga, S.P., W.M. Mars, P. Pediaditakis, A. Bell, K. Mule, W.C. Bowen, X. Wang, R. Zarnegar, and G.K. Michalopoulos, Hepatocyte growth factor induces Wnt-independent nuclear

translocation of beta-catenin after Met-beta-catenin dissociation in hepatocytes. Cancer Res, 2002. 62(7): p. 2064-71.

102. Roberts, L.R. and G.J. Gores, Hepatocellular carcinoma: molecular pathways and new therapeutic targets. Semin Liver Dis, 2005. 25(2): p. 212-25.

103. Dal Bello, B., L. Rosa, N. Campanini, C. Tinelli, F. Torello Viera, G. D'Ambrosio, S. Rossi, and E.M. Silini, Glutamine synthetase immunostaining correlates with pathologic features of hepatocellular carcinoma and better survival after radiofrequency thermal ablation. Clin Cancer Res, 2010. 16(7): p. 2157-66.

104. Mirandola, L., P. Comi, E. Cobos, W.M. Kast, M. Chiriva-Internati, and R. Chiaramonte, Notch-ing from T-cell to B-cell lymphoid malignancies. Cancer Lett, 2011. 308(1): p. 1-13.

105. De Strooper, B., W. Annaert, P. Cupers, P. Saftig, K. Craessaerts, J.S. Mumm, E.H. Schroeter, V. Schrijvers, M.S. Wolfe, W.J. Ray, A. Goate, and R. Kopan, A presenilin-1-dependent gamma-secretase-like protease mediates release of Notch intracellular domain. Nature, 1999. 398(6727): p. 518-22.

106. Grabher, C., H. von Boehmer, and A.T. Look, Notch 1 activation in the molecular pathogenesis of T-cell acute lymphoblastic leukaemia. Nat Rev Cancer, 2006. 6(5): p. 347-59.

107. Weng, A.P., A.A. Ferrando, W. Lee, J.P.t. Morris, L.B. Silverman, C. Sanchez-Irizarry, S.C. Blacklow, A.T. Look, and J.C. Aster, Activating mutations of NOTCH1 in human T cell acute lymphoblastic leukemia. Science, 2004. 306(5694): p. 269-71.

108. Santagata, S., F. Demichelis, A. Riva, S. Varambally, M.D. Hofer, J.L. Kutok, R. Kim, J. Tang, J.E. Montie, A.M. Chinnaiyan, M.A. Rubin, and J.C. Aster, JAGGED1 expression is associated with prostate cancer metastasis and recurrence. Cancer Res, 2004. 64(19): p. 6854-7.

109. Nicolas, M., A. Wolfer, K. Raj, J.A. Kummer, P. Mill, M. van Noort, C.C. Hui, H. Clevers, G.P. Dotto, and F. Radtke, Notch1 functions as a tumor suppressor in mouse skin. Nat Genet, 2003. 33(3): p. 416-21.
110. Moeini, A., H. Cornella, and A. Villanueva, Emerging Signaling Pathways in Hepatocellular Carcinoma. Liver Cancer, 2012. 1(2): p. 83-93.
111. Qi, R., H. An, Y. Yu, M. Zhang, S. Liu, H. Xu, Z. Guo, T. Cheng, and X. Cao, Notch1 signaling inhibits growth of human hepatocellular carcinoma through induction of cell cycle arrest and apoptosis. Cancer Res, 2003. 63(23): p. 8323-9.
112. Wang, C., R. Qi, N. Li, Z. Wang, H. An, Q. Zhang, Y. Yu, and X. Cao, Notch1 signaling sensitizes tumor necrosis factor-related apoptosis-inducing ligand-induced apoptosis in human hepatocellular carcinoma cells by inhibiting Akt/Hdm2-mediated p53 degradation and up-regulating p53-dependent DR5 expression. J Biol Chem, 2009. 284(24): p. 16183-90.
113. Villanueva, A., C. Alsinet, K. Yanger, Y. Hoshida, Y. Zong, S. Toffanin, L. Rodriguez-Carunchio, M. Sole, S. Thung, B.Z. Stanger, and J.M. Llovet, Notch signaling is activated in human hepatocellular carcinoma and induces tumor formation in mice. Gastroenterology, 2012. 143(6): p. 1660-1669 e7.
114. Giovannini, C., L. Gramantieri, P. Chieco, M. Minguzzi, F. Lago, S. Pianetti, E. Ramazzotti, K.B. Marcu, and L. Bolondi, Selective ablation of Notch3 in HCC enhances doxorubicin's death promoting effect by a p53 dependent mechanism. J Hepatol, 2009. 50(5): p. 969-79.
115. Wang, F., H. Zhou, Y. Yang, X. Xia, Q. Sun, J. Luo, and B. Cheng, Hepatitis B virus X protein promotes the growth of hepatocellular

carcinoma by modulation of the Notch signaling pathway. Oncol Rep, 2012. 27(4): p. 1170-6.

116. Koeller, K.K. and E.J. Rushing, From the archives of the AFIP: Oligodendroglioma and its variants: radiologic-pathologic correlation. Radiographics, 2005. 25(6): p. 1669-88.

117. Kros, J.M., S.T. Lie, and S.Z. Stefanko, Familial occurrence of polymorphous oligodendroglioma. Neurosurgery, 1994. 34(4): p. 732-6; discussion 736.

118. Van den Bent, M.J., M. Reni, G. Gatta, and C. Vecht, Oligodendroglioma. Crit Rev Oncol Hematol, 2008. 66(3): p. 262-72.

119. Jenkins, R.B., H. Blair, K.V. Ballman, C. Giannini, R.M. Arusell, M. Law, H. Flynn, S. Passe, S. Felten, P.D. Brown, E.G. Shaw, and J.C. Buckner, A t(1;19)(q10;p10) mediates the combined deletions of 1p and 19q and predicts a better prognosis of patients with oligodendroglioma. Cancer Res, 2006. 66(20): p. 9852-61.

120. Pilkington, G.J. and P.L. Lantos, The role of glutamine synthetase in the diagnosis of cerebral tumours. Neuropathol Appl Neurobiol, 1982. 8(3): p. 227-36.

121. Cairncross, J.G. and D.R. Macdonald, Successful chemotherapy for recurrent malignant oligodendroglioma. Ann Neurol, 1988. 23(4): p. 360-4.

122. van den Bent, M.J., Diagnosis and management of oligodendroglioma. Semin Oncol, 2004. 31(5): p. 645-52.

123. Barcellos-de-Souza, P., V. Gori, F. Bambi, and P. Chiarugi, Tumor microenvironment: bone marrow-mesenchymal stem cells as key players. Biochim Biophys Acta, 2013.

124. Friedenstein, A.J., J.F. Gorskaja, and N.N. Kulagina, Fibroblast precursors in normal and irradiated mouse hematopoietic organs. Exp Hematol, 1976. 4(5): p. 267-74.

125. Ilancheran, S., Y. Moodley, and U. Manuelpillai, Human fetal membranes: a source of stem cells for tissue regeneration and repair? Placenta, 2009. 30(1): p. 2-10.
126. Dominici, M., K. Le Blanc, I. Mueller, I. Slaper-Cortenbach, F. Marini, D. Krause, R. Deans, A. Keating, D. Prockop, and E. Horwitz, Minimal criteria for defining multipotent mesenchymal stromal cells. The International Society for Cellular Therapy position statement. Cytotherapy, 2006. 8(4): p. 315-7.
127. Wang, M., Q. Yu, L. Wang, and H. Gu, Distinct patterns of histone modifications at cardiac-specific gene promoters between cardiac stem cells and mesenchymal stem cells. Am J Physiol Cell Physiol, 2013. 304(11): p. C1080-90.
128. Inaba, H., M. Greaves, and C.G. Mullighan, Acute lymphoblastic leukaemia. Lancet, 2013. 381(9881): p. 1943-55.
129. Pui, C.H., L.L. Robison, and A.T. Look, Acute lymphoblastic leukaemia. Lancet, 2008. 371(9617): p. 1030-43.
130. Stanulla, M. and M. Schrappe, Treatment of childhood acute lymphoblastic leukemia. Semin Hematol, 2009. 46(1): p. 52-63.
131. Mendez-Ferrer, S., T.V. Michurina, F. Ferraro, A.R. Mazloom, B.D. Macarthur, S.A. Lira, D.T. Scadden, A. Ma'ayan, G.N. Enikolopov, and P.S. Frenette, Mesenchymal and haematopoietic stem cells form a unique bone marrow niche. Nature, 2010. 466(7308): p. 829-34.
132. Andre, V., D. Longoni, S. Bresolin, C. Cappuzzello, E. Dander, M. Galbiati, C. Bugarin, A. Di Meglio, E. Nicolis, E. Maserati, M. Serafini, A.J. Warren, G. Te Kronnie, G. Cazzaniga, L. Sainati, M. Cipolli, A. Biondi, and G. D'Amico, Mesenchymal stem cells from Shwachman-Diamond syndrome patients display normal functions and do not contribute to hematological defects. Blood Cancer J, 2012. 2: p. e94.

133. Rodriguez-Pardo, V.M., J.A. Aristizabal, D. Jaimes, S.M. Quijano, I.D. Reyes, M.V. Herrera, J. Solano, and J.P. Vernot, Mesenchymal stem cells promote leukaemic cells aberrant phenotype from B-cell acute lymphoblastic leukaemia. Hematol Oncol Stem Cell Ther, 2013.
134. Bergfeld, S.A. and Y.A. DeClerck, Bone marrow-derived mesenchymal stem cells and the tumor microenvironment. Cancer Metastasis Rev, 2010. 29(2): p. 249-61.
135. Armeanu-Ebinger, S., J. Wenz, G. Seitz, I. Leuschner, R. Handgretinger, U.A. Mau-Holzmann, M. Bonin, B. Sipos, J. Fuchs, and S.W. Warmann, Characterisation of the cell line HC-AFW1 derived from a pediatric hepatocellular carcinoma. PLoS One, 2012. 7(5): p. e38223.
136. Tardito, S., M. Chiu, J. Uggeri, A. Zerbini, F. Da Ros, V. Dall'Asta, G. Missale, and O. Bussolati, L-Asparaginase and inhibitors of glutamine synthetase disclose glutamine addiction of beta-catenin-mutated human hepatocellular carcinoma cells. Curr Cancer Drug Targets, 2011. 11(8): p. 929-43.
137. Bustin, S.A., Absolute quantification of mRNA using real-time reverse transcription polymerase chain reaction assays. J Mol Endocrinol, 2000. 25(2): p. 169-93.
138. Dall'Asta, V., O. Bussolati, R. Sala, A. Parolari, F. Alamanni, P. Biglioli, and G.C. Gazzola, Amino acids are compatible osmolytes for volume recovery after hypertonic shrinkage in vascular endothelial cells. Am J Physiol, 1999. 276(4 Pt 1): p. C865-72.
139. Cairo, S., C. Armengol, A. De Reynies, Y. Wei, E. Thomas, C.A. Renard, A. Goga, A. Balakrishnan, M. Semeraro, L. Gresh, M. Pontoglio, H. Strick-Marchand, F. Levillayer, Y. Nouet, D. Rickman, F. Gauthier, S. Branchereau, L. Brugieres, V. Laithier, R. Bouvier, F. Boman, G. Basso, J.F. Michiels, P. Hofman, F. Arbez-Gindre, H.

Jouan, M.C. Rousselet-Chapeau, D. Berrebi, L. Marcellin, F. Plenat, D. Zachar, M. Joubert, J. Selves, D. Pasquier, P. Bioulac-Sage, M. Grotzer, M. Childs, M. Fabre, and M.A. Buendia, Hepatic stem-like phenotype and interplay of Wnt/beta-catenin and Myc signaling in aggressive childhood liver cancer. Cancer Cell, 2008. 14(6): p. 471-84.

140. Minet, R., F. Villie, M. Marcollet, D. Meynial-Denis, and L. Cynober, Measurement of glutamine synthetase activity in rat muscle by a colorimetric assay. Clin Chim Acta, 1997. 268(1-2): p. 121-32.

141. Burcombe, R., G.D. Wilson, M. Dowsett, I. Khan, P.I. Richman, F. Daley, S. Detre, and A. Makris, Evaluation of Ki-67 proliferation and apoptotic index before, during and after neoadjuvant chemotherapy for primary breast cancer. Breast Cancer Res, 2006. 8(3): p. R31.

142. Laplante, M. and D.M. Sabatini, mTOR signaling in growth control and disease. Cell, 2012. 149(2): p. 274-93.

143. Jewell, J.L., R.C. Russell, and K.L. Guan, Amino acid signalling upstream of mTOR. Nat Rev Mol Cell Biol, 2013. 14(3): p. 133-9.

144. Fenton, T.R. and I.T. Gout, Functions and regulation of the 70kDa ribosomal S6 kinases. Int J Biochem Cell Biol, 2011. 43(1): p. 47-59.

145. Chiu, M., S. Tardito, A. Barilli, M.G. Bianchi, V. Dall'Asta, and O. Bussolati, Glutamine stimulates mTORC1 independent of the cell content of essential amino acids. Amino Acids, 2012. 43(6): p. 2561-7.

146. Wen, H.Y., S. Abbasi, R.E. Kellems, and Y. Xia, mTOR: a placental growth signaling sensor. Placenta, 2005. 26 Suppl A: p. S63-9.

147. Bussolati, O., V. Dall'Asta, R. Franchi-Gazzola, R. Sala, B.M. Rotoli, R. Visigalli, J. Casado, M. Lopez-Fontanals, M. Pastor-Anglada, and G.C. Gazzola, The role of system A for neutral amino

acid transport in the regulation of cell volume. Mol Membr Biol, 2001. 18(1): p. 27-38.

148. Baird, F.E., K.J. Bett, C. MacLean, A.R. Tee, H.S. Hundal, and P.M. Taylor, Tertiary active transport of amino acids reconstituted by coexpression of System A and L transporters in Xenopus oocytes. Am J Physiol Endocrinol Metab, 2009. 297(3): p. E822-9.

149. Karunakaran, S., S. Ramachandran, V. Coothankandaswamy, S. Elangovan, E. Babu, S. Periyasamy-Thandavan, A. Gurav, J.P. Gnanaprakasam, N. Singh, P.V. Schoenlein, P.D. Prasad, M. Thangaraju, and V. Ganapathy, SLC6A14 (ATB0,+) protein, a highly concentrative and broad specific amino acid transporter, is a novel and effective drug target for treatment of estrogen receptor-positive breast cancer. J Biol Chem, 2011. 286(36): p. 31830-8.

150. Gaccioli, F., C.C. Huang, C. Wang, E. Bevilacqua, R. Franchi-Gazzola, G.C. Gazzola, O. Bussolati, M.D. Snider, and M. Hatzoglou, Amino acid starvation induces the SNAT2 neutral amino acid transporter by a mechanism that involves eukaryotic initiation factor 2alpha phosphorylation and cap-independent translation. J Biol Chem, 2006. 281(26): p. 17929-40.

151. Anderson, C.M., A. Howard, J.R. Walters, V. Ganapathy, and D.T. Thwaites, Taurine uptake across the human intestinal brush-border membrane is via two transporters: H+-coupled PAT1 (SLC36A1) and Na+- and Cl(-)-dependent TauT (SLC6A6). J Physiol, 2009. 587(Pt 4): p. 731-44.

152. Boukhettala, N., S. Claeyssens, M. Bensifi, B. Maurer, J. Abed, A. Lavoinne, P. Dechelotte, and M. Coeffier, Effects of essential amino acids or glutamine deprivation on intestinal permeability and protein synthesis in HCT-8 cells: involvement of GCN2 and mTOR pathways. Amino Acids, 2012. 42(1): p. 375-83.

153. Tardito, S., M. Chiu, R. Franchi-Gazzola, V. Dall'Asta, P. Comi, and O. Bussolati, The non-proteinogenic amino acids L-methionine sulfoximine and DL-phosphinothricin activate mTOR. Amino Acids, 2012. 42(6): p. 2507-12.
154. van der Vos, K.E., P. Eliasson, T. Proikas-Cezanne, S.J. Vervoort, R. van Boxtel, M. Putker, I.J. van Zutphen, M. Mauthe, S. Zellmer, C. Pals, L.P. Verhagen, M.J. Groot Koerkamp, A.K. Braat, T.B. Dansen, F.C. Holstege, R. Gebhardt, B.M. Burgering, and P.J. Coffer, Modulation of glutamine metabolism by the PI(3)K-PKB-FOXO network regulates autophagy. Nat Cell Biol, 2012. 14(8): p. 829-37.
155. Eisenberg, D., H.S. Gill, G.M. Pfluegl, and S.H. Rotstein, Structure-function relationships of glutamine synthetases. Biochim Biophys Acta, 2000. 1477(1-2): p. 122-45.
156. Kimball, S.R., Eukaryotic initiation factor eIF2. Int J Biochem Cell Biol, 1999. 31(1): p. 25-9.
157. Cheng, T., J. Sudderth, C. Yang, A.R. Mullen, E.S. Jin, J.M. Mates, and R.J. DeBerardinis, Pyruvate carboxylase is required for glutamine-independent growth of tumor cells. Proc Natl Acad Sci U S A, 2011. 108(21): p. 8674-9.
158. Kwon, C., P. Cheng, I.N. King, P. Andersen, L. Shenje, V. Nigam, and D. Srivastava, Notch post-translationally regulates beta-catenin protein in stem and progenitor cells. Nat Cell Biol, 2011. 13(10): p. 1244-51.
159. Rodilla, V., A. Villanueva, A. Obrador-Hevia, A. Robert-Moreno, V. Fernandez-Majada, A. Grilli, N. Lopez-Bigas, N. Bellora, M.M. Alba, F. Torres, M. Dunach, X. Sanjuan, S. Gonzalez, T. Gridley, G. Capella, A. Bigas, and L. Espinosa, Jagged1 is the pathological link between Wnt and Notch pathways in colorectal cancer. Proc Natl Acad Sci U S A, 2009. 106(15): p. 6315-20.

160. Ahn, S., J. Hyeon, and C.K. Park, Notch1 and Notch4 are markers for poor prognosis of hepatocellular carcinoma. Hepatobiliary Pancreat Dis Int, 2013. 12(3): p. 286-94.
161. Zeng, G., U. Apte, B. Cieply, S. Singh, and S.P. Monga, siRNA-mediated beta-catenin knockdown in human hepatoma cells results in decreased growth and survival. Neoplasia, 2007. 9(11): p. 951-9.
162. Zhang, B., L.W. Dong, Y.X. Tan, J. Zhang, Y.F. Pan, C. Yang, M.H. Li, Z.W. Ding, L.J. Liu, T.Y. Jiang, J.H. Yang, and H.Y. Wang, Asparagine synthetase is an independent predictor of surgical survival and a potential therapeutic target in hepatocellular carcinoma. Br J Cancer, 2013. 109(1): p. 14-23.
163. Aslanian, A.M. and M.S. Kilberg, Multiple adaptive mechanisms affect asparagine synthetase substrate availability in asparaginase-resistant MOLT-4 human leukaemia cells. Biochem J, 2001. 358(Pt 1): p. 59-67.
164. Zhuang, Z., M. Qi, J. Li, H. Okamoto, D.S. Xu, R.R. Iyer, J. Lu, C. Yang, R.J. Weil, A. Vortmeyer, and R.R. Lonser, Proteomic identification of glutamine synthetase as a differential marker for oligodendrogliomas and astrocytomas. J Neurosurg, 2011. 115(4): p. 789-95.
165. Domercq, M., M.V. Sanchez-Gomez, C. Sherwin, E. Etxebarria, R. Fern, and C. Matute, System xc- and glutamate transporter inhibition mediates microglial toxicity to oligodendrocytes. J Immunol, 2007. 178(10): p. 6549-56.
166. Ohgaki, H. and P. Kleihues, Population-based studies on incidence, survival rates, and genetic alterations in astrocytic and oligodendroglial gliomas. J Neuropathol Exp Neurol, 2005. 64(6): p. 479-89.
167. Panosyan, E.H., N.L. Seibel, S. Martin-Aragon, P.S. Gaynon, I.A. Avramis, H. Sather, J. Franklin, J. Nachman, L.J. Ettinger, M. La,

P. Steinherz, L.J. Cohen, S.E. Siegel, and V.I. Avramis, Asparaginase antibody and asparaginase activity in children with higher-risk acute lymphoblastic leukemia: Children's Cancer Group Study CCG-1961. J Pediatr Hematol Oncol, 2004. 26(4): p. 217-26.

168. Hermanova, I., M. Zaliova, J. Trka, and J. Starkova, Low expression of asparagine synthetase in lymphoid blasts precludes its role in sensitivity to L-asparaginase. Exp Hematol, 2012. 40(8): p. 657-65.

SCIENTIFIC PRODUCTION

8.1 Scientific production relative to the present work:

1. “Asparagine levels in the bone marrow of patients with acute lymphoblastic leukaemia during asparaginase therapy.” **M. Chiu**, R. Franchi-Gazzola, O. Bussolati, G. D’Amico, F. Dall’Acqua, C. Rizzari. Pediatric Blood Cancer 2013; 60(11):1915.
2. “Changes in the expression of the glutamate transporter EAAT3/EAAC1 in health and disease.” M.G. Bianchi, D. Bardelli, **M. Chiu**, O. Bussolati. Cell Mol Life Sci 2013; in press.
3. “Towards a metabolic therapy of cancer?” Review. **M. Chiu**, L. Ottaviani, M.G. Bianchi, R. Franchi-Gazzola, O. Bussolati. Acta Biomedica 2012; 83:168-176
4. “Valproic acid induces the glutamate transporter EAAT3 in human oligodendroglioma cells” M.G. Bianchi, R. Franchi-Gazzola, L. Reia, M. Allegri, J. Uggeri, **M. Chiu**, R. Sala, O. Bussolati. Neuroscience 2012; 277:260-70
5. “Glutamine stimulates mTORC1 indipendent of the cell content of essential amino acids.” **M. Chiu**, S. Tardito, A. Barilli, M.G. Bianchi, V. Dall’Asta, O. Bussolati. Amino Acids 2012; 43(6):2561-2567
6. “The non-proteinogenic amino acids L:-methionine sulfoximine and DL:-phosphinothricin activate mTOR” S. Tardito, **M. Chiu**, R. Franchi-Gazzola, V. Dall'asta, P. Comi, O. Bussolati. Amino Acids 2012;42(6):2507-12.
7. “L-Asparaginase and Inhibitors of Glutamine Synthetase Disclose Glutamine Addiction of β-Catenin-Mutated Human Hepatocellular Carcinoma Cells.” S. Tardito, **M. Chiu**, J. Uggeri, A. Zerbini, F. Da

Ros, V . Dall'Asta, G. Missale, O. Bussolati. Curr Cancer Drug Targets 2011;11(8):929-43

8.2 Oral presentations of the author relative to the present work:

1. “Pharmacologically induced glutamine depletion impairs liver cancer growth” **M. Chiu**, S. Tardito, A. Armento, D. Bardelli, S. Pillozzi, A. Arcangeli, N. Campanini, E.M. Silini, O. Bussolati. 25th Petzcoller Symposium. June 20-22, 2013 Trento, Italy.
2. “Drug-induced glutamine depletion hinders the growth of β-catenin mutated human liver cancer xenografts" **M. Chiu**, S. Tardito, S. Pillozzi, A. Arcangeli, N. Campanini, E.M. Silini, O. Bussolati. Experimental Biology 2013, Boston (MA, USA) April 20-24, 2013. FASEB J April 9, 2013 27:387.9
3. “β-catenin mutated human Hepatocellular Carcnoma (HCC) cells show features of glutamine addiction” **M. Chiu**, S. Tardito, R. Franchi-Gazzola, M. Bianchi, L. Ottaviani, J. Uggeri, A. Arcangeli, S. Pillozzi, O. Bussolati. 1st Joint Meeting of Pathology and Laboratory Diagnostics, 2012 September 12-15, Udine, Italy. Am J Pathol 2012, 81(Suppl):S1 Abstract NAMT7

8.3 Poster presentations of the author relative to the present work:

1. “Pharmacologically induced glutamine depletion is a metabolic approach for the control of liver cancer” **M. Chiu**, S. Tardito, A. Armento, S. Armeanu-Ebinger, S. Pillozzi, A. Arcangeli, O. Bussolati. Young Scientist Meeting. October 23-24, 2013 Rome, Italy.
2. “Pharmacologically induced glutamine depletion impairs liver cancer growth” **M. Chiu**, S. Tardito, A. Armento, D. Bardelli, S. Pillozzi, A. Arcangeli, N. Campanini, E.M. Silini, O. Bussolati. 25th Petzcoller Symposium. June 20-22, 2013 Trento, Italy. (**Begnudelli Pezcoller award winner**)
3. “Le cellule mesenchimali stromali midollari si adattano alla L-asparaginasi tramite innesco dell’autofagia ed aumento dell’attività di Glutamina Sintetasi” **M. Chiu**, G. Foderà, R. Franchi-Gazzola, G. D'Amico,G. Cazzaniga, F. Dell'Acqua, C. Rizzari ed O. Bussolati. XXXVIII Congresso Nazionale AIEOP 2013. June 9-11, 2013 Rome, Italy
4. “Drug-induced glutamine depletion hinders the growth of β-catenin mutated human liver cancer xenografts" **M. Chiu**, S. Tardito, S. Pillozzi, A. Arcangeli, N. Campanini, E.M. Silini, O. Bussolati. Experimental Biology 2013, Boston (MA, USA) April 20-24, 2013. FASEB J April 9, 2013 27:387.9
5. “Glutamine Synthetase plays a dual role in the dependence of human cancer cells on glutamine” **M. Chiu**, S. Tardito, R. Franchi-Gazzola, M. G. Bianchi, J. Uggeri, O. Bussolati. Experimental Biology 2012, San Diego (CA, USA), April 21-25, 2012. FASEB J March 29, 2012 26:145.18

ACKNOWLEDGEMENTS

I want to express my gratitude to my tutor Prof. Raffaella Chiaramonte of University of Milan, for being always helpful, and, in particular, for kindly giving me the opportunity to pursue my project on cancer cell metabolism. I have truly appreciated it.

Thanks to the Doctoral School in Molecular Medicine of University of Milan for funding my fellowship and my participation to the Experimental Biology 2013 meeting.

This work would not have existed without the help, the advice and the support of my co-tutor Prof. Ovidio Bussolati of University of Parma to whom I am particularly indebted. Thanks for all your teaching, your patience and assistance during these years.

Thanks to all the people who sustained and helped me during this work; in particular, I am grateful to: Dr. Saverio Tardito, now at the Beatson Institute for Cancer Research, for teaching me how to carry on this project and for all the advice he gave me at the beginning of my PhD training; Prof. Renata Franchi-Gazzola and Dr. Massimiliano Bianchi of University of Parma for the support with radiolabeled solute transport; Prof. Valeria Dall'Asta and Dr. Amelia Barilli of University of Parma for the help with HPLC analysis; Prof. Annarosa Arcangeli and Dr. Serena Pillozzi of University of Florence, and Prof. Sorin Armeanu-Ebinger of University Children's Hospital, Eberhard Karls University Tübingen for the support with *in vivo* experiments; Prof. Enrico Maria Silini and Dr. Nicoletta Campanini of University of Parma for the histological evaluation of liver and tumor specimens; Prof. Paul Monga of University of Pittsburgh for providing me

the TOPflash assay for the measurement of β-catenin activity; Prof. Carmelo Rizzari and Dr. Giovanna D'Amico of Centro Ricerca Tettamanti, University of Milan-Bicocca for providing mesenchymal stem cells; Prof. Prisco Mirandola of University of Parma for the help with flow cytometry.

Thanks to Dr. Bruno Rago of EUSAPharma, an Internal Division of Jazz Pharmaceutics, for providing L-Asparaginase and funding my participation to Experimental Biology 2012 meeting.

Many thanks to my lab mates and students I had the pleasure to work with; in particular, thanks to Paola, Gianvito, Angela and Donatella, with you I realized that teaching is another way of learning.

Finally, I would like to specially thanks all my family for their love, their patience, their support. Thank you dears for everything.